HYPERACTIVATED MOTILITY OF STALLION SPERMATOZOA

A Dissertation

By

SHAVAHN CALLAHAN LOUX

Submitted to the Office of Graduate and Professional Studies of
Texas A&M University
In partial fulfillment of the requirements for the degree of

DOCTOR OF PHILOSOPHY

Committee Chair,	Katrin Hinrichs
Committee Members,	Charles R. Long
	Larry Johnson
	Dickson D. Varner
Head of Department,	Glen Laine

December 2013

Major Subject: Biomedical Sciences

ABSTRACT

In vitro fertilization does not occur readily in the horse. Recent evidence suggests that this is due to failure to initiate hyperactivated motility in vitro; however, little is known about the induction of hyperactivated motility in equine sperm. In mice, hyperactivated motility requires the CatSper channel, a pH-gated calcium channel, therefore we investigated this channel and its related intracellular changes, alkalinization and calcium influx, in equine sperm. Motility was assessed by computer-assisted sperm motility analysis, and changes in intracellular pH and calcium were determined via the calcium and pH-specific fluorescent probes, BCECF-AM, Fluo 3-AM and Fluo 4-AM. Additionally, a demembranated sperm model was developed to investigate the direct effect of major regulators of sperm motility on axonemal function.

Increasing intracellular pH induced a rise in intracellular calcium, which was inhibited by the known CatSper blocker mibefradil, supporting the presence of a pH-gated calcium channel, presumably CatSper, in equine sperm. Hyperactivation was induced by treatment with high-pH medium, procaine and 4-aminopyridine. Hyperactivation was associated with moderately increased intracellular pH, but appeared inversely related to increases in intracellular calcium. Sperm treated with procaine in calcium-deficient media both maintained motility and underwent hyperactivation, suggesting that extracellular calcium was not required for hyperactivation. CATSPER1 protein was localized to the principal piece of equine sperm on immunocytochemistry.

Analysis of the predicted equine CATSPER1 protein revealed species-specific differences in structure in the pH-sensor region.

Demembranated equine sperm required ATP for reactivated motility, but did not require cAMP. Motility of demembranated equine sperm was not inhibited by elimination of calcium (chelation to below 20 pM). Excess calcium inhibited motility at concentrations lower than those reported in other species. Calcium-inhibited sperm arrested with a straight tail rather than in a curve, as seen with calcium arrest in other species. Hyperactivated-like motility was not induced at any pH or calcium concentration. Equine sperm were not inhibited by cadmium at concentrations that profoundly inhibit motility in demembranated sperm in other species. These findings indicate species-specific differences in calcium regulation of sperm motility which may relate directly to the inefficiency of functional capacitation of equine sperm under standard in vitro conditions.

DEDICATION

I dedicate this dissertation to my children, Tyler and Daxton, who still believe I know everything.

ACKNOWLEDGEMENTS

I would like to thank my committee chair, Dr. Katrin Hinrichs for the enthusiasm she puts into her work. Her love of research is inspirational and our hours of discussion have been instrumental in getting me to where I am today. I would also like to thank my committee members, Dr. Charles Long, Dr. Dickson Varner and Dr. Larry Johnson for their assistance and input into my education and for helping me make my work the best it can be.

Thanks also to my friends and colleagues, particularly to the members of the Equine Embryo Laboratory at Texas A&M University for their support with all of my research, and the members of the Section of Theriogenology, particularly Sheila Teague and Katrina LaCaze, for the countless stallions which they helped collect semen from for this research.

NOMENCLATURE

4-AP	4-aminopyridine
ÕM	Micromolar
AKAP	A-Kinase Anchor Proteins
ALH	Amplitude of Lateral Head Displacement
BCF	Beat Cross Frequency
Ca_i	Intracellular Calcium
CAMK2	Calmodulin-Dependent Protein Kinase II
CAMK4	Calmodulin-Dependent Protein Kinase IV
CASA	Computer Assisted Sperm Analysis
DMBT1	Deleted in Malignant Brain Tumor
EGTA	Ethylene Glycol Tetraacetic Acid
HRP	Horseradish Peroxidase
ICSI	Intracytoplasmic Sperm Injection
IVF	In Vitro Fertilization
LIN	Linearity
Mib	Mibefradil
mM	Millimolar
MOT	% Total Motility
MT	Modified Tyrodes
MTBD	Microtubule Binding Domain

MW	Modified Whittens
NH_4Cl	Ammonium Chloride
nM	Nanomolar
ODF	Outer Dense Fibers
P4	Progesterone
PGE1	Prostaglandin E1
PHE	Penicillamine, Hypotaurine and Epinephrine
pH_i	Intracellular pH
PI	Propidium Iodide
PKA	Protein Kinase A
pM	Picomolar
PMCA4	Plasma Membrane Calcium ATPase Pump
PVA	Polyvinyl Alcohol
PY	Protein Tyrosine Phosphorylation
sAC	Soluble Adenylyl Cyclase
sNHE	Sodium Hydrogen Exchanger
STR	Straightness
VCL	Curvilinear Velocity

TABLE OF CONTENTS

CHAPTER Page

LIST OF FIGURES

Page

Page

LIST OF TABLES

Page

CHAPTER I

INTRODUCTION

In vitro fertilization (IVF) is problematic in the horse. Historically, success rates have sporadically reached 33% with few trials providing repeatable results [1-5]. This is unfortunate as IVF provides a more physiological method for study of fertilization than does its alternative, intracytoplasmic sperm injection (ICSI). Additionally, ICSI requires highly trained personnel and costly equipment, whereas IVF in most species can be performed with a minimal amount of equipment and supplies.

In 2009, McPartlin et al. reported a fertilization rate of 61% by pharmacologically stimulating hyperactivated motility in capacitated equine sperm [6]. These results suggest that the block to successful in vitro fertilization in the horse is a lack of hyperactivated motility following incubation in standard capacitating conditions. Therefore, the focus of this dissertation research is the regulation of hyperactivated motility in equine sperm, and the role of the kinetics of intracellular calcium and pH in induction of this essential function. This literature review summarizes the most pertinent background on fertilization, IVF in the horse, the ultrastructure of the sperm flagellum, pathways associated with activated and hyperactivated motility and research on demembranated sperm.

FERTILIZATION

Before ejaculated sperm are capable of fertilizing an oocyte, they must undergo preparatory steps, collectively termed capacitation. This was first reported in1951 when two groups independently found that sperm required a period of time in the female reproductive tract before they were capable of fertilizing an oocyte. In his study, M.C. Chang not only determined that rabbit sperm required 6 h to gain the capacity to fertilize an oocyte when surgically placed in the oviduct, he also observed that sperm which were deposited into the vagina gained the ability to fertilize an oocyte much sooner than those placed in the oviduct, indicating a role of the cervix and uterus in capacitating sperm [7]. The study performed by C.R. Austin yielded similar results, showing that oocytes were not fertilized until the sperm had spent at least 4 h in the female reproductive tract, despite the finding that the sperm were in the presence of the ovulated eggs as early as 2 h post-insemination [8].

Capacitation as it is defined today consists of changes to the sperm plasma membrane, cytosol and axonemal structures, including increased protein tyrosine phosphorylation (PY, [9]), increased intracellular pH [10-13], increased intracellular calcium [14-16], changes in membrane fluidity [17, 18] and acquisition of hyperactivated motility [19]. The canonical capacitating medium requires three major components to aid with these changes; calcium, serum albumin and bicarbonate. Calcium is required for the acquisition of hyperactivation [20] as well as the induction of the acrosome reaction [21-23]. Serum albumin is believed to act as a cholesterol acceptor to induce changes in membrane fluidity and may also play a role in allowing

sperm to gain the capacity to undergo the acrosome reaction [24-26]. Bicarbonate stimulates the protein kinase A pathway via stimulation of the sperm soluble adenylate cyclase and production of cAMP [27] and also facilitates an increase in medium pH, which directly correlates to an increase in intracellular pH [13].

Recent work from our laboratory suggests that two components of standard capacitation medium, calcium and BSA, actually suppress the acquisition of protein tyrosine phosphorylation (PY) in stallion sperm at ~pH 7.4 [28]. At this pH, calcium at levels as low as 0.02 mM inhibited PY; this calcium concentration is over 100-fold lower than the calcium concentration seen in standard capacitating medium. Concomitantly, incubation of equine sperm in calcium-free, EGTA-containing medium was associated with high levels of PY. The calcium induced inhibition appeared to be acting through calmodulin, as addition of W-7, a specific calmodulin inhibitor, restored PY to a level similar to that in calcium-free medium. Medium pH played a major role in protein tyrosine phosphorylation of equine sperm. When the pH was high (>7.8), acquisition of PY occurred in the presence or absence of calcium and BSA. This effect was also independent of bicarbonate concentration. These findings appear to be physiologically meaningful, as the pH at which PY could be induced in vitro (>7.8) was similar to that found in the mare uterus immediately after insemination (mean of 7.9). Raw semen was found to have an average pH of 7.47 ± 0.10, which increased to 7.85 ± 0.08 following insemination; the increase in pH could be as important as the actual pH itself [29].

A subsequent study in our laboratory showed that the PY observed in calcium-free medium was occurring through the canonical cAMP/protein kinase A (PKA) pathway [29]. Inhibition of calmodulin kinase II/IV interrupted this pathway, suggesting involvement of this kinase downstream of PKA. Notably, the PY occurring in the presence of calcium with calmodulin suppressed occurred through a separate pathway, which was not affected by inhibition of factors in the canonical PKA cascade. This was a novel finding which has not been reported in other species. Combined, these studies suggest that capacitation in stallion sperm respond differently to the actions of calcium and BSA as compared to sperm of other species.

During in vivo capacitation, sperm of many species are known to bind to the epithelial cells in the oviduct prior to fertilization [30]. It is currently hypothesized that sperm are unable to break free from the oviductal wall until they are fully capacitated, an event which appears to coincide with the acquisition of hyperactivated motility, a whip-like motility required for successful fertilization [31, 32]. This attachment/detachment appears to occur repeatedly during fertilization in vivo, and hyperactivated motility appears to be crucial for providing the sperm with sufficient power to detach from the oviductal wall [33].

Once the sperm have detached from the oviductal epithelial cells and reached the cumulus-oocyte complex, they must penetrate the matrix formed by the cumulus cells. It is thought that hyperactivation, possibly stimulated by the excretion of progesterone from the cumulus cells, is required to allow the sperm to penetrate the cumulus cells [34]. There is some debate about the role of the acrosome reaction in cumulus

penetration [35]; however, the large majority of sperm present in the oviduct and surrounding the oocyte are acrosome-intact, providing support for the theory that hyperactivation alone is sufficient to allow sperm to penetrate the cumulus. Mammalian sperm, including equine sperm, possess a hyluronidase on the plasma membrane of the sperm head, which may aid in cumulus penetration [36].

The necessity for hyperactivated motility in traversing the oviduct is documented largely by work from the laboratory of Susan Suarez at Cornell University. In 1991, this group found that hyperactivated sperm were able to move with greater velocity and generated a greater amount of force than did sperm with typical post-ejaculatory ("activated") motility while swimming through a series of viscous gradients composed of Ficoll, a highly-branched, high mass polysaccharide [37]. Notably, hyperactivated sperm were able to maintain a significantly straighter trajectory in this viscous medium when compared to control sperm, despite the tortuous path of hyperactivated sperm through standard aqueous medium.

After penetration of the cumulus, sperm must bind to, and penetrate, the zona pellucida. The exact method of binding and penetration is not well understood; however, it has been proposed that there are two separate steps involved in penetration of the zona pellucida (ZP). The first involves binding of the acrosome-intact sperm to the ZP, a process which stimulates the acrosome reaction [38-40]. Once the acrosome reaction is complete, a second binding event occurs, allowing the penetration of the sperm through the zona pellucida [41-43].

The above is compatible with the dogma of mammalian fertilization: the fertilizing sperm approaches the ZP with the acrosome intact, then undergoes the acrosome reaction in response to contact with the ZP. This leads to release of enzymes from the acrosome, which causes dissolution of the ZP in the area of the sperm, allowing the sperm to penetrate the protein meshwork of the ZP. Recently, a theory has evolved which suggests that the sperm cells undergo the acrosome reaction within the cumulus cells and thus are acrosome-reacted at the time of sperm-ZP binding. As early as 1998 [44], evidence was reviewed to support the hypothesis that the previously described sequence of events occurs only in lower orders of animals, sub-eutherian mammals, and, rarely, in those eutherian mammals having a thin ZP and spherical-headed sperm, such as bandicoots. In these species, a large hole is dissolved in the ZP and the sperm proceeds into the perivitelline space. However, in most eutherian mammals, there is a thick ZP and no dissolution of the ZP is found in the area of sperm penetration; furthermore, acrosome-reacted sperm are plentiful in the cumulus. Under this theory, the acrosome reaction occurs before contact with the ZP, and the spatulate (flattened) sperm head is then driven through the ZP by the action of the flagellum (hyperactivated motility). In support of this theory, Jin et al. [35] noted that the majority of sperm which managed to successfully fertilize an oocyte in vitro actually began the acrosome reaction within the cumulus cells, and that the rate of successful IVF was increased by the presence of cumulus cells. This has recently been confirmed in an elegant study which found that acrosome-reacted mouse sperm are able to successfully fertilize oocytes [45]. Sperm were allowed to penetrate the ZP of oocytes recovered from mice null for CD9, a

fusion protein. After ZP penetration, the sperm were removed from the perivitelline space of the CD9-null oocytes and placed with wild-type cumulus-oocyte complexes, which they subsequently fertilized, resulting in live offspring.

Hyperactivation appears to be a requirement for the penetration of sperm through the ZP. In a convincing study, Stauss et al. capacitated sperm and added them to 3 separate groups of oocytes [46]. Two of the three groups had inhibitors of hyperactivated motility, 100 µM verapamil or 500 µM cadmium, added after 10 min of exposure, while the third group acted as a control. Only one out of 82 oocytes was penetrated in the groups with hyperactivation inhibited, while 25 out of 40 were penetrated in the control group. An additional experiment in the same study examined sperm capacitated in either 2.9 or 25 mM bicarbonate. Although both groups had equivalent rates of acrosome reaction and ZP binding, only the sperm exposed to 25 mM bicarbonate exhibited hyperactivation. The 25 mM bicarbonate group also had significantly higher rates of fertilization (36% vs. 2%). Sperm which are unable to undergo hyperactivation, such as those from mice null for genes for CatSper, a sperm-specific calcium channel, are sterile, further supporting the requirement for hyperactivated motility during fertilization [47]. A more detailed review of hyperactivation follows below.

After the sperm penetrate the zona pellucida, they must fuse with the oocyte plasma membrane, the oolemma. Fusion of the sperm and oolemma initiates at the equatorial segment of the sperm and involves the microvilli of the oolemma engulfing the sperm head and connecting piece [48]. The microvilli are present over the entire

surface of the oolemma, except for the region directly above the meiotic spindle [49-51]. Little is known about the molecules associated with sperm/egg fusion, although a sperm protein, Izumo, has been shown to be involved, along with the oocyte fusion protein CD9 and its associated integrin, α6β1 [52-54].

Once the sperm has fused with the oolemma, several changes rapidly occur in the oocyte to prevent polyspermy. One of these is the release of cortical granules by the oocyte. Cortical granule release appears to occur in response to oocyte calcium oscillations following exposure to the sperm-derived protein, PLCzeta [55]. During cortical granule release, secretory granules which are evenly distributed along the oocyte cortex fuse with the oocyte plasma membrane and release their contents into the perivitelline space [56, 57]. This induces the cleavage of ZP proteins ZP2 and ZP3 into their truncated forms ZP2f and ZP3f, respectively, and renders the ZP impenetrable by sperm [58]. This process is also known as the zona block or zona hardening [58-60].

The second block to polyspermy occurs at the level of the oolemma, the membrane block. In lower animals, this consists of a change in electrical potential of the oolemma which prevents membrane fusion. The electrical membrane block is present in both lower vertebrates and invertebrates, but is rare in mammalian species [61, 62]. In mammalian oocytes, there appears to be a separate membrane block, but its mechanism is unclear. Cortical tension is higher in the newly fertilized egg than in the unfertilized oocyte [63]. The presence of a membrane block in mammals appears to take more time to develop than the zona block, as it is not yet established at 45 min post-fertilization in the mouse, although it has developed by 90 min post-fusion [64]. This membrane block

appears to be largely independent of cortical granule release because the oolemma of oocytes activated by calcium ionophore, strontium chloride, sperm extract or ICSI, all of which stimulate cortical granule release, are still able to fuse with sperm [64-68].

The efficacy of these blocks to polyspermy varies widely by species. For example, the zona block appears to be weak in species such as the rabbit, pika, pocket gopher and mole, as they are often found with tens to hundreds of surplus sperm in their perivitelline space following fertilization [69-71]. Other species, such as dogs and sheep, rarely have any sperm remaining in the perivitelline space following fertilization [71]. Some species appear to use a combination of both blocks, and between one and ten sperm are often found in the perivitelline space of mice, rats, humans, guinea pigs, cats, pigs and cattle [69-71]. The majority of these observations were recorded with ex vivo recovered embryos, however, human and pig oocytes were also analyzed following in vitro fertilization [70, 71].

IVF IN THE HORSE

Artificial reproductive techniques in the horse have an extensive history. EJ Perry, (1968) wrote that the first artificial insemination occurred in the horse in 1322 A.D., when an Arab chieftain stole the semen from a rival's stallion, and transferred the contents to his own mare who went on to produce a live foal eleven months later [72]. However, the first reliable published account of artificial insemination in the horse was in 1897 by Sir Walter Heape [73].

Despite the long-standing interest in assisted reproduction in the horse, in vitro fertilization (IVF) in this species is still notoriously unsuccessful. Production of equine IVF embryos was first reported in 1989 [74], but the process was inefficient and few successful attempts have been reported since [1, 75-78]. In these subsequent reports, the maximum fertilization rate was 36%; however, these methods have not been repeatable; with the exception of two reports from a German laboratory [4, 5], subsequent reports from the same laboratories have not produced equivalent results.

The methods used for equine IVF have varied among studies, although some techniques have been utilized by multiple groups. For example, several groups used penicillamine, hypotaurine and epinephrine (PHE), compounds which were thought to prevent loss of sperm motility over time, and have been a standard component in the fertilization medium, TALP [4, 5, 79]. Calcium ionophore A23187, a compound that facilitates calcium influx into the sperm, was used by multiple groups [1, 2, 5, 77, 80]. Heparin was also utilized regularly as it has been shown to aid in capacitation of bull sperm, possibly due to its ability to induce intracellular alkalinization, although its role in IVF in humans is debatable [4, 5, 10, 81]. Del Campo et al. used a high concentration of bicarbonate (37 mM), which may have aided in capacitating the sperm through intracellular alkalinization [79]. Lastly, several groups used frozen-thawed sperm, as this process is thought to induce changes similar to capacitation in the sperm [1-5, 82].

Failure of equine IVF to be successful appears to be related to the failure of equine sperm to penetrate the zona pellucida in vitro: when the zona pellucida is breached by partial ZP dissection or by partial dissolution using acid medium, high

fertilization rates and even polyspermy result [83, 84]. The binding and fusion of sperm to the oocyte plasma membrane in these cases suggests that sperm capacitation, that is, preparation of the sperm head for fertilization, may be at least partially adequate using the capacitation techniques in these reports. However, failure of sperm to penetrate the zona pellucida indicates that capacitation is incomplete; this finding could be due to either failure of the acrosome reaction or to the failure of induction of hyperactivated motility. True capacitation of equine sperm has not been achieved because the sperm require pharmacological manipulation to achieve fertilization, however, for simplicity, sperm incubated under conditions promoting protein tyrosine phosphorylation will be designated "capacitated", whereas sperm not exposed to these conditions will be designated "non-capacitated."

Recently, McPartlin et al. [6] obtained an in vitro fertilization rate of 61%, by far the highest ever reported for equine IVF. This group first analyzed the effects of procaine on both non-capacitated and capacitated equine sperm using CASA sperm analysis. Capacitated sperm were those incubated for 6 h in a standard capacitation medium containing protein, bicarbonate and calcium. They noted that procaine treatment of non-capacitated sperm resulted in an increase in lateral head amplitude (ALH), as well as a decrease in linearity (LIN) and straightness (STR). When capacitated sperm were treated with procaine, the sperm had a similar motility pattern, but did not travel as far as did procaine-treated non-capacitated sperm. A decrease in VSL, LIN and STR were noted after procaine treatment of capacitated sperm. However, ALH was not significantly increased in these sperm after procaine treatment, suggesting

that capacitated sperm respond differently to procaine than do non-capacitated sperm. They noted that procaine did not affect PY in either capacitated or non-capacitated sperm.

To perform IVF, this group incubated the sperm for 6 hs in the basic capacitation medium described above before adding sperm to oocyte-containing droplets. Procaine was added to the sperm-oocyte co-incubation medium; while procaine is toxic to oocytes, the authors hypothesized (Bedford-Guaus, personal communication, 2010) that the cumulus cells of the oocytes served to protect the oocytes from the toxic effects of procaine. Overall, a fertilization rate of 61% was achieved using a total of 80 oocytes, as determined by either cell cleavage or the formation of two pronuclei. Capacitated sperm which were not exposed to procaine treatment did not fertilize any oocytes, and neither did non-capacitated sperm which were exposed to procaine. The success of this procedure in promoting equine IVF suggests that the block to IVF in the horse using standard capacitating procedures is failure of sperm to spontaneously undergo hyperactivated motility. Although the paper of McPartlin et al. was published in 2009, the same level of fertilization has not been reported by others using this protocol, which may indicate that repeatability of the procedure is still a problem.

In 2011, a group from Italy presented a brief report outlining success (19% embryo development to the 8-cell stage) using a similar capacitation procedure but treating to induce hyperactivated motility using follicular fluid instead of procaine [85]. However, it is not clear whether the follicular fluid, in fact, induced hyperactivated motility, or had other effects on the sperm or oocyte. In 2013, a group from France

achieved a 37% fertilization rates using the same technique as outlined by McPartlin et al. [6]. The fertilization rate rose to 62% when the oocytes were incubated in post-ovulatory oviductal fluid for 30 min prior to fertilization [86]. However, this group did not perform IVF without procaine addition, so the role of procaine in these results is unclear. Ambruosi et al. hypothesized that the protein deleted in malignant brain tumor 1 (DMBT1) was responsible for the increase seen in fertilization after exposure to oviduct secretions, as DMBT1 was found in both equine and porcine oviductal secretions, and exposing porcine oocytes to DMBT1 for 30 min prior to fertilization (equine oocytes were not studied) resulted in a significant increase in fertilization rates.

The above results highlight the two basic components of successful preparation of sperm for in vitro fertilization that comprise capacitation: adequate preparation of the sperm head to allow it to undergo the acrosome reaction in response to the correct stimulus, and to fuse with the oocyte plasma membrane after ZP penetration; and properly-timed induction of hyperactivated motility, essential to the movement of the sperm through the zona pellucida. The Suarez laboratory at Cornell University has pioneered the investigation of these two components as separate entities, primarily in bovine and murine sperm: in these species, proper environmental conditions for capacitation eventually lead to the induction of hyperactivated motility. However, notably, this motility can also be induced in non-capacitated sperm with appropriate stimuli such as procaine [87].

ULTRASTRUCTURAL ANATOMY OF THE SPERM FLAGELLUM

The above findings underline the importance of hyperactivated motility in fertilization. To understand the mechanisms regulating hyperactivated motility, we must understand the anatomy of the sperm flagellum, and the basics of activated (normal) sperm motility.

The sperm flagellum can be divided into four sections; the connecting piece, the midpiece, the principal piece and the end piece [88]. The entire flagellum of stallion sperm, beginning immediately distal to the proximal centriole in the connecting piece and continuing the entire length of the flagellum, contains the 9 + 2 microtubule structure seen in all eukaryotic flagella. This includes nine outer microtubule pairs known as the outer doublets which surround one inner pair of microtubules. These outer doublets each consist of an A microtubule and a B microtubule and are numbered 1 – 9 [89]. Microtubule nomenclature is determined by drawing an imaginary line down the central axis of the axoneme, directly between the central pair which consists of two microtubules known as C1 and C2. The outer doublet dissected by this line is numbered "1", and the remaining numbers ascend in the direction of the dynein arms (Figure 1.1).

The outer doublets are connected to the adjacent outer doublets by protein-rich nexin links, and are connected to the inner sheath which surrounds the inner microtubules via the radial spokes [90]. Each of the nine outer doublets possesses both inner and outer dynein arms, described in detail below, which are responsible for generating the driving force of the flagellum. Surrounding the outer doublets are the outer dense fibers (ODFs), passive elastic structures composed of cysteine- and proline-

rich intermediate filament-like proteins and are associated in a 1:1 ratio with the outer doublets.

The connecting piece, so named because it connects the flagellum to the sperm head, is one of the first sections formed during spermiogenesis. It is a short piece which contains the proximal centriole in mature sperm [88]. The proximal centriole is involved in the assembly of the connecting piece and also plays a role later in development when it is engulfed by the oocyte during fertilization and becomes the aster which draws the female pronucleus towards the male pronucleus [91]. In the mouse and rat, the entire proximal centriole degenerates during epididymal transit, and centrosomal inheritance is entirely maternal [92-94]. Paternal inheritance of the centrosome seems to be conserved over the remaining mammalian species, including rhesus monkeys, humans, sheep, and bull [95-97]. The status of the proximal centriole in stallion sperm and its role in fertilization is not currently known.

The midpiece immediately follows the connecting piece and is easily distinguished by an increased girth due to the presence of the mitochondrial sheath [90]. This sheath consists of helically-arranged mitochondria which surround the axoneme and outer dense fibers. The annulus marks the transition from the midpiece to the principal piece, and is distinguished by the cessation of mitochondria as well as the replacement of the ODFs associated with microtubule doublets 3 and 8 with the longitudinal columns of the fibrous sheath (Figure 1.1). Additional support for the fibrous sheath comes from circumferential ribs, extensions of the fibrous sheath which wrap around the sperm's circumference. At the distal end of the principal piece, the

ODFs and FS taper off, leaving only the axoneme surrounded by the plasma membrane, a short segment known as the end piece (review, [98]).

The fibrous sheath may play a large role in sperm motility, as it serves as scaffolding for a number of metabolic enzymes and signaling molecules associated with sperm motility [99]. Unsurprisingly, this structure is rich in A-kinase anchor proteins (AKAP) family proteins which are integral in securing various enzymes and proteins in place. It has also been hypothesized that the fibrous sheath helps protect sperm from oxidative stress due to the presence of a mu-class glutathione-s-transferase [100].

The dyneins are ancient ATPases which are highly conserved throughout flagella and cilia [101]; dyneins were first discovered in 1963 by Gibbons who was working with *Tetrahymen* cilia [102]. The dyneins are considered the force-generating structure of sperm, as well as cilia. Dyneins consist of 2-3 heavy chains, known as α, β and γ subunits, as well as intermediate and light chains which aid in attaching the dyneins to the A microtubule [103-105].

Dyneins work as minus-end motors; they attach to the A tubule in an ATP-independent fashion, and appear to walk in a hand-over-hand fashion, with the two heavy chains repeatedly binding and releasing the B microtubule while moving toward the minus-end of the microtubule [106]. To accomplish this, the microtubule binding domain (MTBD) of the dynein binds to the B tubule and the linker region of the heavy chain undergoes a conformational change which generates a winch-like movement of the head, this force-generating movement is known as the powerstroke [107, 108].

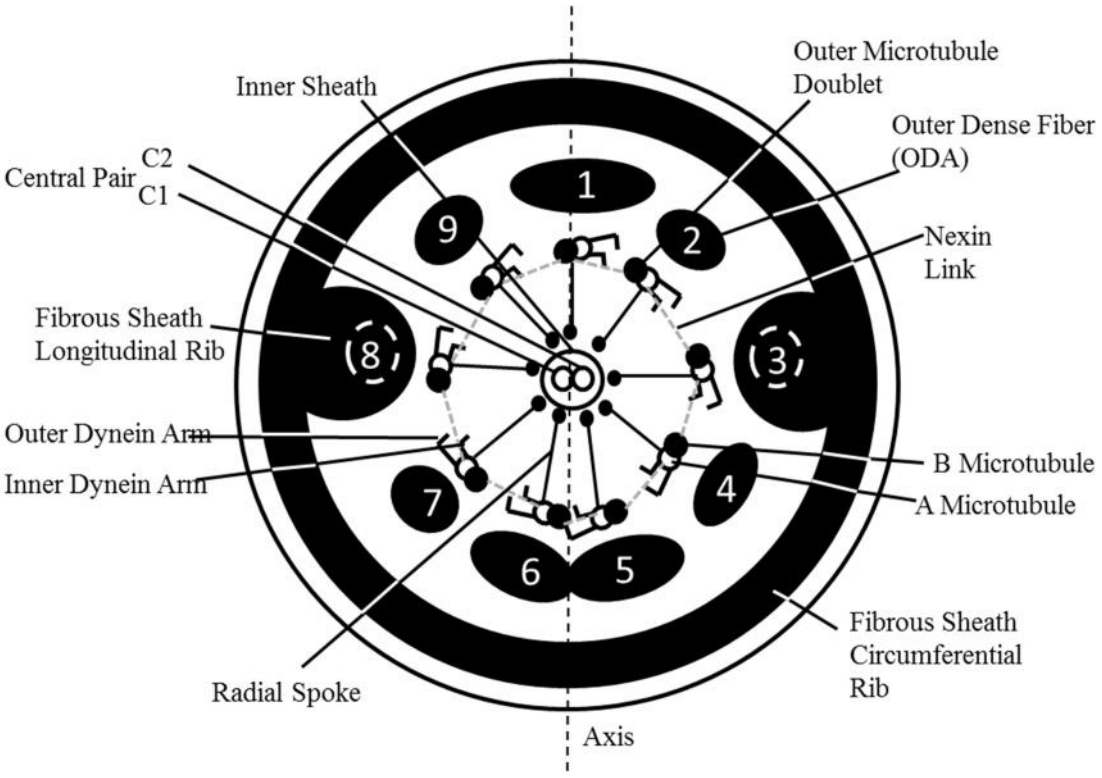

Figure 1.1. Ultrastructure of the sperm flagellum. The axoneme of sperm cells consists of a 9 + 2 microtubule structure, with 9 outer microtubule doublets surrounding a central pair of microtubules. The outer doublets are numbered by drawing a line along the axis, dissecting the central pair. The doublet intersected by the line is considered number 1, with the numbers increasing in the direction of the dynein arms which are connected directly to the A tubule. Each of the outer microtubule doublets consists of an A and B microtubule and is connected to the surrounding microtubule doublets via nexin links, and to the inner sheath by radial spokes. The outer dense fibers are passive elastic structures which are associated with the outer microtubule doublets and numbered correspondingly. At the initiation of the principal piece, the 3 and 8 ODFs are replaced by the longitudinal ribs of the fibrous sheath. Figure adapted from Afzelius, 1988, and Turner, 2003.

Each heavy chain consists of six AAA domains, the site of conformational changes to induce the powerstroke. Because the microtubules are fixed within the axoneme by nexin links, microtubule sliding on one side of the axoneme causes lengthening of that side, generating sufficient force to induce axonemal bending; (Figure 1.2) [107, 108].

Although the dynein motor domain is the structure which physically binds to the microtubule and induces motility, the light chains also appear to be involved in regulating motility [109, 110]. Specific proteins associated with the light chains, such as Tctex2, are phosphorylated in the presence of cAMP when motility is initiated [109] and known motility regulator, calmodulin, has been shown to be bound to the light chains of outer-arm dynein [110]. The intermediate chains appear to be primarily involved in binding the dynein to the A microtubule [111].

The central pair of microtubules is believed to determine the plane of bending, as the C1 microtubule is oriented towards the direction of active sliding [112]. The radial spokes may also play a role in controlling motility, as they have been shown to regulate inner arm dynein activity through protein phosphorylation/dephosphorylation [113]. These changes are possibly mediated through a cAMP-dependent kinase or through calmodulin, both of which are anchored to the radial spokes [114, 115].

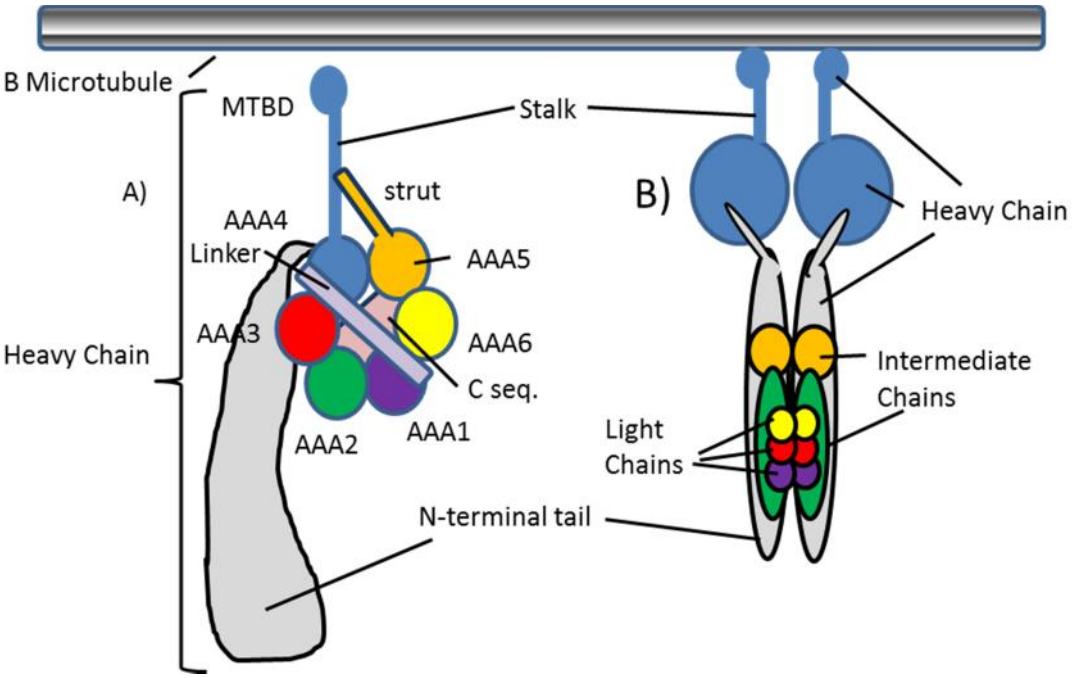

Figure 1.2. Dynein structure. The model (A) shows the dynein motor domain, along with the N-terminal tail, also known as the heavy chain. This model includes the linker which is thought to act as a winch to generate force, the C terminal sequence, the microtubule binding domain (MTBD) and the AAA sequences, thought to act as ATP cleavage sites. The linker changes binding location depending on the state of the dynein; this model shows the un-primed state, with the tip of the linker in close proximity to AAA4, however, in the primed state, it can be found proximal to the AAA2 domain. (B) Contains the entire structure of the dynein, including the intermediate and light chains. This figure depicts a dynein with two heavy chains. Figure modified from [101, 116, 117].

CHAPTER II

LITERATURE REVIEW

DEMEMBRANATED SPERM

The first study on demembranated cells was published in 1949 by Szent-Gyorgyi who used glycerol to strip the membrane from skeletal muscle cells and was able to perform elegant experiments demonstrating the central role of ATP and calcium in muscle contraction [118]. In 1955, Hoffman-Berling used glycerol to demembranate sperm, but were unable to achieve coordinated motility [119]. The first successful restoration of movement in demembranated sperm was achieved by Brokaw and Benedict in sea urchin sperm using glycerol [120]. Subsequently, Gibbons and Gibbons showed that use of Triton X-100 to demembranate the sperm in place of glycerol supported restoration of normal flagellar activity [121]. This model was widely used in the 1970s to analyze the basic forces which directly affect the axoneme. By perforating the plasma membrane, demembranization allows the axonemal environment to be rigidly controlled simply by altering the bathing medium, permitting observation of the effects of min changes in environment on sperm motility without interference from plasma membrane components such as ion channels.

Historically, there has been little or no consensus on the ideal protocol for demembranating sperm. Although Triton-X 100 is the most commonly used method of sperm demembranization, concentrations used vary greatly from 0.2% to 0.04% (v/v) [122-125].

ATP has been shown to be an absolute requirement for reactivation of demembranated sperm, and requires a divalent cation, typically magnesium, to exert its action [126]. If ATP is not present in the medium, the sperm will not reactivate regardless of the other substrates contained in the medium [122, 127, 128]. This is logical, as dyneins hydrolyze ATP molecules to ADP to create energy to induce conformational changes, which allows flagellar beating to occur [129]. Without ATP, the dynein arms are unable to complete the power stroke and the flagellum remains immotile.

The role of cAMP in sperm motility is less clear; it appears to be required for reactivation in some species, but its effects vary widely. It has been reported in the hamster [130, 131], and boar [130] that sperm will not regain motility until cAMP is added to the media. In several other species, including human [132], dog [133] and ram [134], cAMP does not appear to be an absolute requirement, but does increase motility parameters such as beat frequency and % total motility. In the dog, cAMP appears to exert its effect through a protein which is soluble in NP-40, a non-ionic detergent, and which appears to be highly conserved among species [133]. In this study, cAMP was unable to increase motility in the absence of this NP-40 soluble protein; however, adding the NP-40 extracted fraction of human, sea urchin or Chlamydomonas flagella allowed the original sperm to regain their responsiveness to cAMP. In demembranated bull [122] and rabbit sperm [135], cAMP did not affect any motility parameters. Cyclic AMP thus affects motility parameters in certain species, but this effect is not universal. Interestingly, the effect of cAMP may relate to the treatment of sperm before

demembranization. In the hamster, it has been shown by several laboratories that sperm exposed to calcium before demembranization do not require cAMP following demembranization; it appears that exposure to calcium allows intact sperm to produce adequate cAMP to activate the pathways necessary for later motility [136]. Therefore, the apparent differences in requirement for cAMP seen among species may relate to both the method of sperm collection (from the epididymis or ejaculated) as well as how the sperm is handled post-collection (presence or absence of calcium in medium).

Calcium is required for motility activation of intact sperm in the mouse, rat, hamster and bull [22, 136-138]. In hamster sperm, epididymal sperm are only weakly motile until they are exposed to medium containing 3 mM extracellular calcium, at which point motility is maximized [136]. Epididymal bovine sperm also require extracellular calcium to gain motility [137]. In 1978, Morton et al. [138] analyzed the calcium concentrations within the epididymis of rats, mice and hamsters and found a positive relationship between epididymal calcium concentrations and epididymal sperm motility.

The requirement of demembranated sperm for calcium appears to be species specific. Addition of 50 μM free calcium is required to stimulate motility in demembranated bull sperm [139]. Total motility in this model dropped significantly from 55% to 25% when free-calcium was reduced to <1 nM by extending sperm in medium containing 2 mM EGTA and no added calcium. In the bull, increasing free-calcium levels results in an increase in hyperactivated motility without change in total motility [122]. In this study, increasing free-calcium levels from 50 to 1000 nM resulted

in a dose-dependent increase in the percent of hyperactivated sperm. Other species which experience an increase in hyperactivated motility parameters in response to increasing calcium levels include mouse, rat, monkey and sea urchin sperm [124, 140-142].

In many species including the mouse, rat and sea urchin, excessive calcium levels in demembranated sperm induce quiescence marked with a significant flagellar bend, known as a "curlicue," "fish hook" or "candy cane," respectively [122, 140, 143-147]. In the rat and mouse, this curvature has been shown to be initiated when the dyneins on doublets 1 through 4 are arrested in the fully activated position [148-150]. These are also the dyneins which are dominant in calcium-induced asymmetrical beating. The calcium-induced curvature of rat sperm has been shown to be inhibited by vanadate, a substance which inhibits dynein-tubulin cross-bridge cycling, further supporting the involvement of dyneins in the calcium-induced curvature [140, 151, 152]. This curvature is inhibited by both nickel and cadmium; in mouse sperm, the curlicue configuration is relaxed by the presence of both nickel and cadmium until the sperm exhibit only a mild bending [140]. Human sperm appear to be more sensitive to high calcium concentrations than are sperm of other species, as demembranated human sperm experience a decline in motility at free-calcium levels as low as 500 nM [153], as compared to demembranated bull, mouse and rat sperm which do not experience a decrease in motility until exposed to 1 mM free calcium, a 2000-fold difference [122, 125, 142].

Medium pH is an important factor in the motility of demembranated sperm, as seen in human and bovine sperm [122, 154, 155]. In bovine sperm, motility is initiated at pH 6.5, is maximal from pH 7 to pH 8 and the sperm become fully immotile by pH 10.5 [122]. This sensitivity to pH appears to be due primarily to the outer dynein arms, as human sperm lacking the outer dynein arms are insensitive to increasing pH [155]. To determine this, sperm were demembranated then reactivated in bathing medium at either pH 7.1 and 7.8. Sperm lacking outer dynein arms did not exhibit a higher level of reactivation at pH 7.8, as was seen in control sperm. A pH-dependent increase in hyperactivated motility parameters has not been seen in demembranated sperm, despite the integral role of intracellular pH in hyperactivation in intact sperm [156]. This suggests that the role of the increase in intracellular pH in hyperactivation may be to signal membrane-related proteins, such as the CatSper calcium channel, discussed below, rather than to stimulate the axoneme directly.

Both nickel and cadmium severely inhibit motility of demembranated bull and rat sperm [140, 150, 157]. In the rat, Lindemann and Goltz [140] found that nickel completely inhibited motility at 200 µM, while doses of cadmium as low as 1 µM cadmium were able to severely inhibit motility, but complete inhibition was not seen. The inhibition by cadmium appeared to be dose-dependent, however high doses of cadmium could not be evaluated as, when cadmium was raised to 30 µM, sperm began to disintegrate. In demembranated bull sperm, nickel has been shown to inhibit spontaneous axonemal wave *initiation*; interestingly, if a wave was initiated by inducing a bend between two fixed points of the flagellum via micromanipulation, the bend was

propagated as a wave along the flagellum distally [158]. Thus, nickel-inhibited sperm retained ATPase and dynein activity of at least a subset of microtubules, and underwent microtubule sliding, but lacked the ability to generate an initial bend without assistance. Without mechanical intervention, these sperm were irreversibly immotile. This suggests that in normal sperm motility, a mechanism exists to stimulate the development of the initial flagellar bend, which then is propagated essentially automatically distally down the axoneme via microtubule sliding.

In the technique known as microtubule extrusion, as described in [150], the mitochondrial sheath is disrupted significantly to allow the microtubule pairs to exit the fibrous sheath when the dyneins are activated. Therefore, in this technique, only microtubules which have active dyneins are seen outside the fibrous sheath. Using this model, both nickel and cadmium appear to exert their inhibitory effects specifically on the 9, 1, 2 bundle of doublets, as doublets 4, 5-6, 7 are extruded almost exclusively in demembranated sperm treated with nickel [150]. This effect appears to be due to a lack of inter-doublet sliding between microtubule doublets 2 and 3.

Despite their similarities, nickel and cadmium appear to have different mechanisms of action [140]. Nickel requires a significantly higher concentration to exert its effect, with studies using concentrations ranging from 200 µM to 1.33 mM [140, 159, 160], but cadmium is able to inhibit motility at concentrations as low as 1 µM [140]. Addition of EGTA to the medium is able to diminish the effect of nickel but not of cadmium, although both are strongly chelated by EGTA.

The inhibition of the flagellum by nickel appears to be due to an inhibition of the dynein α heavy chain [161]. In paramecium, nickel induced cessation of movement of 14S dynein, a detergent-isolated fraction containing only the α heavy chain [105]. This was determined evaluating the effect of nickel on sliding of isolated microtubules, as well as on ATPase activity of the dynein fractions [161]. Activity was regained following washing the cells with EGTA. 22S dynein, which is intact (has α, β and γ heavy chains) [105], was affected only slightly by the addition of nickel [161].

The action of cadmium is less clear; it has been suggested that cadmium works via a calmodulin-mediated effect [140, 162, 163], and, like nickel, has been shown to block sliding of the 9,1,2 microtubule doublets [150]. It is possible that cadmium serves as a calcium agonist or antagonist, depending on the system.

REGULATION OF INTRACELLULAR ENVIRONMENT

Pre-ejaculatory spermatozoa located in the epididymis are quiescent. This quiescence may be induced by the relatively acidic epididymal environment, as these conditions inhibit axonemal dynein activity [164-166]. Sodium concentration is also believed to be important in maintaining quiescence [167], and the concentration of sodium is much lower in the cauda epididymis compared to the seminal plasma (30 mM vs 100-150 mM, respectively). Calcium concentrations appear to be important as well; calcium concentration is lower in the epididymis (between 0.031 and 0.05 mM [168]) than in serum (0.94-1.33 mM [169]) and there is a direct correlation between epididymal calcium concentration and motility of sperm within the epididymis [138].

Once the sperm are ejaculated, they immediately gain activated motility due to the dramatic increase in pH, bicarbonate, sodium and calcium found in the seminal plasma [167]. The sperm axoneme may require basal levels of calcium to operate, as detailed above, at least in some species [170]. The mechanism by which calcium is required for motility is unclear. The calcium-adenylyl cyclase-PKA pathway in sperm has been shown to increase flagellar beat frequency, but has not been shown to be required for activated motility [171]. There is evidence that calmodulin is involved in stimulating activated motility in bovine sperm [139]. When calmodulin is removed from the fibrous sheath during demembranization, motility is fully inhibited and is not restored until calmodulin is reintroduced. Calmodulin requires calcium to be activated [139].

Activated motility requires a specific intracellular environment, including low sodium and high potassium concentrations which are achieved by sodium potassium ATPases [172]. Calcium concentrations within the sperm cell are kept between 50 to 100 nM due to a plasma membrane calcium ATPase pump (PMCA4) [27, 173, 174], and intracellular pH is maintained through the Hv1 channel, at least in human sperm [13, 175-177]. The HV1 channel is not present in the mouse, therefore Na^+/H^+ exchangers (sNHE), which also regulate intracellular pH, are hypothesized to be integral in this species [13, 178].

An increase in intracellular calcium plays a significant role in the induction of hyperactivated motility [179], a whip-like motility required for successful fertilization [19], which is described in further detail below. There appear to be two distinct calcium

signaling pathways in mouse sperm, one which is initiated via entry of extracellular calcium and one which is initiated when intracellular stores are released [180]. These can be appreciated because of the asymmetrical hook-shaped head of the mouse sperm. When hyperactivation is stimulated via extracellular calcium influx through the CatSper channel, standard hyperactivation occurs (i.e. pro-hook); however, when the calcium influx is initiated via the intracellular stores, a "reverse" hyperactivation occurs (anti-hook), where the direction of the dominant flagellar bend is the opposite from that seen during hyperactivation due to calcium influx. This difference in bending is thought to help the sperm redirect its path to more efficiently reach the oocyte. Surprisingly, sperm present in the oviduct of mice exhibit anti-hook bending, suggesting that calcium release from internal stores are involved in stimulating hyperactivated motility in vivo [33]. Clinical support for the role of calcium in motility comes from a study by Alasmari et al. [181], which found that sub-fertile men presenting at a fertility clinic are significantly less likely to have a normal influx of calcium in response to progesterone or 4-AP (inducers of hyperactivated motility), suggesting that the calcium pathways are intricately tied to fertilization.

Voltage-gated calcium channels such as $Ca_v2.2$, $Ca_v2.3$ and $Ca_v 3.1$ had originally been proposed to be the primary regulators of the calcium influx in sperm cells, however, mice deficient in these genes were able to display normal fertility, suggesting that these channels in and of themselves were not required for fertilization [182-184]. More recently, a sperm-specific calcium-selective cation channel known as

the CatSper channel [47] has been proposed to be the primary modulator of calcium influx during hyperactivation [185].

The laboratory of Dejian Ren, at the University of Pennsylvania, evaluated a CatSper knock-out mouse which has been invaluable in deciphering the functions of the CatSper channel [47]. In this primary study, the CatSper channel was shown to be localized to the principal piece of sperm and was not found in any tissue type except for testis and sperm. Ren et al. proposed that the CatSper channel was gated by cyclic nucleotides and voltage. Although this channel does respond to both these stimuli, it was later shown to be much more responsive to increases in pH [186]. When intracellular pH of mouse sperm is raised from 6.0 to 7.0, there is an approximately seven-fold increase in calcium influx [186]. It appears to be this calcium influx that triggers hyperactivated motility, as the sperm of CatSper-null mice do not show a calcium influx in response to alkalinizing conditions, do not exhibit hyperactivated motility, do not fertilize oocytes in vitro, and CatSper-null male mice are infertile when mated naturally [47, 185, 187].

Increasing intracellular alkalinization with NH_4Cl has been shown to increase intracellular calcium concentrations, as well as to induce hyperactivated motility [188]. Mice lacking a functional CatSper channel neither increase calcium influx nor hyperactivate in response to alkalinizing conditions [189]. The sensitivity of the CatSper channel to alkaline pH_i has been theorized to be due to the high concentration of histidines on the N-terminal domain [47, 190]. Blocking the CatSper channel with the proprietary molecule HC-056456 induces similar effects to those seen in CatSper-null

mice [187], and mutations of the CatSper gene in men are associated with infertility [191, 192].

The CatSper channel is made up of seven protein subunits; CatSper 1-4 physically form the channel complex, where CatSper B, CatSper D and CatSper G are auxiliary proteins [47, 185, 189, 193-195]. Of these, CatSper 1-4 and CatSper D have been shown to be essential for proper channel formation and function [185, 189]. Little is known about the three auxiliary proteins CatSper B, CatSper G and CatSper D, but CatSper B is predicted to have two transmembrane helices, whereas CatSper D and CatSper G are both believed to have a single transmembrane helix. All auxiliary proteins appear to have large extracellular domains, including an extracellular domain loop on CatSperB [189, 194-196]. Interestingly, when CatSper1 expression is knocked-out, the remaining six proteins cannot be detected in the resultant sperm, suggesting that all the subunits are required for proper channel formation. A similar reaction occurs when *CATSPER D* is missing [187, 189, 194, 195]. To date, none of the CatSper proteins have been successfully expressed in a heterologous system, even when all four CatSper channel proteins and CatSper B and G were expressed in combination with associated chaperone protein HSPA2 [189].

The CatSper gene is present in a wide range of species, however, identity among species is low, suggesting that regulation of the CatSper channel may vary widely among species [194, 196-198]. This is confirmed by the number of factors which stimulate the CatSper channel, including albumin, cAMP, cGMP, progesterone and PGE1, which have been shown to be species specific [196, 199-201]. Progesterone and

prostaglandin E1 specifically have been shown to stimulate the CatSper channel in human sperm, but not in mouse [200, 201].

Previous work in our laboratory has confirmed the presence of CatSper1 mRNA in the equine testis and spermatozoa by PCR, as well as by immunocytochemistry [202]. Reverse-transcription PCR confirmed the presence of *CATSPER1* mRNA within equine testes, while real-time PCR confirmed that mature equine sperm carry *CATSPER1* mRNA. It appears that *CATSPER1* mRNA is abundant in mature horse sperm, suggesting that the CatSper channel remains in these cells after spermiogenesis. Immunocytochemistry using an antibody raised against the C-terminus of the human protein showed specific staining of the principal piece in equine sperm. Additionally, increasing intracellular alkalinization in the equine sperm with ammonium chloride (NH_4Cl) induced hyperactivation in a dose-dependent manner, providing further support for a functional CatSper channel in mature equine sperm [202].

Recent work by Olson et al. has provided a mathematical model for the calcium mechanics during hyperactivated motility which suggests that the calcium influx through the CatSper channel itself is not sufficient to maintain hyperactivated motility [203]. Instead, the calcium influx initiated at the CatSper channel travels up the sperm flagellum to the redundant nuclear envelope and triggers a calcium-induced calcium release. It is unclear whether the calcium stimulates the IP3 receptor directly, by initiating the activation of PLC and therefore the breakdown of PIP2 to IP3, or by a combination of both. This model takes into account the parameters of calcium, IP3, the IP3 receptor and the secretory pathway calcium-ATPase. A later publication by the

same group breaks down the calcium kinetics in sperm while taking into account calcium dynamics from both the CatSper channel and IP3 calcium channels within a moving flagellum, the viscous fluid mechanics as well as the elasticity of the flagellum [204], and creates an inclusive equation to predict the swimming behavior of sperm.

PHYSIOLOGY OF HYPERACTIVATED MOTILITY

As described above, motility of spermatozoa is powered by the movement of the dynein arms which induce the sliding between pairs of outer doublet microtubules [102]. This basic process is powered by ATP hydrolysis occurring on the dynein heavy chains [205]. As detailed above, the requirements for initiation of activated sperm motility seem to be minimal, with ATP being the only consistent requirement for motility in demembranated sperm across all observed species, although there may be several species-specific requirements as well, including calcium, pH and cAMP [122, 124, 136, 137, 140, 141, 157, 206-209].

Hyperactivated motility was first characterized in 1970 in golden hamster sperm. Yanagimachi [19] reported that sperm seen within the oviductal ampulla were extremely motile, and he theorized that this motility aided the sperm in reaching the oocyte and penetrating its outer vestments. Further research has supported this theory, showing that when hyperactivated sperm are placed in a viscous medium similar to that encountered in the oviduct, their trajectory becomes straight and they are able to move through it more effectively than non-hyperactivated sperm [37, 210]. Additionally, sperm that are not hyperactivated appear to be incapable of penetrating the zona pellucida. In an

elegant study performed by Stauss et al. [46], capacitated hamster sperm were allowed to bind to the zona pellucida, at which point calcium channel blockers were introduced, preventing hyperactivated motility. This effectively inhibited penetration, with only 1% of oocytes being fertilized compared to 63% of controls.

Hyperactivated motility is characterized by rapid, whip-like motion of the sperm tail, which causes an increase in the amplitude of lateral head movement when sperm are in a medium with low viscosity. This results in a star-like or circular motility pattern, and methods to use the bounding square of a sperm trajectory track as a measure of hyperactivated motility have been developed [211]. In species where adequate sperm numbers can be obtained, motion characteristics are commonly analyzed using Computer Assisted Sperm Analysis (CASA). This system measures a minimum of nine different parameters to assess motility, of which five are commonly used to categorize hyperactivation, including an increase in curvilinear velocity (VCL) and lateral head amplitude (ALH), and a decrease in progressive (straight-line) velocity, linearity and straightness. In bovine sperm, increased VCL and ALH have been used to define hyperactivated motility [87]. Use of a decrease in straight-line velocity, linearity and straightness alone to characterize hyperactivation can be problematic, as these values also decrease as sperm are dying.

Recently, it was discovered that, even though hyperactivation spontaneously occurs when sperm are fully capacitated, the acts of hyperactivation and capacitation are controlled by two different or divergent signaling pathways [87]. Capacitation is widely believed to be partially due to the high levels of bicarbonate found in the oviduct, which

is known to stimulate soluble adenylyl cyclase (sAC) activity, which in turn increases the production of cAMP in a pH-dependent manner [212]. This increase in cAMP triggers the activation of protein kinase A (PKA), which is involved in a number of cellular functions including serine/threonine phosphorylation and the subsequent protein tyrosine phosphorylation [213]. Serine and threonine phosphorylation has been shown to increase following hyperactivation induced by 4-AP or procaine [180]. Both serine and threonine phosphorylation were found to occur on the principal piece of sperm, however, serine phosphorylation is concentrated primarily at the base of the flagellum. The localization of this phosphorylation on the principal piece suggests a role in serine/threonine phosphorylation in the regulation of motility.

This bicarbonate/sAC/PKA pathway has also been implicated in increasing flagellar beat frequency (Figure 2.1). In this pathway, bicarbonate induces an increase in intracellular pH which leads to an increase in intracellular calcium, as well as stimulating sAC activity which then stimulates PKA [27]. Bicarbonate-induced sAC activity has been shown to increase flagellar beating and sAC itself can be activated directly by calcium [171, 214, 215]. PKA has been shown to increase phosphorylation of the axonemal dyneins, which increases beat frequency as well [209, 216]. Despite these actions in the mouse, PKA does not appear to be required for the initiation of activated sperm motility as mouse sperm lacking cAMP-dependent PKA still maintain normal activated motility in vitro [217]. Along similar lines, sperm lacking soluble adenylyl cyclase are able to swim normally, but do not experience an increase in

flagellar beat frequency or a rise in intracellular calcium levels in response to extracellular bicarbonate [218]

Although the bicarbonate/sAC/PKA signaling pathway increases flagellar beat frequency, this pathway is likely redundant and its role in motility may be species specific. The inhibition of cAMP or PKA does not significantly inhibit either activated motility or hyperactivated motility stimulated by caffeine or procaine [87]. Additionally, as noted above, the role of cAMP in sperm motility is controversial, with some researchers stating it is essential for sperm motility [128, 157, 207, 208, 219], while others have found that the effect of cAMP is calcium dependent, and only affects motility at calcium levels of 10^{-7} and below [124], and others report it has little to no effect on motility or hyperactivation under any circumstances [122].

An increase in intracellular pH (pH_i) and intracellular calcium levels are associated with hyperactivated motility (Figure 2.2). As pH_i increases, dynein activity is stimulated, effectively increasing the flagellar beat frequency of the sperm [155]. While no relationship between bath medium and hyperactivated motility has been shown in demembranated sperm, as noted above, it appears that the outer dynein arms are sensitive to pH. Both sperm with and without outer dynein arms were dependent on ATP concentrations for activation at pH 7.1; however, at pH 7.8, demembranated sperm lacking outer dynein arms were still reliant on ATP, whereas control sperm were not [155]. A similar phenomenon was seen in a study in the bull [209]. In this study, demembranated sperm exposed to an alkaline environment (7.4 - 7.8) were much less

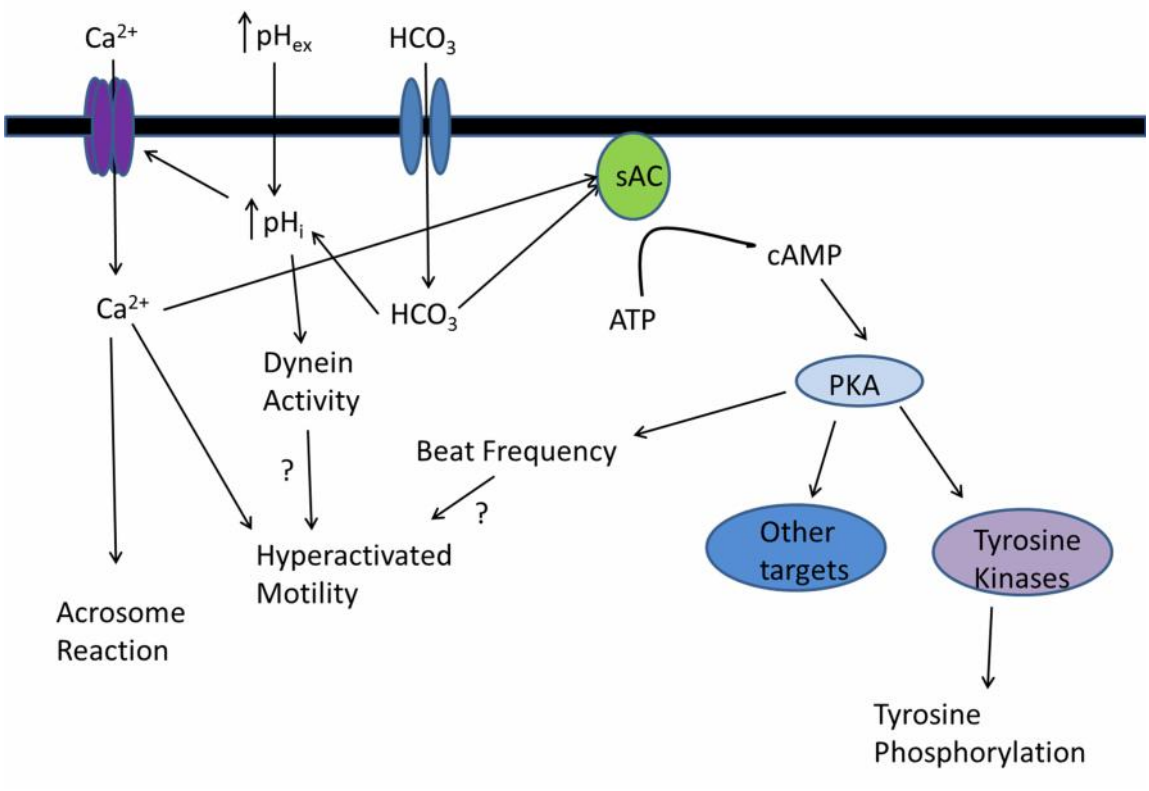

Figure 2.2. Factors affecting capacitation and hyperactivated motility. This figure depicts a simplified version of the PKA pathway which is believed to be involved in stimulating protein tyrosine phosphorylation and may be involved in hyperactivated motility. Figure modified from [220, 221].

reliant on cAMP and ATP concentrations for reactivation and flagellar beat frequency than those reactivated in a more acidic environment (pH 6.6 - 7.1).

The differing sensitivity of axonemal microtubules and dyneins to pH likely plays a role in the asymmetrical flagellar beating seen during hyperactivation. The dynein arms on certain microtubule doublets appear to have differing responses to environmental stimuli [148]. Rat sperm were demembranated, then exposed to either high pH (pH 9 at 4°C) or to high temperature (pH 7.8 at 37°C) until microtubule sliding occurred. In sperm treated with high pH, microtubule doublets 4-7 were preferentially extruded, whereas doublets 9, 1 and 2 were extruded following incubation at 37°C. The 9-1-2 bundle was frequently observed in a hook-like shape, such as is commonly seen in response to excess calcium, although the extrusion did not appear to be calcium-sensitive in this study.

Mechanisms which induce hyperactivated motility commonly do so by inducing either intracellular alkalinization or by directly inducing calcium influx. Thus, hyperactivated motility typically seen following capacitation is likely to be induced by the intracellular alkalinization which occurs during standard capacitation. Treatment of bovine sperm with high-pH medium or with NH_4Cl (a weak base that raises intracellular pH) also induces intracellular alkalinization, and can result in hyperactivated motility independently of capacitation [188]. However, because of the lack of direct effect of pH on hyperactivation in demembranated sperm, the effect of increasing intracellular pH probably is exerted via induction of changes in the intracellular environment, most notably by opening of the CatSper channel, which is pH sensitive. Interestingly, the

hyperactivating effect of progesterone appears to be via a non-genomic progesterone receptor which opens the CatSper channel, as calcium influx induced by progesterone is identical to that induced by direct CatSper channel effectors [200] and blockage of the channel inhibits the effect of progesterone [201]. Progesterone is able to induce calcium influx in human sperm, but not in mouse sperm, a phenomenon which suggests regulation of the CatSper channel may vary widely between species [201]. Capacitation increases the responsiveness of the progesterone receptor, but it is still unclear whether this is a response of the CatSper channel itself, or of an associated receptor molecule.

As discussed above, the molecular pathway of induction of hyperactived motility by calcium is unclear. Results of evaluation of different pathways appear to differ among species, and even within species, such as the mouse, protein phosphorylation patterns differ in sperm activated via external or internal calcium sources [180]. Roles of cAMP, cAMP-dependent kinase (protein kinase A), protein kinase C, phospholipase D, pyruvate dehydrogenase A, serine/threonine phosphatases, and serotonin, among others, have been presented without an overall consensus; some findings differ, either by species or due to differences in experimental protocol [222-230].

Very little is known about the role of calmodulin and its associated kinases in hyperactivated motility. Ignotz and Suarez [139] showed that calmodulin was required for motility in demembranated bovine sperm. Additionally, these authors reported that inhibition of calmodulin-dependent protein kinase II (CAMK2) and/or calmodulin-dependent protein kinase IV (CAMK4) by KN-93 inhibited hyperactivated motility in demembranated sperm without affecting activated motility. The KN-93 also inhibited

caffeine-induced hyperactivation in intact bovine sperm. This finding suggests a role of CAMK2/4 in hyperactivated motility.

CAMK2 and CAMK4 are serine/threonine kinases which are activated by calmodulin and have been implicated in the regulation of flagellar and ciliary motility [231, 232]. The CAMK4 has been localized to the flagellum of human sperm, and ATP levels dropped significantly following inhibition of CAMK4 with KN-62 or KN-93, suggesting that CAM kinase inhibitors decrease motility by reducing ATP availability, or by an increased consumption of ATP in other pathways. These authors concluded that the effect of KN-93 was specific to CAMK4 in human sperm, as CAMK2 was not found via Western blot or immunocytochemistry of human sperm. Here, CAMK4 appeared to be involved in the regulation of activated motility over time. In this trial, motility was not analyzed immediately following exposure to KN-62 or KN-93, but instead one to eighteen h later and % motile sperm were reported over time.

Other membrane channels beyond the CatSper channel play a role in controlling sperm motility by maintaining the intracellular environment. These include the Slo3 channel, a pH-sensitive potassium channel which is thought to be responsible for the I_{KSPER} current in sperm. This current is the only detectable hyperpolarizing current in sperm, and as such, plays a large role in the function of all voltage gated channels in sperm [233]. The *Slo3* -/- mice have been found to have minor defects in motility which include lower average path velocity and linear velocity than WT mice, as well as significantly lower progressive motility [234, 235]. Additionally, *Slo3* -/- mice are infertile and their sperm do not hyperpolarize during capacitation [234].

The Hv1 channel, a voltage-gated proton channel found in human sperm, also plays an important role in capacitation [13, 236, 237]. This is a unidirectional channel which rapidly conducts protons to the extracellular space [236]. This is essential during activated motility, as a high level of lactic acid is produced during glycolysis in the sperm tail [238-240]. Zinc inhibits the Hv1 channel at low micromolar concentrations; therefore the relatively high concentration of zinc in human seminal plasma likely helps prevent premature capacitation [177]. The gene coding for the HV1 channel is present in the mouse (*VSOP*), as this channel is found in many cell types, notably macrophages [241]. However, the channel does not appear to be present in mouse sperm [13]. There is no current corresponding with HV1 present in mouse sperm [13], and the *HV1* knock-out mouse is fertile [242].

HYPERACTIVATION IN STALLION SPERM

Information on hyperactivation of stallion sperm has been notable primarily by its absence. In 2001, Rathi et al. [243] performed a flow-cytometric study of sperm capacitation, comparing the standard capacitation assessment technique, chlortetracycline (CTC) staining of fixed cells, with staining with merocyanine 540 and FITC-PNA, followed by flow-cytometric analysis in an attempt to create a more user-friendly assessment of capacitation in stallion sperm. In addition to static capacitation analysis, changes in motility of stallion sperm during capacitation were analyzed via CASA. Despite seeing a *decrease* in hyperactivated motility parameters following "capacitation" (60% before capacitation, compared to 30% following capacitation), this

group was the first to propose that CASA values of VCL ≥ 180 and ALH ≥ 12 denoted hyperactivation of stallion spermatozoa.

Some specific factors have been shown to increase hyperactivation-related motility parameters in stallion sperm. These include estrogen-like mycotoxins, which were found to increase ALH in stallion sperm while reducing straight-line velocity and linearity [244]. Three mycotoxins were studied (zearalenone, α-zearalenol, β-zearalenol) and results were compared to those for 17-β estradiol. Only β-zearalenol did not induce some level of hyperactivated motility; however, effects were weak from all compounds studied. Only the highest concentration tested (0.1 mM) of any compound exerted an effect, so it is possible that higher doses would exert a more significant effect. Lange-Consiglio and Cremonesi found indications of hyperactivation (decrease in straightness parameters) in stallion spermatozoa exposed to follicular fluid from preovulatory follicles [85].

A slight increase in hyperactivated motility parameters has been noted after cryopreservation [245]. Overall sperm motility declined significantly (70% to 11%); however, the sperm which maintained motility following cryopreservation were significantly more likely to exhibit increased VCL and VSL, although this may be due to the erratic response of these parameters when total motility is low.

McPartlin et al. [6] induced hyperactivated motility using 5 mM procaine, as detailed previously under IVF in the Horse In their study, procaine induced a significant increase in ALH and a significant decrease in straightness and linearity, whereas after incubation in modified Whitten's medium for "capacitation", procaine induced

significant decreases in straight-line velocity, straightness and linearity. Because the motility induced after capacitation was associated with successful fertilization, these authors considered this motility to represent true hyperactivated motility in stallion spermatozoa. However, as noted previously, using only decreases in motility parameters can be misleading as these values also decrease with sperm death.

A recent publication confirmed that procaine induced hyperactivation of sperm after capacitation in a modified Whitten's medium, increasing ALH while decreasing straightness parameters [246]. In this study, the only article which examines the effects of various compounds on hyperactivation of stallion sperm specifically, Ortgies et al. [246] examined the effect of two separate media, modified Whitten's (MW) and modified Tyrodes (MT), as well as three separate agents known to affect motility parameters in sperm; procaine, pentoxifylline and trolox, a vitamin E analog. Procaine had previously been shown to induce hyperactivation in stallion sperm [6], while pentoxifylline increases hyperactivated motility parameters in human sperm [247] although not in horses [248]. Trolox had been shown to aid in preserving stallion sperm motility over time [248]. There was no significant difference in motility parameters with either media examined; however, MW maintained a higher proportion of viable, capacitated sperm, as measured by merocyanine 540. Hyperactivation was induced only by procaine, however pentoxifylline increased the proportion of viable, capacitated sperm after capacitation, as assessed by merocyanine 540 staning. Trolox had no effect on either motility or capacitation. The authors concluded that MW medium combined

with procaine, as described in [6], provided the best conditions for in vitro fertilization in stallion sperm.

Procaine, the compound associated with successful fertilization in the study of McPartlin et al., works as a local anesthetic via its action as a sodium channel blocker [249]. It also has effects on internal calcium stores, inhibiting calcium release from the endoplasmic reticulum via its inhibitory effect on ryanodine receptors [250], and is a weak base, thus causing intracellular alkalinization [251]. Procaine has numerous other less well-defined cellular activities, which may include displacement of calcium at the membrane level [252] or a direct effect on membrane calcium permeability [253]. The actions of procaine that induce hyperactivated motility are essentially unknown.

Carlson et al. [254] found that 10 mM procaine increased flagellar beat asymmetry in CatSper2 null mutant mice, indicating that there was a partial rescue of hyperactivation in these mice, which are unable to hyperactivate spontaneously. Marquez et al. [255] studied this phenomenon later, and concluded that this motility was not truly hyperactivation. These authors found that only CatSper wild-type mice responded to procaine. Thus, it is unclear whether procaine requires the CatSper channel to exert its effects.

CONCLUSIONS AND AIMS

The finding of McPartlin [6] that pharmacological stimulation of hyperactivated motility was associated with high rates of equine in vitro fertilization suggests that standard capacitating regimens fail to initiate this vital aspect of capacitation in the

horse. This, in turn, suggests that the mechanisms governing sperm hyperactivated motility in the horse differ from those of other species.

The studies presented in this dissertation aimed to evaluate for the first time factors associated with control of hyperactivated motility in equine sperm, i.e. to: (1) verify the presence and location of CATSPER1 protein in equine sperm; (2) evaluate the association between alkaline intracellular pH, intracellular calcium levels and hyperactivated motility parameters; (3) evaluate the effect of known pharmacological stimulators of hyperactivated motility and/or intracellular calcium on intracellular pH, intracellular calcium and sperm motility parameters; (4) assess the effect of known blockers of the CatSper channel on intracellular pH, intracellular calcium and hyperactivated motility parameters; and (5) to determine the direct actions of calcium and pH on the equine sperm axoneme using a demembranated sperm model.

CHAPTER III

CATSPER AND THE RELATIONSHIP OF HYPERACTIVATED MOTILITY TO INTRACELLULAR CALCIUM AND PH KINETICS IN EQUINE SPERM*

INTRODUCTION

In vitro fertilization (IVF) does not occur readily in the horse, despite decades of work in this area. Fertilization rates of up to around 30% have been reported [1, 76, 78, 256], but these have not been repeatable. McPartlin and coworkers [6] suggested that the limiting factor in equine IVF may be a failure of sperm to hyperactivate in vitro. These authors reported a 61% fertilization rate after incubating sperm in capacitating conditions and then stimulating hyperactivated motility with procaine. Similar success using procaine-treated sperm (37 to 62% fertilization) has subsequently been reported by another laboratory [86]. The success of equine IVF after pharmacological induction of hyperactivation suggests that typical sperm capacitation procedures, i.e., incubation in calcium, bicarbonate- and protein-containing media, do not adequately stimulate hyperactivated motility in equine sperm. If true, this would indicate that the physiological mechanism for induction of hyperactivated motility in equine sperm differs from those in sperm of most other species.

---

*Reprinted with permission from "CatSper and the Relationship of Hyperactivated Motility to Intracellular Calcium and pH Kinetics in Equine Sperm" by Loux SC, Crawford KR, Ing NH, González-Fernández L, Macías-García B, Love CC, Varner DD, Velez IC, Choi YH, Hinrichs K. *Biology of Reproduction*, In Press. To be published in Volume 89 (5). Copyright [2013] by the Society for the Study of Reproduction.

Hyperactivated motility is generally characterized by increased sperm flagellar bend amplitude and asymmetry. It is hypothesized that hyperactivation assists sperm in detaching from the wall of the oviduct, increases swimming efficiency in a viscous medium, and supplies the force required for sperm to penetrate the zona pellucida [reviewed in 257]. In mice, hyperactivated sperm motility in response to capacitation is dependent upon the presence of sperm-specific pH-gated cation (CatSper) channels [47, 258]. In humans, mutations in *CATSPER* genes are associated with infertility and abnormal sperm motility [259-261]. CatSper channels are composed of multiple proteins, including CATSPERS 1 through 4, which make up the pore-forming complex, and accessory proteins CATSPERB, CATSPERG and CATSPERD [review, 170]. The CatSper channels are localized to the principal piece of mouse sperm and open in response to increased intracellular pH, which is typically associated with sperm capacitation [47].

The exact mechanism for CatSper-mediated induction of hyperactivated motility is unclear; it may involve environmental calcium influx as well as the release of calcium from an internal store near the neck of the sperm, possibly the redundant nuclear envelope [156, 204, 262]. Mechanisms for CatSper-mediated hyperactivation have currently been investigated essentially only in the mouse and human. While many aspects are similar between these species, notable differences exist; for example, progesterone and prostaglandin E_1 directly stimulate CatSper activation in human sperm, but not in murine sperm [200, 201, 203]. Little is known about CatSper or CatSper-mediated functions in other species. Presence of *CATSPER1* to *-4* mRNA has been

verified in the testes of pigs [263]. While CatSper channels have not been specifically identified in the bull, Marquez and Suarez [188] reported an increase in hyperactivated motility in bull sperm following treatment with ammonium chloride (NH_4Cl), a weak base that raises intracellular pH (pH_i), and this rise was followed by an increase in cytosolic calcium concentration (Ca_i). Similar responses were found when bovine sperm were incubated in high-pH medium. These effects were likely to have occurred via opening of the CatSper channels, as *Catsper1*-null mice fail to demonstrate either calcium influx or hyperactivated motility in response to intracellular alkalinization [258].

Failure of equine sperm to undergo hyperactivation under standard capacitating conditions may be related to species-specific differences in the presence or function of CatSper channels. There is currently no information available on the relationship of intracellular pH to intracellular calcium or motility parameters in equine sperm, or on the presence or function of CatSper channels in this species. This study was conducted to evaluate the interactions among intracellular alkalinization, calcium influx, and hyperactivated sperm motility in equine sperm, and to determine the presence and localization of equine *CATSPER1* mRNA and protein.

MATERIALS AND METHODS

Chemicals and Media

Chemicals were purchased from Sigma-Aldrich (www.sigmaaldrich.com) with the following exceptions: goat anti-rabbit antibody conjugated to horseradish peroxidase (HRP) and the fluorescent probes BCECF-AM, Fluo 3-AM and Fluo 4-AM (Invitrogen;

www.invitrogen.com). A polyclonal antiserum raised in the rabbit against the C-terminus of human CATSPER1 was obtained from Santa Cruz Biotechnologies (H-300; sc-33153; www.scbt.com). Goat anti-rabbit antibody conjugated to Cy3 was obtained from Jackson ImmunoResearch (www.jacksonimmuno.com). Enhanced chemiluminescence detection reagents and Hyperfilm ECL were obtained from Amersham (www.gelifesciences.com).

Semen Collection

Equine semen was collected from seven sexually-mature light-breed stallions. Semen was collected using an artificial vagina (Nasco, Ft. Atkinson, WI) fitted with a nylon micromesh filter (Animal Reproduction Systems, Chino, CA) to remove gel and debris from the ejaculate. All experimental procedures were performed according to the United States Government Principles for the Utilization and Care of Vertebrate Animals Used in Testing, Research and Training and were approved by the Laboratory Animal Care Committee at Texas A&M University.

For motility studies, semen was diluted 1:5 in a modified Tyrodes medium (Sp-Tyrodes) containing 25 mM HEPES and 25 mM $NaHCO_3$, as described by Marquez and Suarez [188], with BSA replaced by 0.02% poly-vinyl alcohol (PVA) to prevent agglutination and glucose (5 mM) was added as this was associated with increases in both VCL and ALH(data not shown). Sperm were washed twice by centrifuging for 10 min at 400 x g and then were diluted to a final concentration of 30 x 10^6/ml. A

minimum of three replicates, each performed on a separate ejaculate, were performed for each study.

Sperm motility parameters were analyzed using computer-assisted sperm analysis (CASA; IVOS Version 12.2 L, Hamilton Thorne Inc., Beverly, MA) according to manufacturer's directions. The preset values for the IVOS system were as follows: frames acquired – 45; frame rate – 60 Hz; minimum contrast – 70; minimum cell size – 4 pixels; minimum static contrast – 30; straightness (STR) threshold for progressive motility – 50; average-path velocity (VAP) threshold for progressive motility – 30; VAP threshold for static cells – 15; cell intensity – 106; static head size – 0.60 to 2.00; static head intensity – 0.20 to 2.01; static elongation – 40 to 85; LED illumination intensity – 2200.

Parameters analyzed included total percent motility (% motile), percent progressively motile (% progressive), curvilinear velocity (VCL), amplitude of lateral head displacement (ALH), beat cross frequency (BCF) and linearity (LIN). Values for VCL and ALH were used as markers of hyperactivated-like motility. For simplicity, only the results from VCL and/or % motile are shown when ALH mirrored the values for VCL. STR was not included in analysis of hyperactivated motility, as it decreases during hyperactivation as well as when sperm are losing motility. For motility trials, between 750 and 1600 sperm were analyzed per treatment for every replicate. A minimum of three replicates per experiment were performed.

Effect of Increasing Extracellular pH on Equine Sperm Hyperactivated Motility

To prepare different pH media, Sp-Tyrodes containing 5 mM glucose and 0.02% PVA instead of BSA, as outlined above, was modified by alteration of [$NaHCO_3$] to 12.5 - 25 mM and inclusion of 25 mM HEPES or 10 mM TAPS, according to the pH desired, and adjustment to pH 7.25, 7.75, 8.25, 8.75 or 9.25 using 1 N NaOH. Sperm were processed in pH 7.25 medium and resuspended to 300 x 10^6/ml in pH 7.25 medium after the final centrifugation. Aliquots (50 µl) of this sperm suspension were diluted to 500 µl using the different pH media, for a final concentration of 30 x 10^6/ml. Sperm motility was evaluated at time 0 after extension in pH 7.25 medium, then aliquots were extended in high-pH media and evaluated after 1, 5, 10, 15, 20, 30, 40, 60, 80 and 100 min incubation at 37 °C in air. The pH values of the sperm suspensions were evaluated immediately after the 100-min time point to determine the final medium pH. An exponential regression model was used to evaluate the significance of final pH vs. time required to achieve maximum VCL values. Values for ALH mirrored those for VCL.

Comparison of Effects of Known Inducers of Hyperactivation on Motility, Intracellular Ca^{2+} and Intracellular pH of Equine Sperm

To determine the effect of both physiological and pharmacological inducers of hyperactivated motility on intracellular calcium and pH, stallion sperm were prepared as outlined above, using pH 7.25 medium, then aliquots were extended to a final concentration of 30 x 10^6/ml using pH 8.5 or 9.5 medium, or were extended using pH 7.25 medium then treated with 5 mM procaine, 4 mM 4-aminopyridine (4-AP), or 0.1, 1

or 10 µM ionomycin, an inducer of hyperactivated sperm motility in other species [188, 264]. The concentration of procaine was that used in previous reports [6, 86]; the concentration of 4-AP was selected based on maximum response in dose-response trials (data not shown). CASA readings were taken at 0, 5, 15, 30 and 60 min post-treatment to verify the effect of the reagents on motility.

Subsequently, pH_i and Ca_i were evaluated in sperm treated with the stimuli given above. Stallion sperm processed in pH 7.25 medium were incubated in 5 µM BCECF-AM or in 5 µM Fluo 3-AM at 25°C for 30 min in the dark, washed, and resuspended to 30 x 10^6 sperm/ml. Aliquots (200 µl) were loaded into a 96-well plate of a Synergy MX microplate reader (Bio-Tek; www.biotek.com) and excited at 488 nm and at 440 nm; emission was read at 535 nm. Three baseline measurements were recorded for each well, then treatments were added (high-pH treatments were resuspended at this time), and readings were taken every 2 min for 30 min.

The changes in intracellular calcium concentration (Ca_i) were expressed as the ratio $\Delta F/F_0$ after adjusting for background, with ΔF being the change in fluorescent signal, and F_0 the baseline as calculated by averaging the first three readings prior to adding reagents. Since the high-pH medium-treated sperm were exposed to the stimulus at the time of extension, they did not have a true Time 0 (pre-stimulus) reading; in this case the average of all other Time 0 readings in pH 7.25 medium was used to estimate this value. Quenching of Fluo 3-AM by procaine was confirmed by measuring the fluorescence of Fluo 3-AM-loaded, Triton-X-treated sperm before and after the addition of procaine: Control sperm maintained 100.5 ± 1.0% of their original fluorescence;

however procaine-treated sperm dropped to 60.0 ± 1.7% of their original fluorescence. Intracellular pH (pH_i) was assessed by calculating the ratio of emission after excitation at 488 nm to that after excitation at 440 nm (the isosbestic point) to control for loading and quenching; this allowed evaluation of procaine-treated sperm.

To ensure that motility was not significantly affected by either Fluo 3-AM or BCECF-AM, sperm were loaded as above, then treated with each of the reagents and motility was evaluated for 30 min. With the plate reader, approximately 6 million sperm were analyzed per well per treatment. A minimum of three replicates per experiment were performed.

Single-cell Imaging for Intracellular Ca^{2+}

To further evaluate the effect of 4-AP on calcium kinetics, single-cell imaging was performed. Equine sperm were processed in modified Sp-Tyrodes as above, containing 25 mM bicarbonate and 10 mM HEPES, then extended after the final wash to 10 x 10^6 sperm/ml in the same medium without PVA or BSA, and incubated in the presence of 10 µM Fluo 4-AM for 30 min at 37 °C in air in the dark in a poly-l-lysine coated 4-well coverglass slide. Fluo 4-AM was used for this study due to its increased sensitivity to intracellular calcium levels. After incubation, excess fluorophore was removed by replacing the medium on the slide with fresh medium via pipette. Sperm which were not stuck securely to the bottom of the slide were removed with the medium. Sperm were then incubated for an additional 30 min at 37°C to allow for full de-esterification of the probe before analysis. Between 30 and 50 sperm were analyzed per

treatment during each replicate, depending on how many were present in the field of view. All sperm whose heads were completely in the field of view were included. A minimum of three replicates per treatment were performed.

Fluorescence was monitored before and after addition of 4 mM 4-AP, 1 µM ionomycin (positive control), or deionized water. Sperm were imaged using a 63 x water-immersion objective on an inverted microscope (Carl Zeiss Inc.) using a 505-530 nm emission filter, 470 nm excitation filter and a 493 dichroic mirror. Preliminary trials at different frame capture speeds, from 0.5 to 5 s, showed that exposure at 5 s intervals minimized photobleaching without loss of sensitivity, thus frames were captured at 5 s intervals in the main study. Images were captured for a total time of 10 min, with treatments added after the initial 5 readings. A 4 x 4 binning was used to increase signal, and images were analyzed using Image-J software (NIH, Bethesda, MD). Each sperm head was selected as a region of interest and analyzed using the multi-measure tool, with the mean level of fluorescence for each region of interest at each time point calculated as a $\Delta F/F_0$ ratio (F_0 = the average of the first five readings prior to reagent addition).

Viability Assessment

Viability (membrane integrity) in sperm exposed to the above treatments was measured via staining with propidium iodide, using an automated cell counter (NucleoCounter SP-100; Chemometec, Denmark) according to manufacturer's instructions, as previously validated [265]. The percentage of viable sperm was assessed at 30 min post-treatment. It should be noted that this method used for assessment of PI

staining produces values that are an average of 6% lower than those for flow-cytometric evaluation of PI/SYBR-14-stained sperm. In samples with a higher proportion of membrane-damaged sperm, the discrepancy between the values obtained by the nucleocounter and by flow-cytometric analysis increased [265].

Effect of Progesterone and Prostaglandin E_1 on Motility, Intracellular Ca^{2+} and Intracellular pH

To determine if progesterone or prostaglandin E_1 had an effect on the motility of equine spermatozoa, semen was processed as above using pH 7.25 medium, then extended in media at either pH 7.25 or pH 8, as the effect of progesterone has been shown to be pH-dependent [200]. Three stock solutions each of progesterone and prostaglandin E_1 were prepared in ethanol to allow addition of a fixed volume for each concentration tested. The extended sperm were treated with 0, 0.5, 2 or 5 µM progesterone, or 0, 0.5, 2 or 5 µM prostaglandin E_1, similar to ranges used in the studies by Lishko et al. and Strünker et al. [200, 201]. Sperm were evaluated for motility, pH_i and Ca_i as described above.

Effect of CatSper Channel Inhibitors on Motility, Intracellular Ca^{2+} and Intracellular pH

The effect of mibefradil, a calcium-channel blocker shown to be a CatSper inhibitor in human sperm [201, 266], on motility, pH_i and Ca_i of equine sperm was determined. Evaluation of pH_i and Ca_i was performed using the plate reader as

described above except that readings were obtained every min. Because of the greater sensitivity of Fluo 4-AM shown in the single-cell imaging trials, Fluo 4-AM was used for Ca_i determination. Dose-response trials (mibefradil at 0, 0.5, 1, 2 -2.5, 5 or 10 μM) conducted with equine sperm in pH 8.5 medium indicated that the greatest suppression of Ca_i in this medium occurred with 5 μM mibefradil; increasing the dose to 10 μM resulted in increased Ca_i (Figure 3.1).

The effect of 5 μM mibefradil on Ca_i in sperm treated with the different inducers of hyperactivated motility (high-pH medium, 5 mM procaine, and 4 mM 4-AP) was then determined. To validate the effect of the tested pH medium on hyperactivation, a sample of sperm from each ejaculate was evaluated by CASA for response to pH 7.25 (control), 8, 8.5 and 9 media with and without mibefradil before Ca_i measurement was performed; the medium inducing the greatest VCL and ALH values (pH 8 in two ejaculates and 8.5 in one) was then used to evaluate the Ca_i response to mibefradil in sperm from that ejaculate.

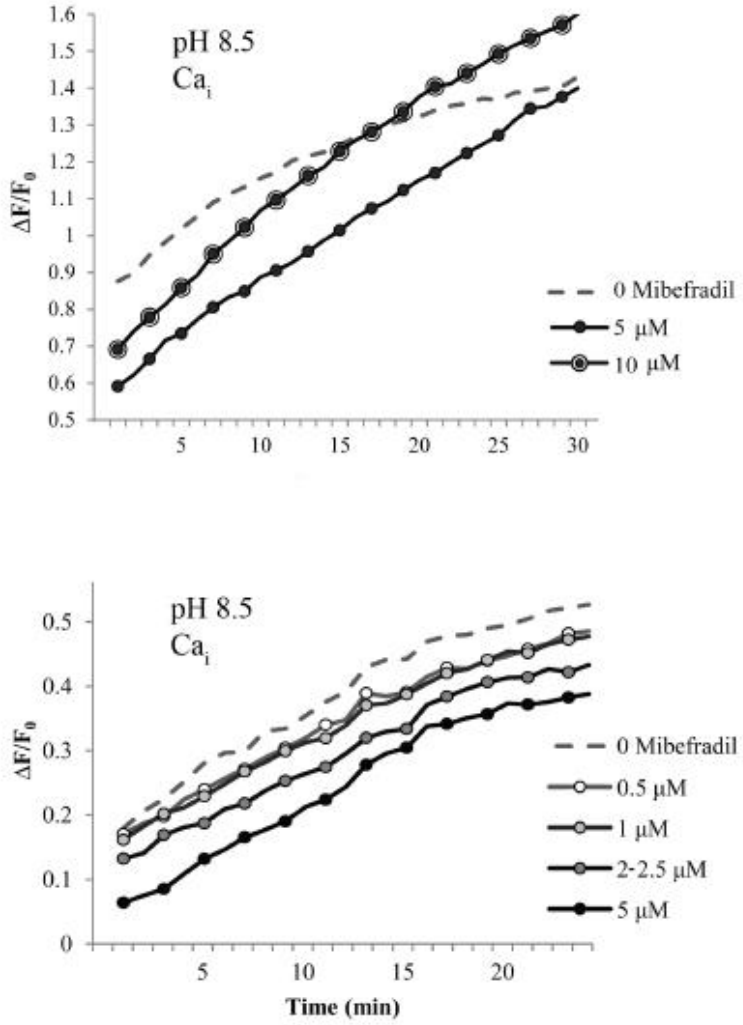

Figure 3.1. Mibefradil dose-response curve. Dose-response of Ca_i, ($\Delta F/F_0$) to mibefradil in equine sperm stained with Fluo 4-AM and extended in pH 8.5 medium.

To ensure that the initial response to hyperactivating stimuli in control and mibefradil-treated sperm was captured, for each hyperactivating stimulus, mibefradil or vehicle was added to sperm in one set of wells, then the stimulus was added and fluorescence was immediately evaluated for 5 min. After the 5 min evaluation, the sperm in the next set of wells was treated with mibefradil or vehicle, then the next stimulus was added and they were evaluated for 5 min, with continuing evaluation of the previous wells. All wells were evaluated for a minimum of 30 min.

The effect of mibefradil on procaine- and 4-AP-treated sperm on motility was subsequently performed using CASA as described above. Motility was evaluated at 0, 1, 15 and 30 min after addition of stimulatory treatments in the presence of either 0 or 5 µM inhibitor.

The above studies were repeated to evaluate the effect of NNC 55-0396 (NNC), another compound reported to block CatSper channel activity [200, 201]. Treatment of equine sperm with NNC resulted in elevated Ca_i at all doses tested (0.2, 0.5, 1, 2 and 5 µM) by a mechanism not yet determined, thus this compound was not evaluated further.

In-situ Immunocytochemistry for the CATSPER1 Protein

Stallion sperm were processed in Sp-Tyrodes medium, as described above. Ten µl of sample was placed on a slide and allowed to air dry, then permeabilized with 0.2% Triton-X, and blocked with 3% BSA in PBS. Primary incubation with the rabbit anti-human CATSPER1 C-terminus antibody (diluted 1:500 in 3% BSA in PBS) was performed at 4°C overnight. The sample was then washed and incubated with goat anti-

rabbit antibody conjugated with Cy3 (diluted 1:2000), washed, and counterstained with DAPI. Control samples were processed as above, but lacked primary antibody. Samples were evaluated using an inverted fluorescent microscope at 400 X, with excitation read at 534 nm and emission at 635 for Cy3 and 350 nm / 470 nm for DAPI.

Western Blot for Presence of CATSPER1 Protein

To extract protein, 300 x 10^6 spermatozoa were diluted 1:5 in a modified Whittens medium without BSA and bicarbonate. The suspension was centrifuged lightly (at 100 x g for 1 min) to remove debris, then the supernatant was transferred to a fresh tube and was re-centrifuged at 600 x g for 5 min to concentrate the pellet. The pellet was resuspended to 30 x 10^6/ml with the modified Whittens medium, then centrifuged at 5,000 x g for 3 min and the supernatant discarded. As a control, previously-frozen equine fibroblasts (~150,000) were thawed and centrifuged at 5,000 x g for 3 min, and the supernatant discarded.

The resulting pellets were diluted in 1 ml PBS, and centrifuged at 5,000 x g for 3 min at room temperature. The supernatant was discarded and samples were diluted in 50 µl of sample buffer containing 65.2 mM Tris HCl- pH 6.8, 25% glycerol, 2% SDS and 0.01% bromophenol blue, and a protease inhibitor cocktail (Complete EDTA-free; Roche (www.roche.com)). Samples were then centrifuged at 10,000 x g for 10 min at 4 °C and the supernatant was collected. Protein concentration was determined using a Bio-Rad DC Protein Assay according to manufacturer's instructions. β-mercaptoethanol

(2.5%) was added, then samples were heated for 5 mins at 95 °C. Samples were stored at -80 °C until further processing.

For electrophoresis, samples containing 40 µg of protein were loaded onto a 12% TGX precast polyacrylamide mini-gel (Bio-Rad Laboratories, Hercules, CA) at 170 V for 40 min, then transferred to a polyvinylidene fluoride (PVDF) membrane at 350 mA for 60 min. The membrane was blocked in 5% non-fat dried milk in TBS-T (0.5 M NaCl, 20 mM Tris and 0.1% TWEEN, at pH 7.4) for one h at room temperature, then washed three times for 5 min each in TBS-T. Primary antibody incubation was performed with the rabbit anti-human CATSPER1 C-terminus antibody detailed above, diluted 1:200 in 5 % non-fat dried milk in TBS-T, for two h at room temperature on an oscillating plate. The antibody was removed by washing 3 times for 5 min each in TBS-T, and a secondary incubation was performed for 45 min at room temperature with goat anti-rabbit antibody conjugated with HRP diluted 1:5,000 in TBS-T. Protein was visualized using a chemiluminescence detection kit (ECL Kit, Amhersham Corp., Arlington Heights, IL) according to the manufacturer's instructions, and exposure to Hyperfilm ECL film (Amersham, Arlington Heights, IL, USA).

Statistical Analysis

All statistical analyses were performed using SigmaPlot ver. 12.0 for Windows (Systat Software, Chicago, IL). Treatment effects for time-series data were detected using repeated measures analysis of variance, followed by the Holm-Sidak method for individual post-hoc comparisons. Paired t-tests were used to evaluate the differences in

pH_i, Ca_i, and motility variables between treatments with and without NNC or mibefradil added for each stimulatory treatment. The linear regression model was used to determine the significance of the relationship between the time of maximum motility and the final pH of the medium. Differences were considered significant when $P < 0.05$.

RESULTS

Effect of Increasing Extracellular pH on Equine Sperm Hyperactivated Motility

Hyperactivated motility parameters VCL and ALH increased in equine sperm with increasing extracellular pH (Figure 3.2). The pH values given for treatments indicate the pH of the medium added to a 50-µl aliquot of sperm prepared in control medium (pH 7.25); final pH values for the 7.25, 7.75, 8.25, 8.75 and 9.25 treatments were 7.55 ± 0.06, 8.00 ± 0.08, 8.20 ± 0.21, 8.51 ± 0.12, and 8.77 ± 0.10, respectively. The greatest stimulation of hyperactivated motility was associated with addition of pH 8.75 medium (maximum VCL of 333 ± 10.3 and ALH of 13.3 ± 0.6 within 10 min after addition). The VCL and ALH of sperm exposed to pH 8.75 medium significantly increased by 5 minutes post-treatment, and remained significantly higher than time 0 until 80 minutes post-exposure ($P < 0.05$). Additionally, sperm treated with pH 8.75 medium had significantly increased VCL and ALH than sperm exposed to either pH 7.25 or pH 7.75 medium at both five and ten minutes post-exposure ($P < 0.001$). Treatment with pH 9.25 medium was associated with a rapid decrease in both VCL and ALH. The time needed to achieve maximum VCL was significantly and inversely correlated to the final medium pH, with higher pH treatments reaching maximal VCL

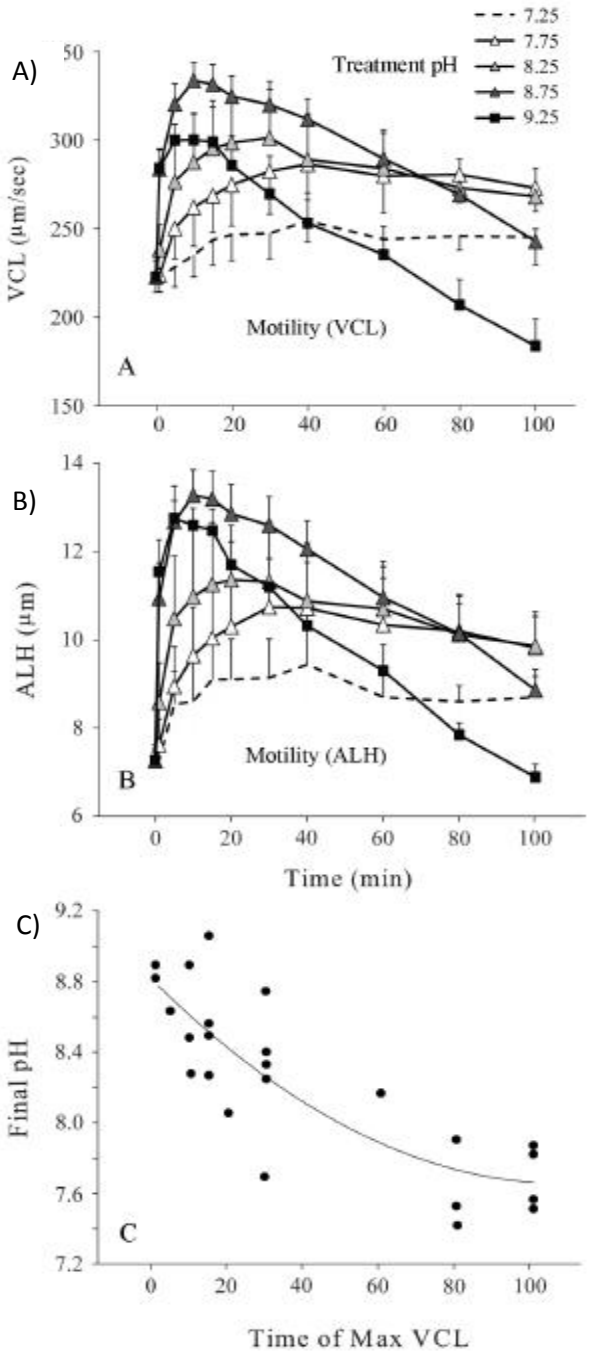

Figure 3.2. **Effect of high pH medium on motility.** Values for A) curvilinear velocity (VCL) and B) amplitude of lateral head movement (ALH) over time in stallion sperm treated with medium of pH 7.25, 7.75, 8.25, 8.75 or 9.25, and C) plot of the pH at the end of the experiment (Final pH) against the time point at which the highest VCL (Max VCL) was recorded, using an exponential regression model; $R^2 = 0.60$. Values represent the mean ± SE for five independent replicates, using three separate stallions.

earlier (Figure 3.2C; $R^2 = 0.60$; $P < 0.001$). These results indicate that increasing extracellular pH increases hyperactivated motility parameters VCL and ALH in equine sperm in a dose-dependent manner, and that rapid onset of hyperactivation can occur in equine sperm under the appropriate conditions. Total motility did not change significantly over time in any treatment ($P > 0.2$).

The concentration of bicarbonate in the medium varied from 15 to 25 mM. The sperm exposed to 15 mM bicarbonate had an average VCL which was 20.7 ± 6.4 µm/sec faster than those treated with 25 mM bicarbonate (271.3 vs. 250.6). The average ALH was 2.4 ± 0.9 µM larger in the 15 mM bicarbonate group (8.58 vs. 10.99). These changes were significantly different ($P < 0.01$).

Comparison of Effects of Known Inducers of Hyperactivation on Motility, Intracellular Ca^{2+} and Intracellular pH of Equine Sperm

Increases in intracellular pH and Ca^{2+} have been proposed to mediate the onset of hyperactivation in sperm of other species. Addition of pH 8.5 medium or of known chemical inducers of hyperactivated motility, procaine and 4-AP (both prepared in pH 7.25 medium), induced an increase in VCL and ALH values in equine sperm (Figure 3.3). Sperm treated with procaine achieved the highest hyperactivated motility values (VCL, 406 ± 11.9; ALH, 14.1 ± 0.18); treatment with pH 9.5 medium was associated with a loss of motility (Figure 3.3.A). The three effective hyperactivating stimuli each induced a similar significant rise in pH_i compared to control ($P < 0.05$); this rise in pH was small compared to that induced by treatment with pH 9.5 medium (Figure 3.3.B).

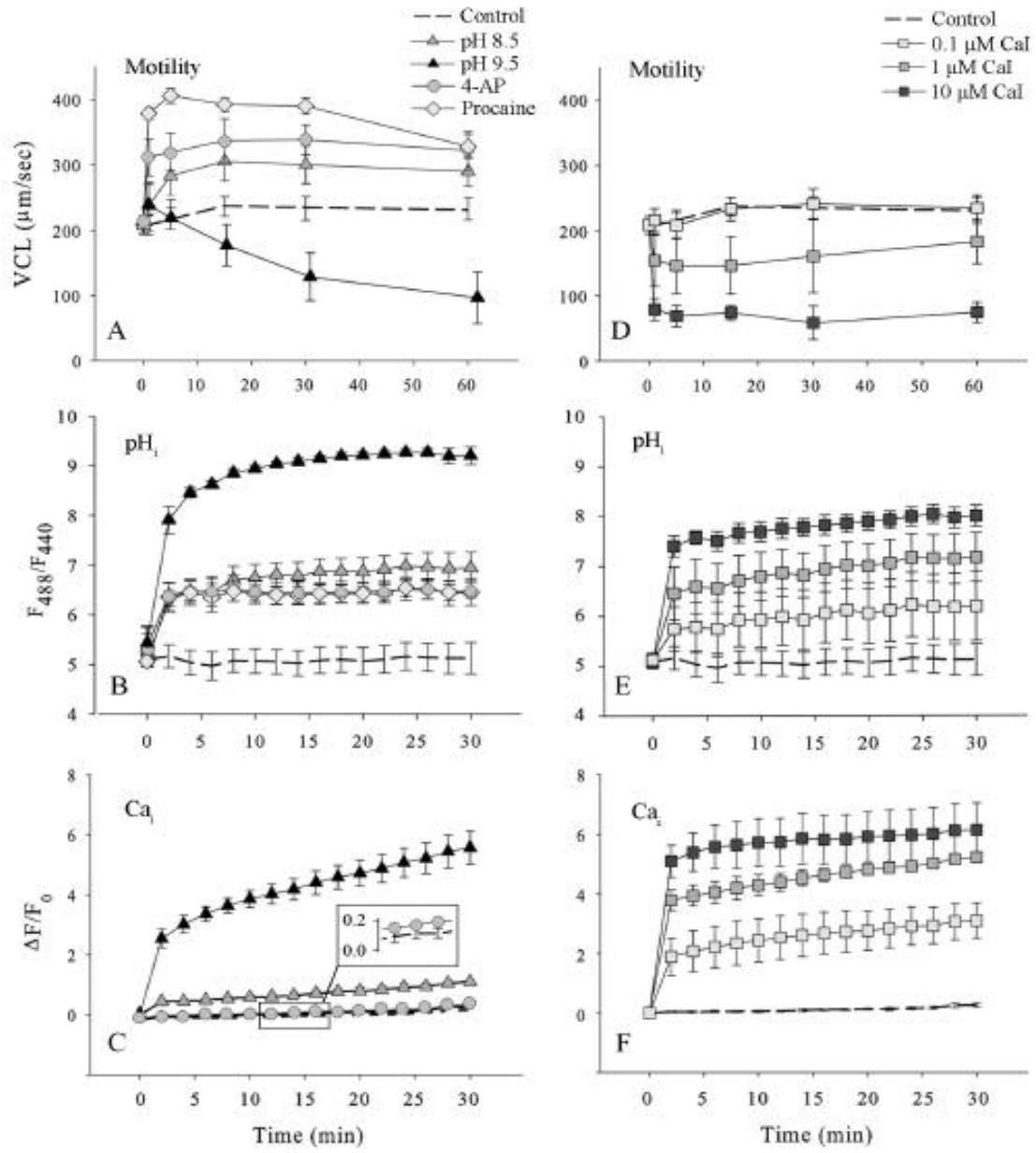

Figure 3.3. Effect of hyperactivating stimuli on VCL, pH_i and Ca_i. Hyperactivated motility (VCL; A,D); pH_i, as determined by BCECF fluorescence (B,E); and Ca_i as measured by Fluo 3-AM fluorescence (C,F) in stallion sperm treated with different pH media, 4 mM 4-AP, 5 mM procaine, or different concentrations of the calcium ionphore ionomycin (CaI); inset in C shows values for 4-AP and Control sperm on an expanded Y axis. Relative pH_i was calculated as emission after excitement at F_{488} / F_{440}. Relative Ca_i was calculated as $\Delta F/F_0$. Values represent the mean ± SE for three independent replicates with a different stallion used for each replicate.

Treatment with 4-AP was associated with only a minimal increase in Ca_i, (inset, Figure 3.3.C) however, using repeated measures ANOVA, this was significantly higher than that for the control ($P < 0.001$). Treatment with pH-8.5 medium resulted in a greater increase in Ca_i than that for 4-AP; treatment with pH-9.5 medium induced the largest rise in Ca_i (Figure 3.3.C). All treatments were significantly different from one another ($P < 0.001$).

We were unable to effectively measure the effect of procaine on Ca_i due to its quenching of fluorescence (see Materials and Methods). None of the above tested treatments had a significant effect on sperm viability (PI exclusion, Table 3.1). The detrimental effect on motility following exposure to pH 9.5 medium, as seen in previous studies with pH 9.25 medium, may be due to abnormally high pH_i, or to excessive Ca_i, as the motility of demembranated sperm exposed to high levels of calcium is inhibited [122, 144]. Because treatment with 4-AP was associated with an increase in VCL and ALH but with only a minimal increase in Ca_i within the sperm population, we evaluated the kinetics of Ca_i in response to 4-AP in individual sperm via single-cell imaging after loading with Fluo 4-AM (Figure 3.4). Some sperm showed a wave in Ca_i fluorescence after 4-AP treatment, followed by a return to lower levels. Individual sperm experienced the wave at different times after 4-AP addition; however, only one wave was noted in any individual sperm in the 4-AP treatment during the 10 min of imaging. In contrast, fluorescence in sperm treated with 1 µM ionomycin increased to high levels and remained high.

Treatment	Viability
Control	66.0 ± 2.4[a]
pH 8.5	66.6 ± 0.6[a]
pH 9.5	68.1 ± 2.0[a]
10 μM Ionomycin	64.8 ± 0.8[a]
1 μM Ionomycin	46.3 ± 5.6[b]
0.1 μM Ionomycin	41.3 ± 3.8[b]
4 mM 4-AP	68.9 ± 2.1[a]
5 mM Procaine	66.9 ± 2.5[a]

Table 3.1. Sperm viability. Viability (PI exclusion) of equine sperm 30 min after treatment with inducers of hyperactivation or calcium influx. Data are expressed as mean ± SE. Values with different superscripts differ significantly ($P < 0.05$). Values represent the mean ± SE for three independent replicates with a different stallion used for each replicate.

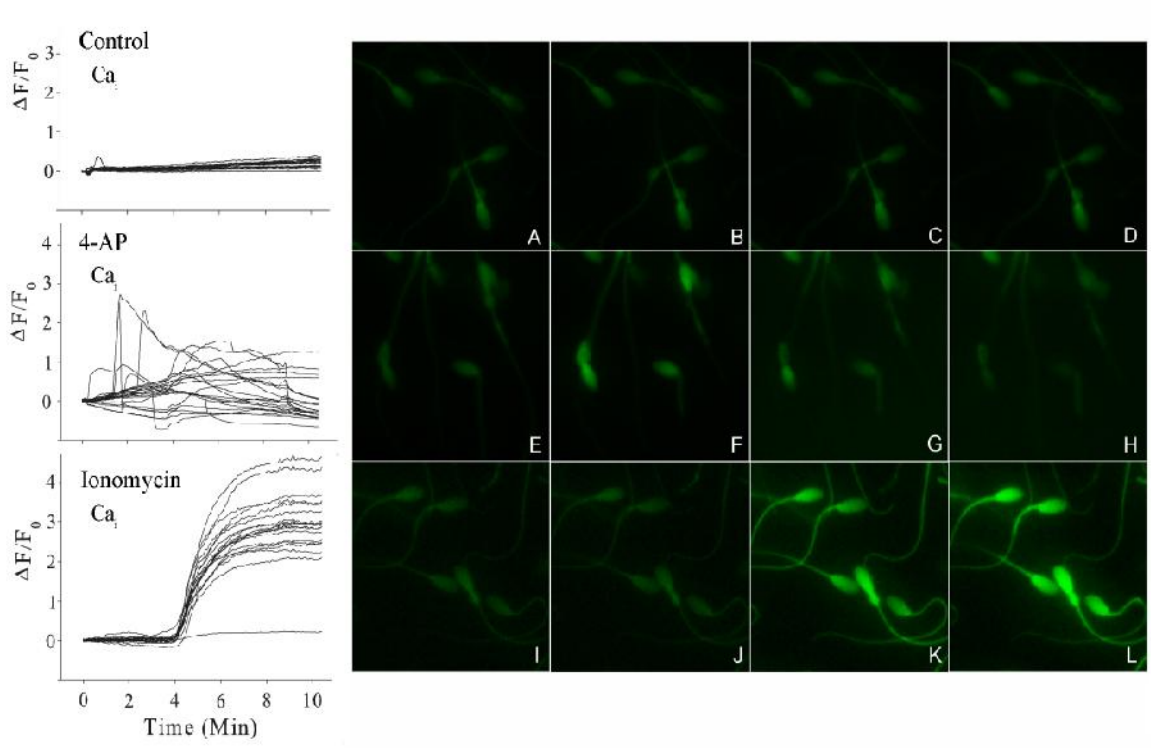

Figure 3.4. **Ca_i in response to 4-AP or ionomyocin.** Single-cell imaging of Fluo 4-AM fluorescence in equine sperm in response to treatment: A-D) Control; E-H) 4 mM 4-AP; I-L) 1 µM ionomycin. Frames were taken before treatment (A,E,I), and at 150 (B,F,J), 300 (C,G,K), and 600 (D,H,L) sec after treatment. Pixel intensity for each treatment was adjusted so that the before-treatment images had equivalent maximum intensity. Relative Ca_i was calculated as $\Delta F/F_0$. Left, measurements for individual sperm in each treatment over the 10 min evaluation period. Each individual sperm is represented by a single line.

As 4-AP increases hyperactivated motility parameters, these findings are consistent with a hypothesis that a transient increase in intracellular calcium is sufficient to induce hyperactivation; alternatively, these data may indicate that the effects of 4-AP on motility in equine sperm are not mediated by a marked rise in Ca_i.

Effect of Ionomycin on Motility, Intracellular Ca^{2+} and Intracellular pH

Exposure to ionomycin induced a dose-dependent increase in pH_i and Ca_i, but did not induce hyperactivated motility (Figure 3.3.D-F); rather, sperm in both 1 µM and 10 µM ionomycin treatments showed significantly reduced motility compared to control sperm ($P < 0.001$). The Ca_i values for ionomycin at all concentrations tested were significantly higher than those for the effective hyperactivating stimuli ($P < 0.001$). Treatment with 1 µM and 10 µM ionomycin significantly decreased viability at 30 min ($P < 0.05$; Table 3.1).

The failure of 0.1 or 1 µM ionomycin to induce hyperactivated motility, despite increases in pH_i similar to that for the effective hyperactivating stimuli, implies that equine sperm have an intracellular threshold for Ca^{2+}, and that an increase over this level has a deleterious effect on hyperactivated motility. Since both calcium ionophore A23187 and ionomyocin have been shown to induce hyperactivated motility at micromolar doses in a variety of other species [188, 264, 267-269], this Ca_i threshold in equine sperm may be lower than that in other species.

Effect of Progesterone and Prostaglandin E_1 on Motility, Intracellular Ca^{2+} and Intracellular pH

Progesterone and prostaglandin E_1 induce CatSper activity and hyperactivated motility in human sperm [200]. Neither compound significantly affected equine sperm motility parameters at any dose tested ($P > 0.2$; Figure 3.5; 3.6). Neither progesterone nor prostaglandin E_1 had a significant effect on pH_i, and neither compound increased Ca_i ($P > 0.2$); rather, prostaglandin E_1 at 2 or 5 μM significantly decreased Ca_i levels at 4 min post-treatment in both pH 7.25 and pH 8 media when compared to the ethanol control ($P < 0.05$; Figure 3.6). These results suggest that these compounds are not associated with Ca^{2+} influx or onset of hyperactivated motility in horse sperm, in contrast to findings for human sperm. Results for ALH mirrored those for VCL, therefore only VCL was shown.

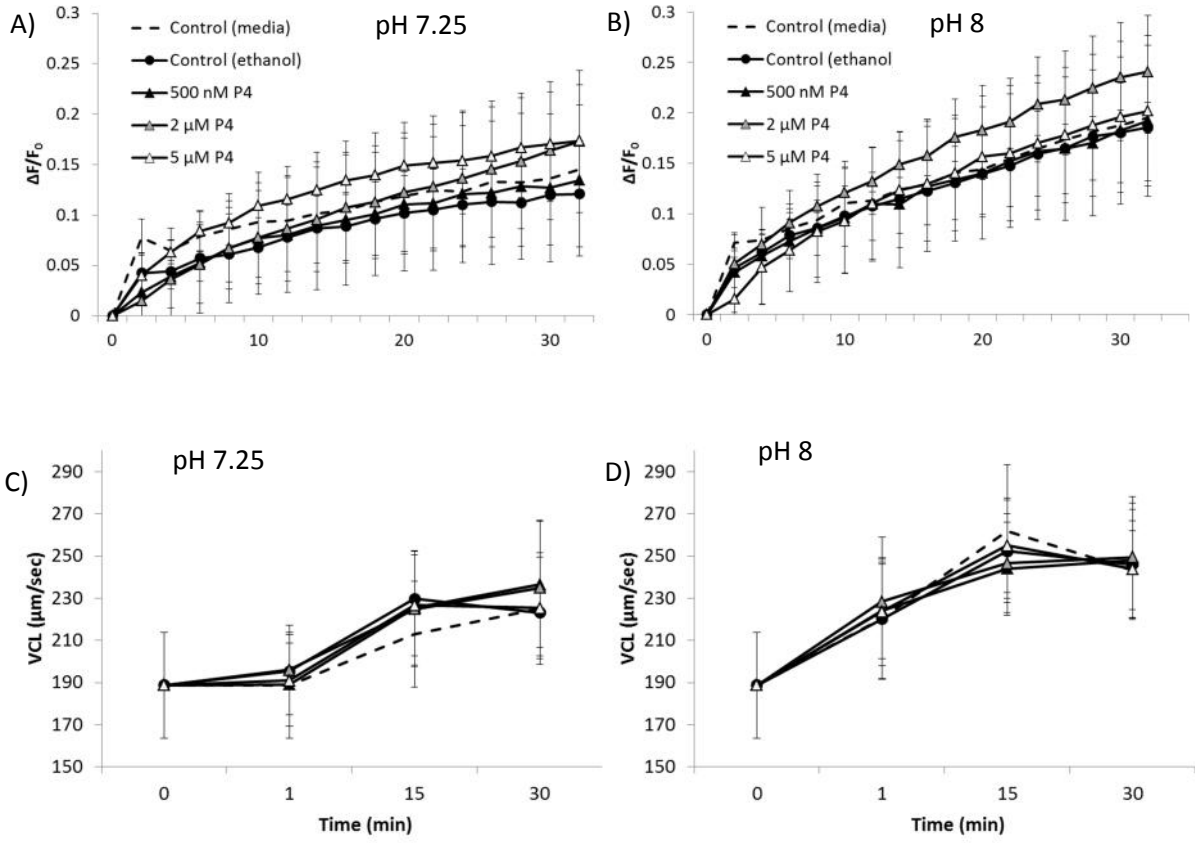

Figure 3.5. Effect of progesterone (P4) on equine sperm The effect of progesterone on sperm was analyzed, including A,B) Ca_i ($\Delta F/F_0$) as determined by Fluo 4-AM fluorescence, and C, D) curvilinear velocity (VCL). Experiments were performed with sperm extended in either A,C) pH 7.25 medium or B,D) pH 8 medium. Values represent the mean ± SE for three independent replicates with a different stallion used for each replicate.

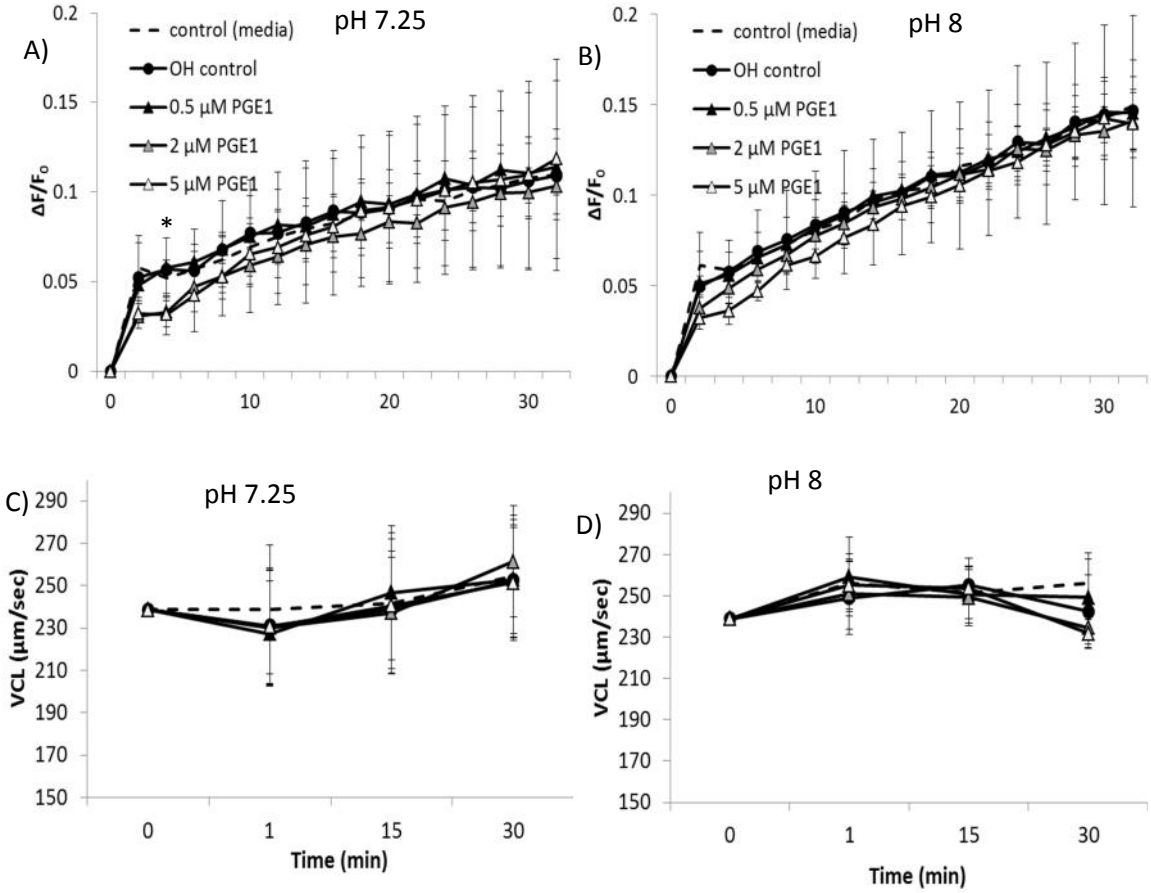

Figure 3.6. Effect of prostaglandin E1 (PGE1) on equine sperm The effect of progesterone on sperm was analyzed, including A,B) Ca_i ($\Delta F/F_0$) as determined by Fluo 4-AM fluorescence, and C,D) curvilinear velocity (VCL). Experiments were performed with sperm extended in either A,C) pH 7.25 medium or B,D) pH 8 medium. Values represent the mean ± SE for three independent replicates, with a different stallion used for each replicate. * denotes a significant difference between treatments at a given time point ($P < 0.05$).

Effect of Mibefradil on Motility, Intracellular Ca^{2+} and Intracellular pH

The calcium-channel inhibitor mibefradil has been reported to block the CatSper current in human sperm [201, 266]. In equine sperm, treatment with mibefradil induced a dose-dependent increase in pH_i (Figure 3.7). The effect of 5 μM mibefradil on VCL and Ca_i of equine sperm as induced by the three effective hyperactivating stimuli (high pH medium, 4-AP and procaine), is shown in Figure 3.8. Values for ALH mirrored those for VCL. Evaluation of Fluo 4-AM-loaded sperm at 1-min intervals immediately after stimulus addition allowed the capture of an initial rise in Ca_i in response to high-pH medium. Treatment with mibefradil significantly reduced Ca_i in control, high-pH and 4-AP treatments ($P < 0.05$). Mibefradil did not significantly affect Ca_i fluorescence in procaine-treated sperm ($P > 0.2$), however, it should be noted that the relationship of the change in fluorescence to actual Ca_i may be altered in the presence of procaine (Figure 3.8).

In spite of its suppressive effect on Ca_i, mibefradil treatment did not inhibit the initial increase (1 min post-addition) in either VCL (Figure 3.8.C-F) or ALH (data not shown) induced by any of the hyperactivating stimuli ($P > 0.2$), and was associated with a significant increase in hyperactivated motility parameters in sperm treated with high-pH medium ($P < 0.001$).

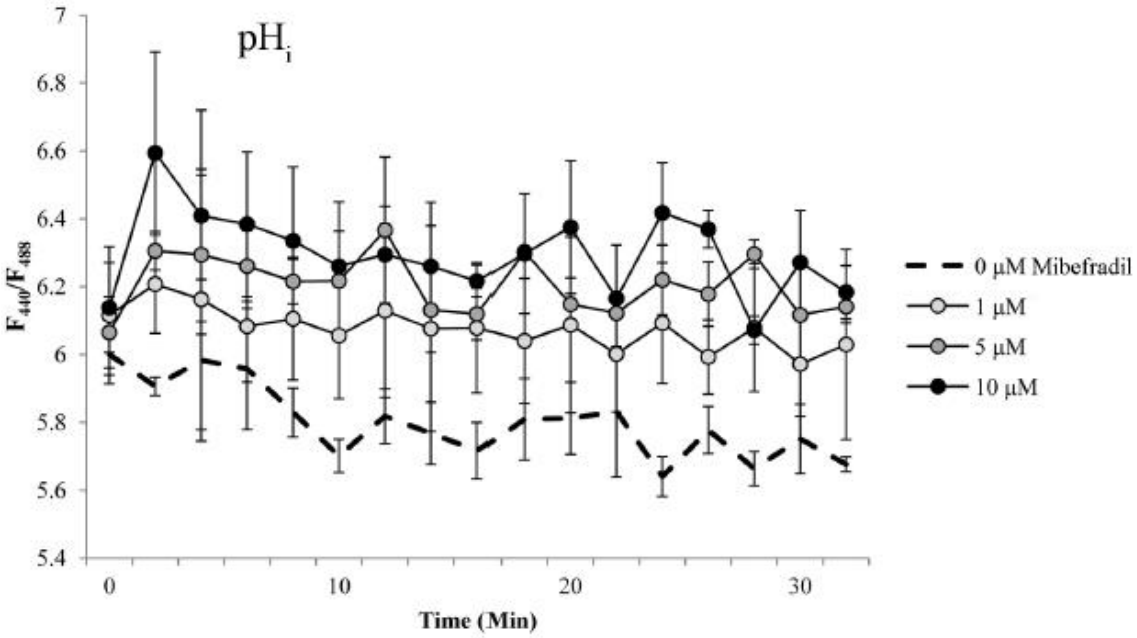

Figure 3.7. Effect of mibefradil on pH_i. Changes in pH_i , as determined by BCECF fluorescence (F_{440}/F_{488}) associated with treatment of equine sperm with different concentrations of mibefradil. Values represent the mean ± SE for three independent replicates using a different stallion used for each replicate.

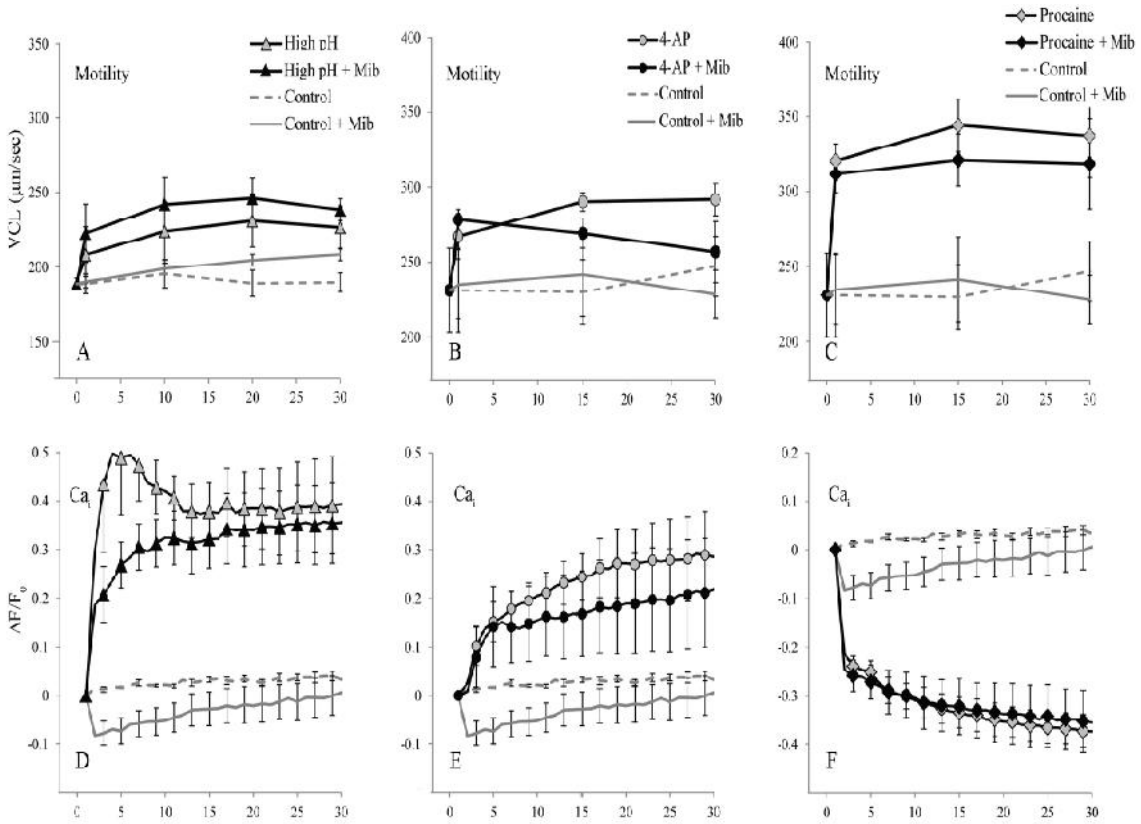

Figure 3.8. Effect of mibefradil on sperm exposed to high pH medium, 4-AP or procaine. VCL and Ca_i levels measured in response to Control (pH 7.25) medium, 4 mM 4-AP, high-pH medium (pH 8 – 8.5, as determined by the medium inducing maximum hyperactivated motility parameters in that ejaculate), or procaine; each treatment was evaluated in sperm treated with vehicle (control) or 5 μM mibefradil (Mib) before application of the stimulus. Values represent the mean ± SE for three independent replicates using a different stallion used for each replicate.

In sperm exposed to high-pH medium or 4-AP, the reduction in Ca_i associated with mibefradil suggests that the increase in Ca_i related to these stimuli is due to opening of CatSper channels. The finding that mibefradil treatment did not inhibit the onset of hyperactivated motility indicates that unimpeded Ca^{2+} influx is not essential for induction of hyperactivated motility in equine sperm. On the contrary, the increase in VCL and ALH in high-pH sperm treated with mibefradil suggests that reduction in Ca_i may be associated with increased hyperactivated motility. The lack of apparent effect of mibefradil on Ca_i fluorescence in procaine-treated sperm, if valid, raises the possibility that procaine works through a mechanism independent of CatSper.

Mibefradil treatment itself induced an increase in $pH_{i,}$ but a decrease in Ca_i. Since mibefradil is known to block CatSper, these findings suggest that the CatSper channel in equine sperm is responsible for the influx of Ca^{2+} associated with increased pH_i, similar to that seen in other species [186].

In agreement with our findings in high-pH medium, Strunker, et al. [201] reported that in human sperm exposed to NH_4Cl, treatment with mibefradil inhibited the initial peak in Ca_i, but had little effect on the static high Ca_i afterward. The paradoxical increase in Ca_i that we found with high concentrations of mibefradil, and in preliminary trials with NNC, agrees with the findings of Strunker, et al. [201], who stated that the pharmacology of these compounds is complex.

Effect of Absence of Environmental Ca^{2+} on Induced Hyperactivated Motility

The effect of the absence of environmental calcium on induction of hyperactivated motility was dependent upon the hyperactivating stimulus applied (Figure 3.9). Procaine treatment induced hyperactivated motility at 1 min both in medium with no added calcium ([-]Ca) and in medium with no added calcium containing 2 mM EGTA ([-]Ca+EGTA). The procaine-induced increase in hyperactivated motility parameters was sustained for over 30 min in the [-]Ca medium. Treatment with 4-AP produced a transient but significant rise in VCL in [-]Ca medium at 1 min ($P < 0.05$) but did not induce hyperactivated motility in [-]Ca+EGTA medium. Treatment with pH 8.5 medium did not induce hyperactivated motility in either medium; in contrast, pH 8.5 treatment was associated with a significant decrease in VCL, ALH and in total motility ($P < 0.05$; Figure 3.9.C,F) in both calcium-deficient media at 15 and 30 min.

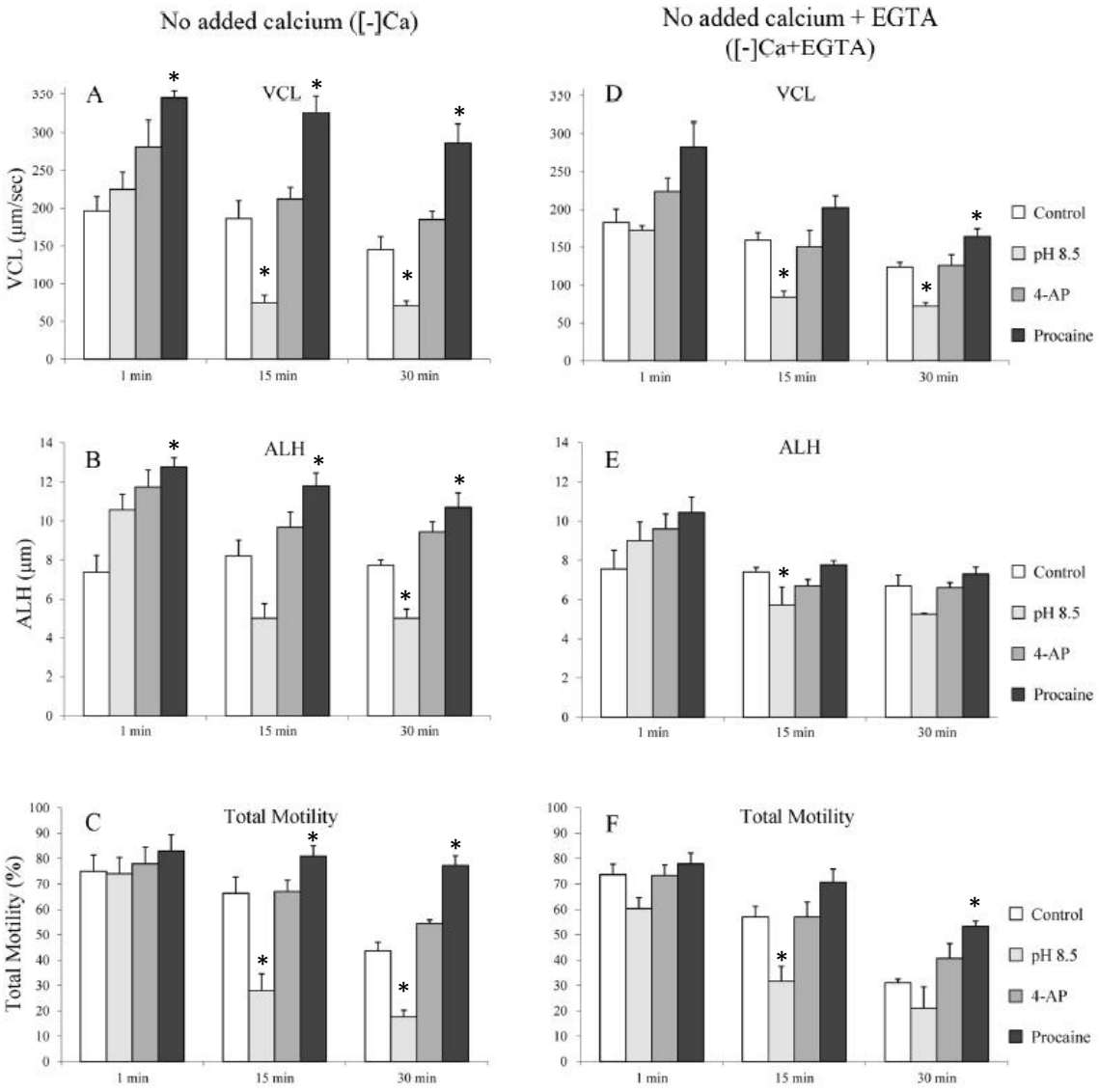

Figure 3.9. Effect of low-calcium media on sperm treated with pH 8.5 medium, 4-AP or procaine. Hyperactivated motility (VCL and ALH) and total motility in sperm treated with pH 8.5 medium, 4 mM 4-AP or 5 mM procaine in medium containing no added calcium ([-]Ca; A-C) or no added calcium with 2 mM EGTA ([-]Ca+EGTA; D-F). Values represent the mean ± SE for three independent replicates with a different stallion used for each replicate. Treatments significantly different from the control (pH 7.25 media) for that time point, are denoted by a * ($P < 0.05$).

The rise in Ca_i associated with treatment with high-pH medium in the preceding studies, and its suppression by mibefradil, suggests that high-pH medium induces opening of CatSper channels, as reported in other species. In this study, the loss of total and hyperactivated motility in high-pH treated sperm in the absence of environmental calcium may also be related to opening of CatSper channels: under Ca^{2+}-free conditions, CatSper channels transport Na^+ ions, and the resulting Na^+ influx directly causes inhibition of sperm motility [270]. The ability of procaine to support total and hyperactivated motility in equine sperm in the absence of environmental Ca^{2+} suggests: 1) that CatSper channels are not opened in equine sperm treated with procaine; 2) that procaine induces hyperactivation in equine sperm through a mechanism independent of CatSper, as suggested in the preceding study by the lack of response of procaine-treated sperm to mibefradil and 3) that this mechanism is largely independent of calcium influx from the environment.

CATSPER1 Peptide Sequence Analysis

Alignment of equine and murine CATSPER1 (Figure 3.10) demonstrated that the equine protein had both functional and morphological homology to that of other species. The S4 voltage-sensor transmembrane helix region of the equine protein was 100% homologous to that identified in the mouse [193]. The putative pore loop P contained the conserved channel pore consensus motif TxDxW, denoting ion specificity, as found in CATSPER1 and other CatSper proteins in other species, and contained the key aspartate residue that is absolutely conserved [193, 271]. A coiled-coil domain was

predicted at the C-terminus of the equine protein, suggesting multimeric protein-protein interactions, as found in CatSper proteins in other species [193, 263]; however, a second coiled-coil domain was predicted at amino acids 302 to 317, immediately prior to the S1 transmembrane region, of the equine protein (Figure 3.10). This mid-protein coiled domain is not present in human, mouse or porcine CATSPER1. A similar region is found in CATSPER2 in other species [193, 263]; however, alignment of the predicted equine CATSPER1 amino acid sequence with that of human or mouse CATSPER2 was poor (maximum 24 and 25% identity, respectively).

A notable finding in equine CATSPER1 was a potential transmembrane domain at aas 98 to 120 (Segment R; Figure 3.10) that was not a signal peptide (prediction score < 0.2) and was not present in human or mouse CATSPER1. Segment R was interpreted to be a transmembrane domain by the DAS and TMpred software, but did not meet probability requirements in TMHMM or TOPCONS. As in the human and murine proteins, the N-terminus of the equine protein included a histidine-rich region; histidines undergo protonation at a physiological pH range, and their presence suggests pH sensitivity. However, in the equine protein, histidine enrichment occurred only in 151 aa between the end of Segment R and the onset of S1, the first consensus transmembrane domain , whereas in human and murine CATSPER1, the entire first 335 (mouse) or 390 (human) amino acids, from the N-terminus to S1, are histidine-rich. The limited histidine-rich area in the equine protein contained a greatly-enriched sequence of 58 aa containing 27 histidines, including 6 repeats of HHH. The histidine-rich region of CATSPER1 is predicted to be intracellular [193].

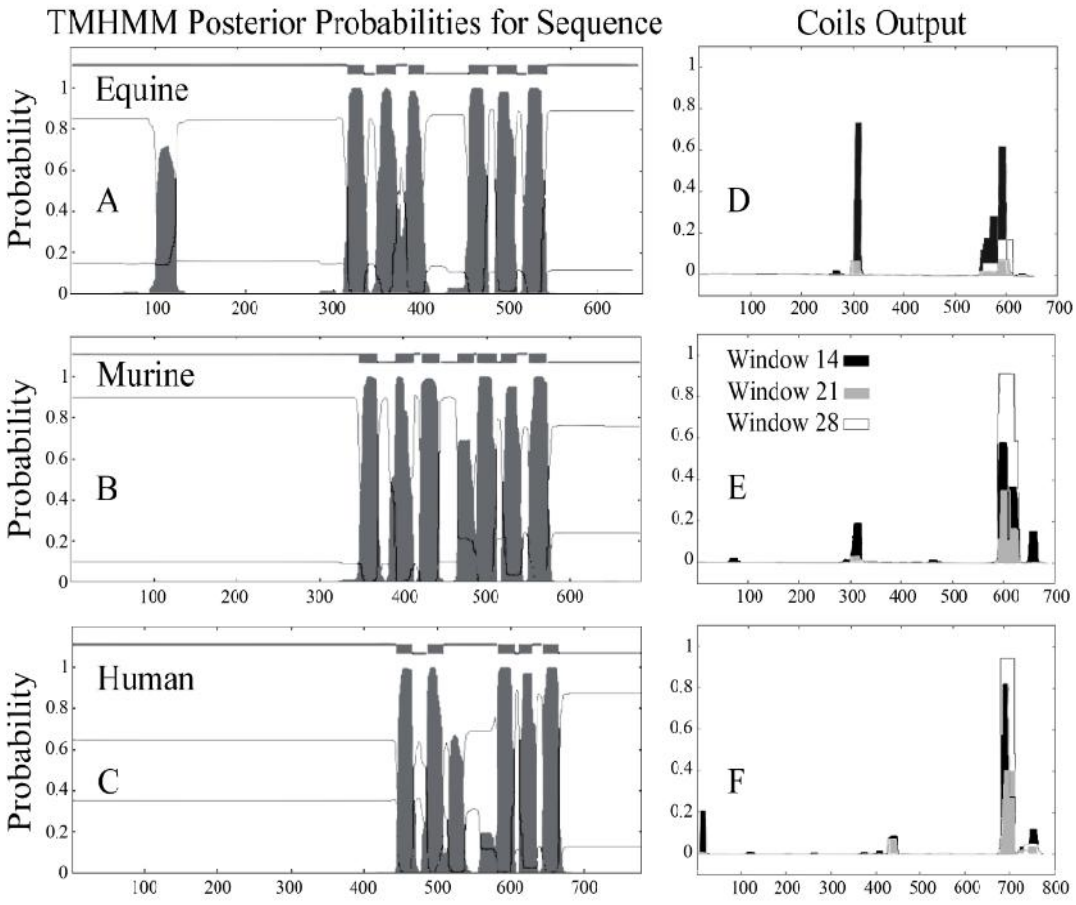

Figure 3.10. Peptide sequence analysis of CatSper1. Transmembrane domain prediction as given by TMHMM software (A-C) and coiled-coil prediction as given by COILS software (D-F) for equine, murine and human CATSPER1 proteins. G, alignment of murine CATSPER1 with the predicted equine protein. Histidine residues, indicating pH sensitivity, are in bold. R, possible N-terminus transmembrane domain present in equine, but not murine protein; S1-6, predicted consensus transmembrane domains; dotted-line boxes show prediction by TMHMM and those reported by [47], solid lines represent areas of agreement. The putative voltage-sensor region of S4 [193] is boxed and shaded. P, putative pore region; consensus ion-specific residues (TxDxW) are shaded individually.

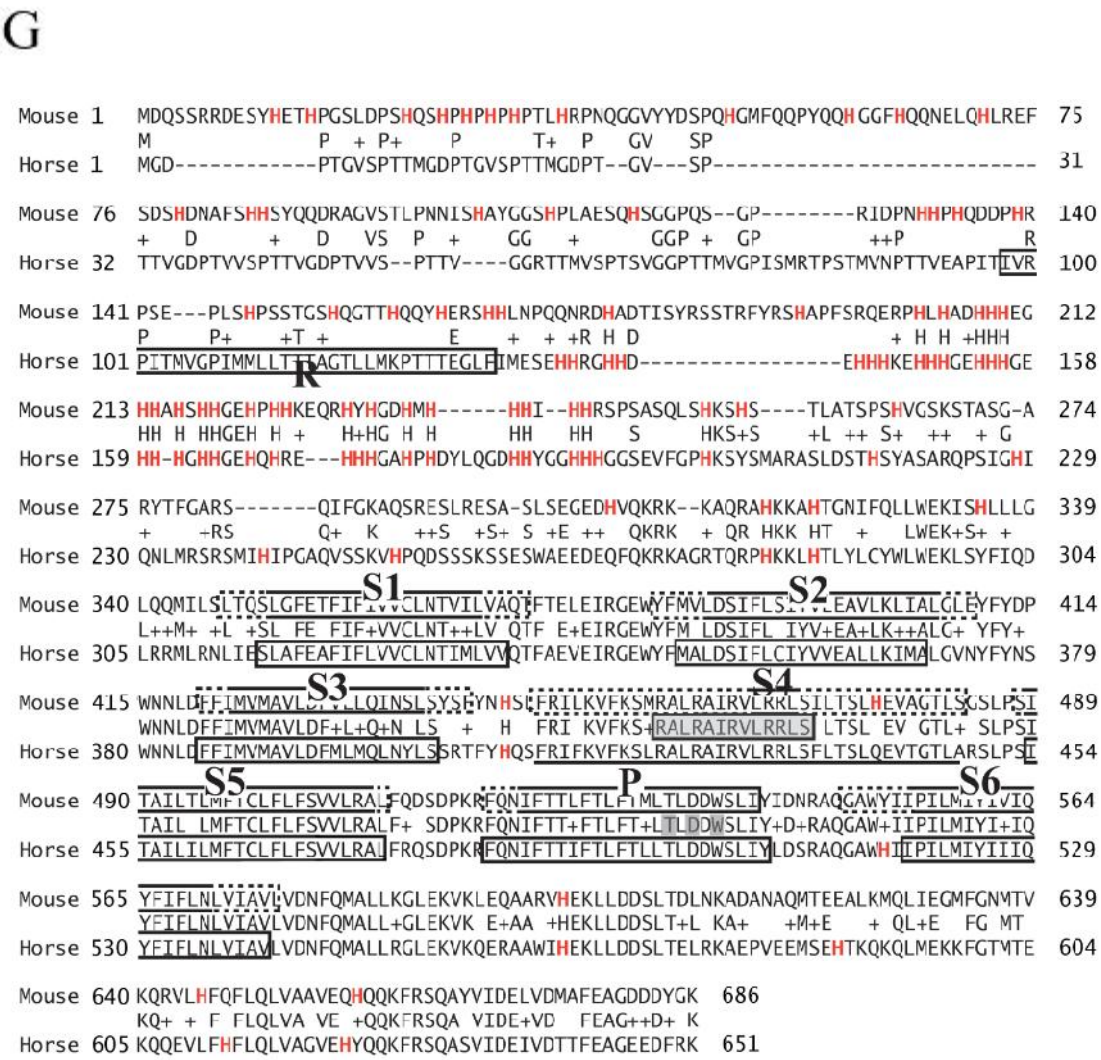

Figure 3.10. Continued

The restriction of histidines in the equine protein to the post-Segment R region suggests that region R is likely to be a transmembrane segment serving to internalize the histidine-rich region, and that the N-terminus of the equine protein may be external. This suggests a marked difference in both protein conformation and pH regulation between equine CATSPER1 and the murine and human proteins, combined with possible increased sensitivity to the extracellular environment if the N-terminus is indeed extracellularly located.

In-situ Immunocytochemistry for the CATSPER1 Protein

CATSPER1 in mouse and human sperm distributes to the principal piece. Fluorescence localized to the principal piece was detected in equine sperm stained with the anti-human C-terminus CATSPER1 antibody (Figure 3.11). Staining was seen in 100% of the sperm examined. A minimum of 100 sperm were analyzed per replicate with 3 replicates performed.

Western Blot for Presence of CATSPER1 Protein

A distinct band was seen at 72 kDa on Western blotting of proteins extracted from ejaculated equine sperm, using the anti-human CATSPER1 C-terminus antibody (Figure 3.12). The size was consistent with the predicted size for CATSPER1 in equine sperm. This band was absent in fibroblasts.

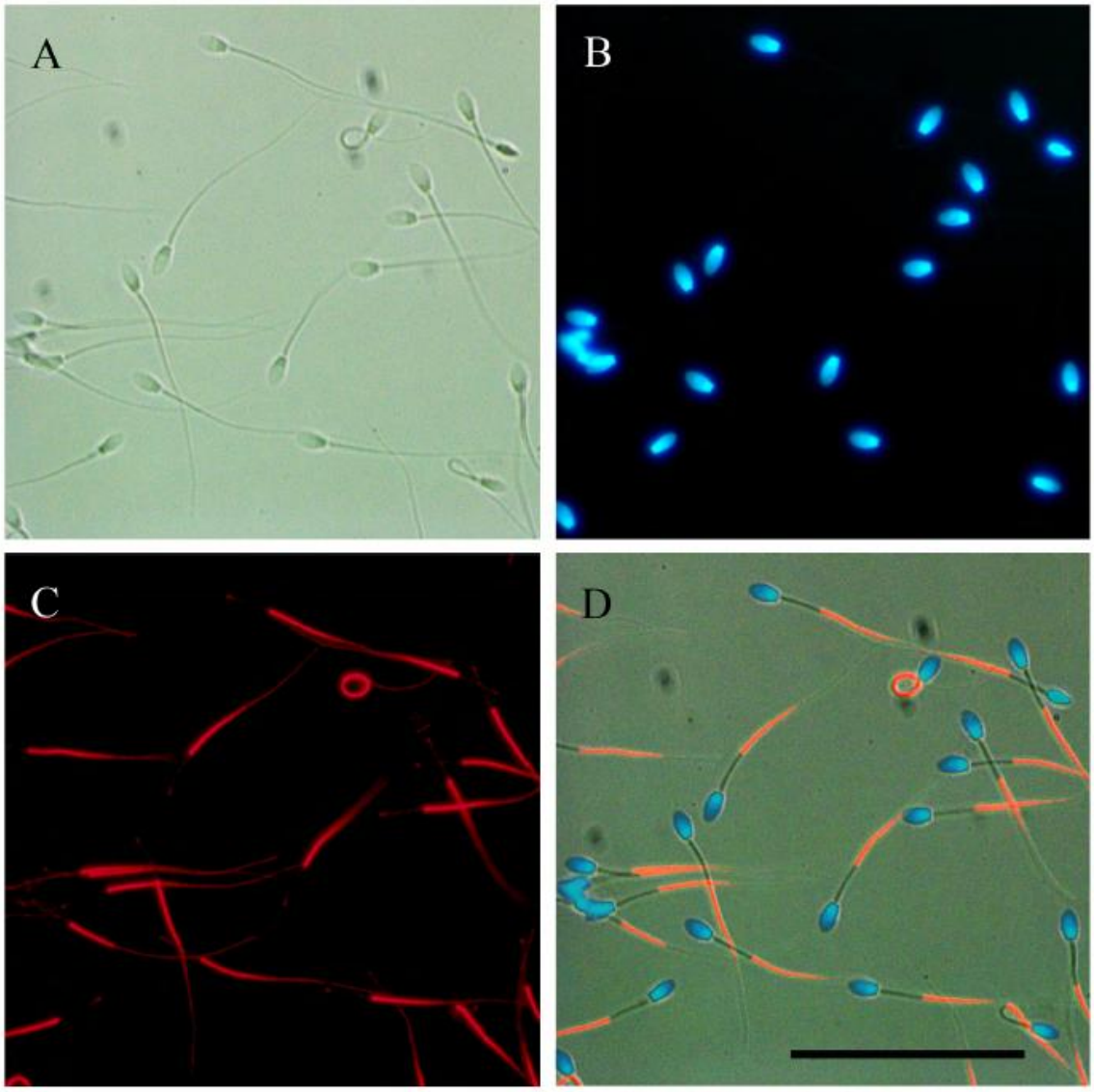

Figure 3.11. Immunocytochemistry of CatSper1 in equine sperm. Photomicrograph of equine sperm after labeling. A) Brightfield; B) DAPI; C) Rabbit anti-human CATSPER1 immunostaining D) Overlay of all three images. Bar = 50 µm. Staining was repeated four times using semen from three separate stallions.

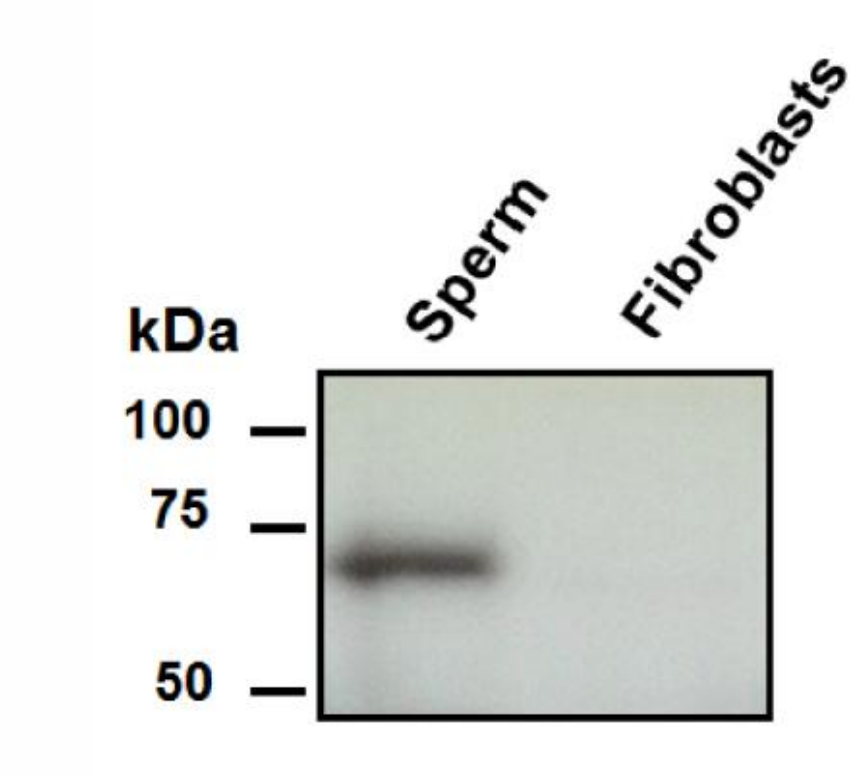

Figure 3.12. **Western blot analysis for CatSper1 protein.** Immunolabeling showed detection of a 72-kDa protein by rabbit anti-human CATSPER1 C-terminus antibody in equine sperm; the protein was not present in equine fibroblasts. The Western blot was repeated three times with a different stallion's semen used for each replicate.

DISCUSSION

This study was conducted to investigate the mechanisms underlying the failure of equine sperm to fertilize oocytes under standard in vitro conditions. The high IVF rate which has been achieved by treating equine sperm with procaine to stimulate hyperactivation [6, 86] suggests that the poor success of standard equine IVF may be related to the inability of typical capacitating conditions to adequately induce hyperactivated motility in equine sperm. Hyperactivation in sperm of other species is dependent upon presence and function of the pH-gated cation channel, CatSper; therefore, we investigated the function and presence of this channel in equine sperm. We found that the three effective hyperactivating stimuli (high-pH medium, 4-AP and procaine) produced a remarkably similar, moderate increase in BCECF fluorescence in equine sperm above that seen in control sperm (F_{488}/F_{440}; control - 5.72 ± 0.22; 4-AP – 6.30 ± 0.20; procaine – 6.40 ± 0.20; pH 8.5 medium - 6.91 ± .15). Increasing pH_i further by increasing treatment pH (pH 7.25, 8.5 or 9.5 medium) induced a dose-dependent increase in $Ca_{i,}$ (Figure 3.2) supporting the existence of functional CatSper channels, as calcium influx in response to intracellular alkalinization is CatSper-dependent in mice [186]. *CATSPER1* mRNA has been shown previously to be present in equine sperm [202], and we confirmed that CATSPER1 protein was present in equine sperm and that the protein was localized to the principal piece, as in other species. Treatment of equine sperm with mibefradil [272], a specific blocker of CatSper channels in human sperm [201, 270], reduced the influx of Ca^{2+} associated with intracellular alkalinization, further supporting the concept that the alkaline-induced Ca^{2+} influx occurs via CatSper.

While these data suggest that equine CatSper channels may operate similarly in response to intracellular alkalinization as do those of other species, we found several unusual features in the equine system. In earlier results from our laboratory [202], peak hyperactivated motility in response to NH_4Cl was seen in bull sperm 5 min after NH_4Cl addition, but occurred at 60 min in stallion sperm, and, in our hands, required a 5% CO_2 atmosphere. This delay to onset of hyperactivation was not constitutive, as subsequent trials with high-pH medium showed that equine sperm were capable of rapid onset of hyperactivation (Figure 3.2). In murine sperm, the alkalinizing effect of NH_4Cl decays over time [273]; it is possible that in the horse, hyperactivation with NH_4Cl occurred only when pH_i decayed to an appropriate level, then potentially only when any excessive increase in Ca_i induced by hyper-alkalinization also was restored to functional levels. Thus, the delay in response to NH_4Cl in equine as compared to bovine sperm suggests differences in regulation of pH_i, or greater pH or Ca^{2+} sensitivity for induction of hyperactivation, in equine sperm. Unfortunately, we were unable to analyze changes in pH_i and Ca_i over time in NH_4Cl-treated sperm due to the requirement for a CO_2 atmosphere since we did not have access to a plate reader with the capability to maintain a 5% CO_2 atmosphere; extensive attempts to achieve repeatable hyperactivation with this compound in air by adjusting medium pH, bicarbonate or buffer system were unsuccessful.

We found that the relationship of onset of hyperactivated motility to calcium influx differed in equine sperm from that reported in other species. The degree of hyperactivated motility appeared to be inversely related to the rise in Ca_i, as shown by

the findings that A) 4-AP induced a lower Ca_i than did pH 8.5 medium, but resulted in a greater degree of hyperactivation; B) treatment with 1 μM ionomycin induced the same pH_i but higher Ca_i than did 4-AP or pH 8.5 medium, and was not associated with hyperactivation, whereas in other species, micromolar concentrations of ionomycin or calcium ionophore A23187 induce hyperactivation [188, 264, 267-269]; C) suppression of Ca^{2+} influx with mibefradil increased hyperactivated motility in response to treatment with high-pH medium; and D) procaine, which induced the greatest degree of hyperactivation, showed no apparent Ca_i response to mibefradil, suggesting that the effects of this compound may not be associated with a CatSper-related calcium influx.

Determining the mechanism by which procaine induces hyperactivated motility in equine sperm is important, as procaine treatment is, thus far, the only sperm treatment associated with efficient IVF in the horse. Unfortunately, the direct Ca_i response to procaine could not be evaluated due to quenching of the fluorophore. However, the actions of procaine on CatSper may be inferred from its action on sperm in calcium-deficient media. In the absence of environmental calcium, CatSper functions as a voltage-independent Na^+ channel [177, 274]. Torres-Flores, et al. [270] demonstrated in human sperm that the loss of motility seen in calcium-deficient media is due to the influx of sodium through CatSper channels, rather than to the absence of calcium. Thus, in calcium-deficient media containing sodium, treatments that result in opening of CatSper channels would be predicted to result in suppression of total motility. We found this effect in equine sperm treated with high-pH medium. The lag in suppression of total motility seen with high-pH medium in our study is comparable to the slow depression of

motility by Na^+ influx (~10 min to steady state) reported by Torres-Flores, et al. [270] In contrast, the maintenance of both total and hyperactivated motility in equine sperm treated with procaine in the absence of environmental calcium suggests that procaine does not induce opening of CatSper channels in equine sperm, and also that it exerts its initial hyperactivating effect without need for influx of external calcium. This may be a species-specific finding, as Marquez and Suarez [87] reported that in bull sperm, procaine did not induce hyperactivated motility in calcium-deficient medium, and procaine has been used as a CatSper activator in mice [180]. Mujica, et al. [275] reported that procaine induced hyperactivation in guinea-pig sperm in medium with no added calcium; however these observations were in pH 7.8 medium and are complicated by the lack of a non-procaine-treated control. The slow loss of procaine-induced hyperactivated motility over time in calcium-deficient media, which occurred more quickly in EGTA-containing medium, indicates that influx of extracellular calcium is eventually required for continued hyperactivated motility in equine sperm.

In our study, while mibefradil treatment lowered Ca_i in the high-pH and 4-AP treatments, it did not suppress the initial (1 min) induction of hyperactivated motility in any treatment. To the best of our knowledge this represents the first study on the effect of mibefradil on sperm hyperactivated motility in any species. In murine sperm, the proprietary compound HC-056456, a potent CatSper blocker, inhibited the rise in Ca_i evoked by alkaline depolarization, prevented the development of hyperactivated motility during capacitation, and reversed hyperactivation after its onset [274], consistent with a direct role of Ca^{2+} influx in stimulation of hyperactivated motility in

this species. The difference in effect of CatSper inhibitors on hyperactivation between mouse and horse sperm again supports the existence of species-specific differences in the relationship of Ca_i to sperm hyperactivated motility.

From these data, we postulate that hyperactivated motility in equine sperm occurs within a narrow window of moderately elevated pH_i, but may not require an increase in Ca_i, and is suppressed by elevations in Ca_i within a range that would support hyperactivated motility in other species. This latter concept is interesting in light of our recent finding that environmental calcium suppresses capacitation-related protein tyrosine phosphorylation in equine sperm in a pH-dependent manner [28]. The current data suggest that calcium may exert a similar suppressive effect on sperm hyperactivated motility in the horse.

The most repeatable and effective methods to induce hyperactivated motility in our study were treatment with 4-AP and procaine. The mechanisms by which these compounds stimulate hyperactivated motility are unclear. Both 4-AP and procaine are weak bases and thus increase pH_i. The effect of 4-AP on sperm ion currents is not well understood; 4-AP is a commonly-used blocker of voltage-gated potassium channels in other systems, and has been shown to block SLO3 K+ channels [276] and the major, multistate ion channel flux of human sperm [277]. However, 4-AP has a stimulatory effect on CatSper current, Ca_i, and I_{ksper} in murine sperm [233, 278], and has been reported to mobilize internal Ca^{2+} stores [156]. In our study, it appeared that 4-AP may have a CatSper-related component, as suggested by the decrease in Ca_i associated with mibefradil treatment. On the other hand, 4-AP maintained motility in calcium-deficient

medium better than did pH 8.5 medium, suggesting that CatSper channels were not completely functional in this treatment. This is in agreement with the lower Ca_i induced by 4-AP than by pH 8.5 medium in calcium-containing medium, at the same pH_i (Figure 3.3.C).

There are conflicting data on the mechanism of procaine-induced hyperactivation. Marquez et al. [255] reported that procaine stimulated hyperactivated motility in sperm from wild-type, but not *Catsper1*-null mice, and concluded that procaine was a CatSper activator. However, Carlson, et al. [254] reported that procaine treatment caused the same increase in wave asymmetry in *Catsper1*-null mice as it did in wild-type mice, and concluded that procaine acted without involvement of CatSper. Our results with procaine in the presence of mibefradil, and in calcium-deficient medium, are consistent with the hypothesis that in equine sperm, procaine treatment does not open CatSper channels.

In conclusion, the findings of these studies demonstrate that CATSPER1, and thus likely the CatSper channel, are present in equine sperm. The equine CATSPER1 protein differs structurally from that of other species in its histidine-rich (pH-sensor) region and N-terminal domain. Our data suggest that, as in other species, the equine CatSper channel opens to allow calcium influx in response to increased pH_i; however it is not clear whether opening of the CatSper channels or an increase in Ca_i is required for onset of hyperactivated motility in this species. Failure of stimulation of hyperactivated motility in equine sperm under conditions that capacitate sperm of other species may be related to a narrow window of pH_i and Ca_i at which this motility occurs in the horse.

Research is thus warranted on the effects of environmental pH and calcium on fertilization both in vivo and in vitro. To the best of our knowledge, this is the first report on intracellular factors associated with sperm hyperactivated motility in the horse, a species in which effective in vitro capacitation is still problematic. These findings add to our knowledge of the comparative biology of sperm motility, and should provide a basis for much future research to define the factors associated with effective sperm-oocyte interactions in this species.

CHAPTER IV

REGULATION OF AXONEMAL MOTILITY BY CALCIUM AND PH IN DEMEMBRANATED STALLION SPERMATOZOA

INTRODUCTION

Historically, equine in vitro fertilization (IVF) has had poor success [1, 2, 5]. This failure is postulated to be due to the lack of induction of hyperactivated motility in equine sperm in standard capacitation media, as one laboratory reported a 60% fertilization rate after treatment of sperm with procaine, a powerful inducer of hyperactivation [6]. Hyperactivated motility is crucial for the final stages of fertilization; it provides sperm with sufficient force to swim through the viscous environment of the oviduct, advance through the cumulus, and penetrate the zona pellucida [37, 46, 47, 210, 279, 280]. The apparent inability of equine sperm to spontaneously undergo hyperactivated motility under standard in vitro capacitating conditions suggests that there is a fundamental difference in regulation of hyperactivated motility between sperm of horses and those of other species.

In other species, hyperactivated motility has been shown to be dependent upon the pH-regulated calcium ion channel, CatSper [47, 188]. The current working model for initiation of hyperactivated motility is that capacitation induces an increase in intracellular pH, causing the CatSper channel to open [47, 188]. The resultant influx of extracellular calcium may directly affect axonemal function, may open intracellular

calcium stores resulting in calcium oscillations, or may act a second messenger to stimulate hyperactivated motility via enzymes such as calmodulin or calmodulin kinase II [47, 139, 188, 203]. We previously found that equine sperm possess CATSPER1 protein, and that intracellular alkalinization induces an increase in intracellular calcium which is partially blocked by the CatSper inhibitor, mibefradil, suggesting functional CatSper channels in this species [281]. However, in contrast to findings in other species, we found that the degree of hyperactivated motility induced by different stimuli appeared to be inversely related to intracellular calcium concentrations, and that calcium may largely play an inhibitory role in induction of hyperactivation in equine sperm. This suggests a major difference in the calcium-related regulation of motility in equine sperm.

One method to directly assess the effect of intracellular factors on axonemal function is the use of demembranated sperm which allows the investigator to directly control the environment of the axoneme and its related proteins. Coordinated motility in a demembranated sperm model was first reported in 1968 [120], and demembranated sperm have proven to be a powerful and useful model for studying the regulation of sperm motility. The most commonly used method of demembranization is treatment with Triton X-100 [121], however, there is no consensus as to the optimal protocol, and concentrations used vary from 0.04% to 0.2% (v/v; [122-125]. To the best of our knowledge, only one report on demembranated sperm is available in the horse [282]. In that report, sperm from the cauda epididymis were empirically treated with the non-ionic detergent Brij-35; treated sperm required ATP to reactivate motility and incorporate

phosphate into protein under stimulation by cAMP. Presence of ATP appears to be a universal requirement for motility in demembranated sperm [122, 127, 128].

Little work has been done to determine the requirement for calcium in demembranated sperm. In the bull, demembranated sperm exposed to <1 nM calcium had a significant decline in motility [122]. In contrast, demembranated hamster sperm have been reported to be motile, and even hyperactivated, in the absence of calcium [283], however the amount of EDTA added to reactivation medium in this study (maximum of 580 μM) would have likely resulted in calcium still present at the nM level. No loss of motility was seen in demembranated sea urchin sperm exposed to free calcium levels as low as 100 pM [284].

In demembranated mouse, rat, bull, monkey and sea urchin sperm, increasing calcium has been shown to increase characteristics of hyperactivated motility, such asymmetrical beating and increased curvilinear velocity (VCL) [122, 124, 140-142]; for example, the percentage of demembranated bull sperm exhibiting hyperactivated motility increased from 20% to 80% as medium calcium concentration increased from 50 to 400 nM [122]. This direct effect of calcium on the axoneme reflects the current understanding of the pathway for hyperactivation in intact sperm, i.e., that capacitation-related changes, notably intracellular alkalinization, cause opening of the sperm-specific cation channel, CatSper, resulting in calcium influx which directly or indirectly stimulates the onset of hyperactivated motility [47, 187].

Medium pH is an important factor in re-establishing motility in demembranated sperm, as sperm fail to reactivate at extreme pHs [122, 154, 155]. Maximum motility is

achieved in demembranated bull sperm from pH 7.0 to 8.1, at pH 7.8 in demembranated human sperm and between 7.5 and 8.0 in demembranated ram sperm [122, 154] [285, 286]. The effect of cAMP is controversial in demembranated sperm, with several groups finding it is essential for motility restoration [130, 131], while others find no effect [122, 135].

Both nickel and cadmium inhibit motility of demembranated sperm and cilia, and also inhibit calcium-induced flagellar curvature in rat sperm [140]; however. these two metals appear to have different mechanisms of action. Nickel requires a relatively high concentration (200 µM to 1.33 mM) to exert its effect on demembranated sperm [140, 159, 160]. In contrast, cadmium inhibits motility at concentrations as low as 1 µM [140]. Addition of EGTA to the medium is able to diminish the effect of nickel but not of cadmium, although both are strongly chelated by EGTA [150]. Nickel is implicated in suppression of ATPase activity in one of the heavy chains of sperm dynein [161], and preferentially blocks interdoublet sliding on one side of the axoneme (9,1,2 [150]). The action of cadmium is less clear, but it has been suggested that cadmium works via a calmodulin-mediated effect [140, 287, 288], and, like nickel, cadmium has been shown to block sliding of 9,1,2 microtubule doublets [150].

Procaine and 4-AP are stimulators of suggestive hyperactivated motility patterns in equine sperm [281], but their mechanisms of action in this area are unknown. As both compounds are known ion channel regulators, it is likely that they induce hyperactivation through changing the intracellular environment via ion channels, such as

the CatSper channel [180, 289]. However, the possibility exists that they may exert their effects directly on the sperm axoneme.

In this study, we determined the optimal protocol for demembranization of stallion sperm and used this model to study the direct effects of calcium concentration, pH, ATP, dibutyryl-cAMP (dbcAMP), nickel and cadmium, as well as the pharmacological stimulators of hyperactivated motility, procaine and 4-AP, on the activated and hyperactivated motility of demembranated equine sperm.

MATERIALS AND METHODS

Chemicals and Media

All reagents were purchased from Sigma Aldrich (St. Louis, MO, USA) unless otherwise stated. Propidium iodide and BCECF-AM was purchased from Invitrogen (Grand Island, NY, USA). Reagents for transmission electron microscopy were purchased from Electron Microscopy Supplies (Hatfield, PA, www.emsdiasum.com). Free calcium levels were calculated using MaxChelator (http://maxchelator.stanford.edu), taking into account the ionic value of the medium (0.0145), the concentrations of EGTA, $MgSO_4$, adenosine 5'-triphosphate disodium salt hydrate (ATP) and calcium added, media pH and incubator temperature.

Demembranization medium (DeM) consisted of 25 mM potassium glutamate, 220 mM sucrose, 10 mM HEPES, with 0.02% polyvinyl alcohol (PVA; v/v) added to minimize agglutination. Medium pH was adjusted to 7.4 ± 0.02 immediately prior to use unless otherwise stated.

Unless otherwise noted, the reactivation medium (ReM) consisted of 25 mM potassium glutamate, 220 mM sucrose, 10 mM HEPES, and 0.02% PVA (v/v) with 2 mM each of EGTA, $MgSO_4$ and ATP. $CaCl_2$ was added in a sufficient quantity to provide 100 nM free calcium, as calculated with MaxChelator, and the medium pH was adjusted to 6.90 ± 0.02 immediately prior to use.

The medium used for capacitation was modified Whittens medium (MW) at pH 7.25 containing 100 mM NaCl, 4.7 mM KCl, 1.2 mM MgCl2, 5.5 mM glucose, 22 mM HEPES, 2.4 mM sodium lactate, 7 mg/mL bovine serum albumin, 1 mM sodium pyruvate and 25 mM sodium bicarbonate.

The medium used for calibration of intracellular pH was a modified TALP medium at pH 7.25, containing 77.5 mM NaCl, 3.1 mM KCl, 1.1 mM $MgCl_2$, 0.4 mM NaH_2PO_4, 5 mM Glucose, 10 mM HEPES, 25.4 mM sodium lactate, 25 mM sodium bicarbonate, 1 mM sodium pyruvate, 2 mM $CaCl_2$ and 0.02% polyvinyl alcohol. High potassium TALP was identical, although the concentrations of NaCl and KCl were changed to 3.1 mM and 102.5 mM, respectively. Bicarbonate was excluded from the high-potassium medium.

Semen Collection, Preparation and Motility Evaluation

Fresh equine semen was collected from five sexually mature, light-breed stallions using an artificial vagina. Removal of debris and the gel fraction of the ejaculate was performed using an inline nylon micromesh filter (Animal Reproduction Systems, Chino, CA, USA). All experimental procedures were performed according to the *United*

States Government Principles for the Utilization and Care of Vertebrate Animals Used in Testing, Research and Training and were approved by the Laboratory Animal Care Committee at Texas A&M University.

For demembranization, semen was diluted 1:5 in DeM, washed twice via centrifugation at 400 x g for 10 min, then resuspended to 300 x 10^6 sperm/ml in DeM prior to treatment with Triton X-100 as described below. Sperm were used within one h of resuspension. Sperm prepared for intracellular pH calculations were processed identically, except were diluted in either modified TALP or high potassium TALP.

For incubation for capacitation, semen was diluted 1:5 in MW. The suspension was centrifuged for 1 min at 170 x g to remove debris, then the supernatant was centrifuged for 5 min at 600 x g to wash. Sperm were extended to 10 x 10^6 in MW and incubated for four h in air in the absence of calcium (Gonzalez-Fernandez et al., 2012). Following the capacitating procedure, sperm were centrifuged for five min at 600 x g, resuspended in DeM at 300 x 10^6 sperm/ml, and demembranated as described below.

Sperm motility was evaluated by computer assisted sperm analysis (CASA; Hamilton Thorne). Parameters analyzed included total percent motility (% motile), percent progressively motile (% progressive), curvilinear velocity (VCL), amplitude of lateral head displacement (ALH), beat cross frequency (BCF) and linearity (LIN). Values for VCL and ALH were used as markers of hyperactivated-like motility [281]. For simplicity, only the results from VCL, ALH and/or % motile are shown. Between 700 and 1600 sperm were evaluated for each replicate of each treatment. A minimum of three replicates were performed for each experiment.

Demembranization

To optimize the protocol for demembranating equine sperm, we evaluated both percent total motility and the percent of the sperm population permeabilized, after treatment with different concentrations of Triton X-100 for varying time periods (immediate, 30 s, 60 s). Motility analysis was performed by CASA, as described above, and an aliquot of sperm was concurrently exposed to 1 µM propidium iodide (PI) for five min at 37°C [290]. The % permeabilized (PI-stained) sperm was determined by processing stained spermatozoa through a FACScan flow cytometer (Becton-Dickinson Immunocytometry Systems, San Jose, CA, USA) set on channel FL2, with excitation at 488 and emission read at 585 / 42 at 400 V. A minimum of 5000 events per sample were recorded.

For preliminary analysis, Triton X-100 was added to sperm suspended in DeM, at final concentrations of 0.5%, 0.1%, 0.01%, 0.05% or 0.001% (v/v), then the suspensions were diluted 1:10 in ReM. Motility was evaluated immediately following dilution. Sperm extended in ReM without exposure to Triton X-100 were analyzed as a control.

Results of the preliminary analysis showed that maximum motility and permeabilization occurred at concentrations of Triton X-100 between 0.01% and 0.05%, therefore a second trial was conducted using Triton X-100 at 0.01%, 0.02%, 0.03%, 0.04% and 0.05%. Maximum motility and permeabilization occurred in sperm exposed to 0.02% (v/v) Triton X-100 for 30 s; therefore, this method was used for demembranization in the remainder of the trials.

Electron Microscopy

Demembranated sperm samples were fixed in 0.1 M sodium cacodylate buffer at pH 7.4 with 2% glutaraldehyde and 2.5% formaldehyde. Samples were stained with 1% OsO_4, with 0.4% potassium ferrocyanide for one h at 4°C, then enrobed in 1% agar with 0.05 M sodium cacodylate buffer and dehydrated with serial ethanol washes prior to embedding in epon araldite with 1.5% DMP-30. Ultrathin sections were taken and analyzed with an FEI Morgagni 268 transmission electron microscope (FEI, Hillsboro, OR, www.fei.com) at an accelerating voltage of 80 kV. Digital images were acquired with a MegaViewIII camera operated with iTEM software (Olympus Soft Imaging Systems, Germany).

Calculation of Intracellular pH

To calculate the intracellular pH of intact sperm for comparison with pH of medium used in demembranated sperm, intact sperm were processed in a modified TALP medium at pH 7.25, as described above. Washed sperm were incubated at 300 x 10^6/mL with 5 µM BCECF-AM for 30 min at 25°C in the dark, then centrifuged to remove excess stain. Sperm were resuspended in fresh medium and incubated for 30 min to allow for full de-esterification of the dye. Aliquots (200 µM) were loaded into a 96-well plate of a Synergy MX microplate reader (Bio-Tek; www.biotek.com) and excited at 440 and 488 nm, with emission read at 535 nm. Three baseline measurements were recorded for each well, then treatments were added (high-pH treatments were resuspended at this time) and wells were read an additional three times.

The sperm used for the calibration curve were processed as described above, except with high-potassium TALP instead of modified TALP. Following the final centrifugation, sperm were extended to 300 x 10^6/mL in pH 7.25 high-potassium medium, then diluted 1:9 in media ranging from pH 5.5 to 8.5. Two aliquots were taken from each pH for fluorescence analysis, then the actual pH of each sample was determined using an Accumet Excel XL60 pH meter (Fisher Scientific; Waltham, MA); this measurement was used to create the calibration curve. Five µM of the H^+/K^+ ionophore, nigericin, was added to equilibrate intracellular and extracellular pH. Sperm for the calibration curve were read on the plate reader concurrently with the control sperm and an equation was derived from the curve to determine the actual intracellular pH of the modified TALP-treated sperm. A representative calibration curve is shown in Figure 4.1.

Motility Trials

To determine the effect of ATP concentration on equine sperm motility, sperm were demembranated as above, and resuspended in ReM containing varying levels of ATP. Concentrations evaluated were 0, 1, 2, 3, 4, 5, 7.5 and 10 mM ATP, with $MgSO_4$ added in a 1:1 ratio with ATP. The "0" sample lacking ATP still contained 1 mM of $MgSO_4$. The effect of cAMP on demembranated sperm was evaluated by including 0, 5, 10, 15, 20, 25, 30, 100, 500 or 1000 µM db-cAMP in ReM containing 2 mM ATP at pH 6.9.

The effect of pH on demembranated sperm was assessed by extending demembranated sperm in ReM whose pH was adjusted to values ranging from 4 to 10.5 (±0.02) in 0.5 pH-unit intervals, with calculated free calcium held constant at 100 nM. To study the effect of calcium concentration on the motility of demembranated equine sperm, samples were demembranated as above and diluted in ReM medium at pH 6.9, as this was found to support the greatest motility in preliminary trials. Free calcium levels were adjusted to 0 (2 mM EGTA; < 200 pM Ca^{2+}), 50 nM, 100 nM, 200 nM, 300 nM, 400 nM, 1 µM, 10 µM, 100 µM, and 1 mM; in addition, preparations with no added calcium and increased EGTA (4, 6, and 8 mM) were also evaluated. Free calcium levels calculated for these EGTA treatments are listed in Table 4.1, while the total calcium added to obtain a specific free calcium level is listed in Table 4.2.

	Free Calcium Level			
Tx	**2 mM EGTA**	**4 mM EGTA**	**6 mM EGTA**	**8 mM EGTA**
pH 5.9	46,770 pM	24,140 pM	16, 270 pM	12,270 pM
pH 6.4	5,032 pM	2,526 pM	1,686 pM	1,265 pM
pH 6.9	515 pM	258 pM	172 pM	129 pM
pH 7.4	54 pM	27 pM	18 pM	13 pM

Table 4.1. Free calcium in EGTA-treated samples. Free calcium levels were calculated in samples with various amounts of EGTA added by MaxChelator (www.stanford.edu/maxchelator). Factors taken into account include ATP, EGTA, initial calcium, magnesium, pH, temperature and ionic strength of the medium.

	Total Added Calcium								
Tx	**50 nM**	**100 nM**	**200 nM**	**300 nM**	**400 nM**	**1 µM**	**10 µM**	**100 µM**	**1 mM**
pH 5.9	2.1×10^{-6}	4.2×10^{-6}	8.3×10^{-6}	1.3×10^{-5}	1.7×10^{-5}	4.1×10^{-5}	3.6×10^{-5}	1.6×10^{-4}	3.6×10^{-4}
pH 6.4	1.9×10^{-5}	3.9×10^{-5}	7.6×10^{-5}	1.1×10^{-4}	1.5×10^{-4}	3.3×10^{-4}	1.4×10^{-3}	2.2×10^{-3}	3.7×10^{-3}
pH 6.9	1.8×10^{-4}	3.2×10^{-4}	5.6×10^{-4}	7.3×10^{-4}	8.7×10^{-4}	1.3×10^{-3}	1.9×10^{-3}	2.3×10^{-3}	3.7×10^{-3}
pH 7.4	9.6×10^{-4}	1.3×10^{-3}	1.6×10^{-3}	1.7×10^{-3}	1.8×10^{-3}	1.9×10^{-3}	2.0×10^{-3}	2.3×10^{-3}	3.8×10^{-3}

Table 4.2. Total calcium added by free-calcium level. Total calcium values added to each treatment to achieve a specified free calcium level as calculated by MaxChelator (www.stanford.edu/maxchelator). Factors taken into account include ATP, EGTA, calcium, magnesium, pH, temperature and ionic strength of the medium.

To determine if there was an interaction between calcium and pH in the induction of hyperactivated motility, sperm motility was evaluated in ReM containing 2, 4, 6 or 8 mM EGTA in the absence of added calcium, or with 50 to 1000 nM calculated free calcium, at pH values of 5.9, 6.4, 6.9 and 7.4.

To determine if the decline in motility seen in sperm exposed to 8 mM EGTA was due to chelation of calcium and magnesium, sperm were resuspended in ReM with 8 mM EGTA in the absence of calcium at pH 5.9, 6.4, 6.9 or 7.4, then were supplemented with magnesium, calcium, both calcium and magnesium, or media alone (control). In these treatments, calcium was added for a final calculated free calcium concentration of 100 nM, and magnesium was added so the final free magnesium concentration was equivalent to that seen in the 100 nM calcium treatment at the corresponding pH.

The above studies demonstrated that excessive calcium (> 400 nM) suppressed motility of equine sperm. To determine if the inhibitory effect of excess calcium was reversible, sperm were demembranated and extended in ReM either with or without 2 mM EGTA, each with the same amount of added $CaCl_2$, sufficient to provide 400 nM free calcium in the presence of 2 mM EGTA. Motility was evaluated in each treatment, then 2 mM EGTA was added to the non-EGTA-containing medium to bring the free calcium concentration down to 400 nM, at which point motility was re-evaluated.

To determine if the sensitivity of the equine sperm axoneme to calcium was altered in response to incubation in capacitating medium (medium which supports protein tyrosine phosphorylation; [28]), we examined the effect of calcium on the axoneme after demembranization of sperm exposed to conditions conducive to protein tyrosine phosphorylation for four h ("capacitated") vs. sperm demembranated immediately following processing ("non-capacitated"). Following demembranization, sperm were extended in ReM at pH 6.9 with calculated free calcium concentrations ranging from 129 pM (8 mM EGTA) to 1 mM, and motility was evaluated by CASA.

To evaluate the effects of cadmium and nickel, sperm were reactivated in ReM medium lacking EGTA with $NiSO_4$ or $CdSO_4$ added between 0 and 250 µM. Motility was analyzed immediately following reactivation. To determine if cadmium was able to counteract the decrease in motility seen with excessive calcium levels, sperm was reactivated in ReM containing either 20 µM cadmium, 2 µM free calcium or both cadmium and calcium combined.

To gain information on their effect on sperm, 5 µM medium or 5 µM medium containing treatments to provide a final concentration of 5 mM procaine or 4 mM 4-AP were added to sperm demembranated as described above. Motility was analyzed immediately prior to reagent addition, as well as one and 15 min following addition.

Statistical Analysis

Statistical analysis was performed by one-way ANOVA within each treatment, unless otherwise stated. The data was tested for an appropriate Gaussian distribution by the Shapiro-Wilk test and analyzed for equal variance. Non-Gaussian samples were transformed by taking the natural log distribution. If the data still did not conform, the non-parametric test, Kruskal-Wallis ANOVA on Ranks was used. Individual pair differences were analyzed post-hoc by Holm-Sidak. The level of significance was set as $P < 0.05$. All analyses were performed using SigmaPlot software (Systat Software, Chicago, IL).

RESULTS

Demembranization

The effect of exposure of sperm to Triton X-100 in concentrations ranging from 0.001% to 0.1% (v/v) is presented in Figure 4.1. The majority of sperm treated with 0.1% or 0.05% Triton X-100 for any time, were permeabilized (allowed PI staining), however, the percentage of motile sperm in both of these groups was significantly lower than that for intact sperm ($P < 0.05$; Figure 4.1.A).

In the second demembranization trial (0.01% to 0.05% Triton X-100; Figure 4.1.B), exposure of sperm to 0.02% Triton X-100 for 30 s provided optimal conditions, as 99% of the sperm stained with PI, independent of stallion, and motility was not significantly different from that for the equivalent intact sperm ($P > 0.2$).

Transmission electron microscopy was utilized to evaluate the extent of demembranization (Figure 4.2). In control sperm, the plasma and mitochondrial membranes were intact (Figure 4.2.A,B,C). Sperm demembranated with 0.02% Triton X-100 for 30 s had little membrane remaining on the principal piece and end piece, however, 70 – 80% of the plasma membrane remained over the midpiece, with multiple perforations visible in the plasma membrane (Figure 4.2.D,E,F). The inner and outer mitochondrial membranes were intact in the sperm demembranated with 0.02% Triton X, however, there was profound damage to the inner mitochondrial membranes in the sperm treated with 0.2% Triton X. Thus, several factors supported the use of the 0.02% Triton X-demembranization protocol for subsequent studies, including a permeabilization rate of 99%, continued integrity of the mitochondrial membranes and

thus potentially other intracellular structures, and greater maintenance of motility. This protocol was used for the remainder of the trials.

ATP and dbcAMP Motility Trials

The effect of ATP concentration on motility of demembranated sperm is presented in Figure 4.3. Sperm with no added ATP were immotile. Above 1 mM, ATP concentration did not affect total motility, however VCL, a measure of hyperactivated motility (Loux et al., *in press;* Chapter III) increased significantly with increasing [ATP] ($P < 0.001$). Sperm were highly agglutinated in media containing 7.5 or 10 mM ATP, making accurate motility analysis difficult. Addition of dbcAMP did not significantly affect any motility parameter ($P > 0.2$; Figure 4.4).

Calcium and pH Motility Trials

The calculated intracellular pH of intact, non-capacitated stallion sperm was 7.14 ± 0.07. Treatment of intact sperm with procaine or 4-AP, or incubation in pH 8.5 medium, resulted in intracellular pH values of 7.34 ± 0.07, 7.30 ± 0.07 and 7.40 ± 0.06, respectively. These treatments were selected due to their ability to induce hyperactivated motility in equine sperm [281].

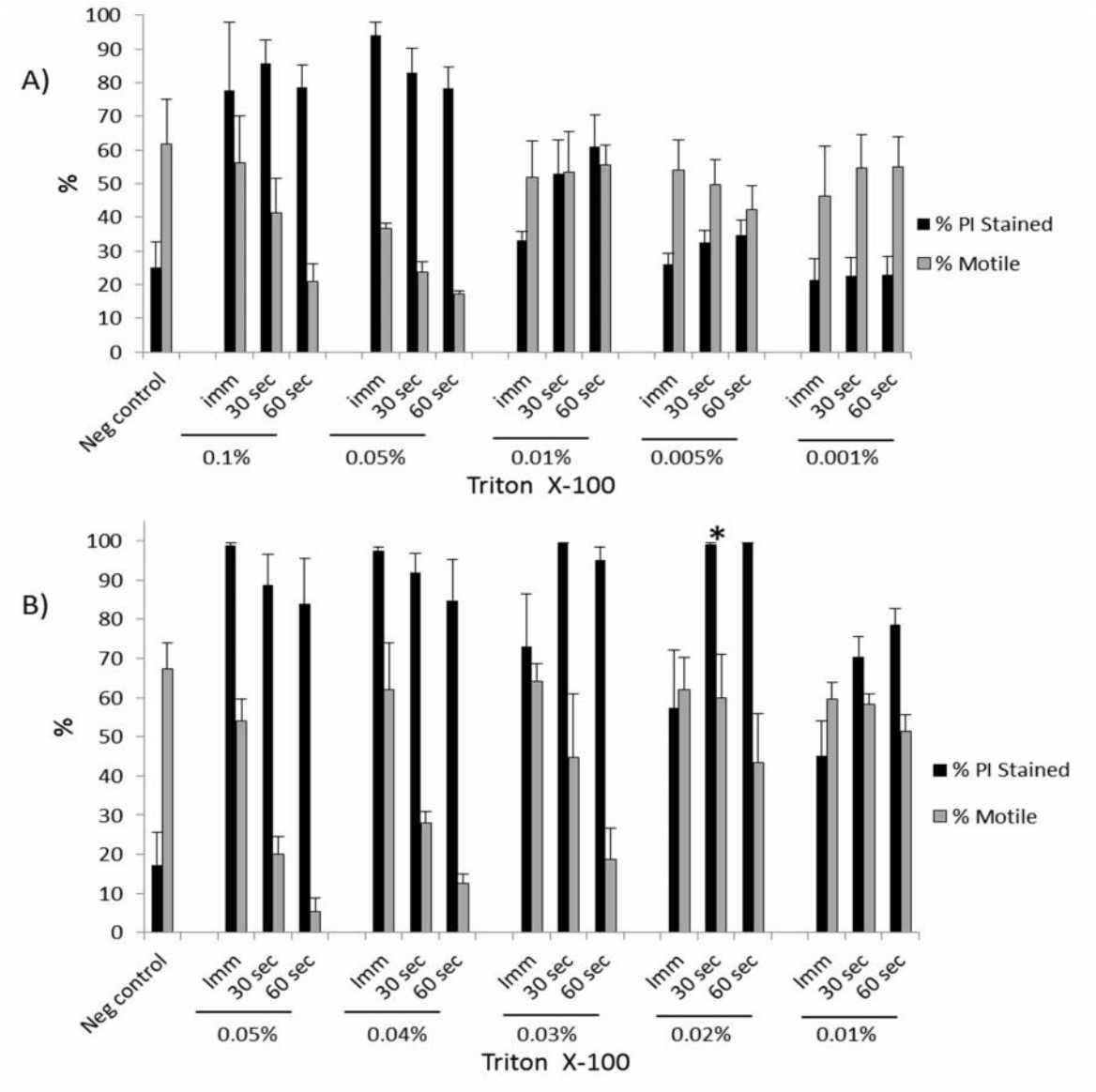

Figure 4.1. Evaluation of sperm following demembranization. Sperm were demembranized by exposure to either A) 0.1%, 0.05%, 0.01%, 0.005%, 0.001% Triton X-100 (v/v) or B) 0.01%, 0.02%, 0.03%, 0.04% or 0.05% Triton X-100 (v/v) for one of three time periods – immediate (~5 s), 30 s or 60 s. Following demembranization, sperm were diluted 1:10 in ReM. Total motility was assessed using CASA and membrane permeabilization was evaluated by staining with 1 µM propidium iodide (PI) stain for 5 min at 37° then processing through a flow cytometer. Concentrations run from highest (left) to lowest (right). Values represent the mean ± SE for three independent replicates with a different stallion used for each replicate.

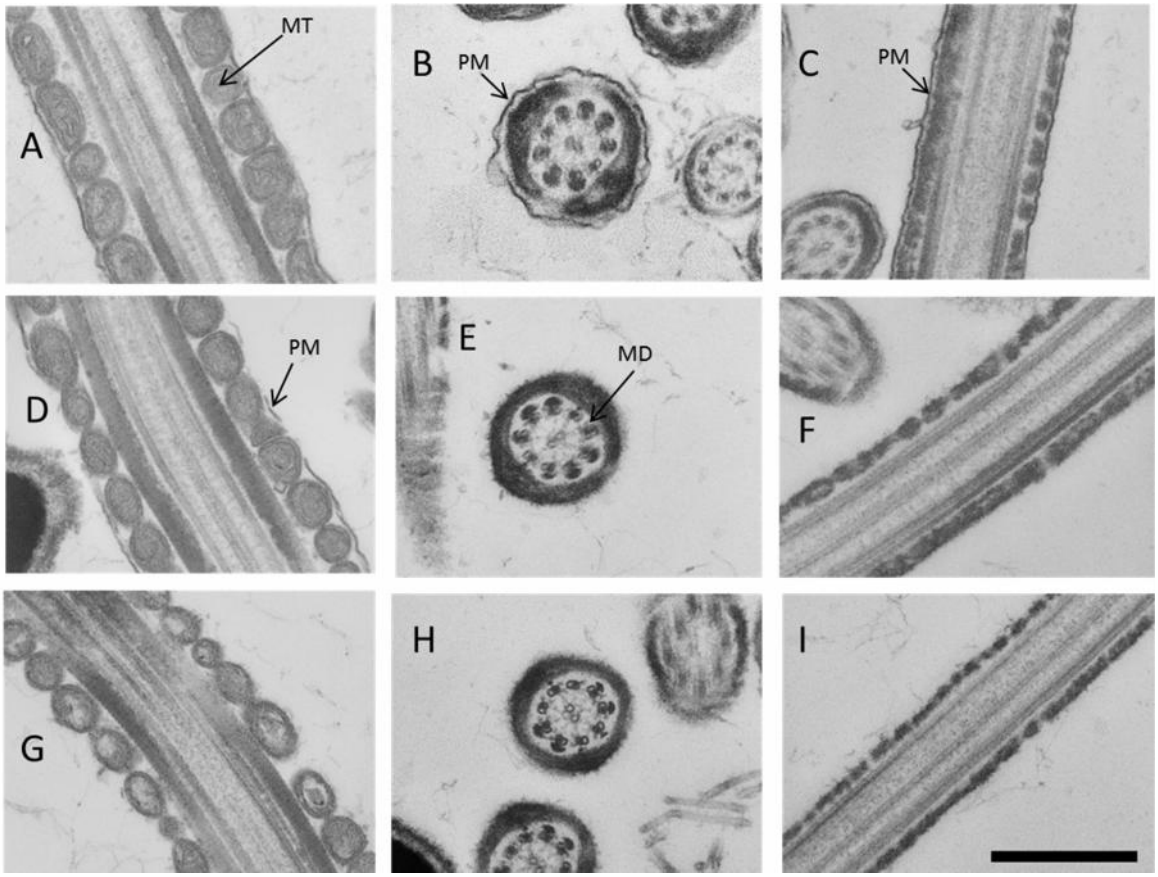

Figure 4.2. Transmission electron microscopy. Sperm were exposed to either (A,B,C) 0%, (D,E,F) 0.02% or (G,H,I) 0.2% Triton-X and subsequently analyzed via transmission electron microscopy. Sections examined included (A,D,G) the midpiece, (B,E,H) a cross section of the axoneme, or (C,F,I) a longitudinal section of the principal piece. (A,B,C) Control sperm maintained plasma membrane integrity in the majority of the specimens examined, while (D,E,F) sperm demembranated with 0.02% Triton X had little to no plasma membrane remaining on the principal piece, however, the plasma membrane on the midpiece (D) was 70-80% intact and mitochondrial membranes maintained their integrity well. (G,H,I) Sperm demembranated with 0.2% Triton X-100 had little to no plasma membrane remaining, regardless of location and (G) mitochondrial membranes were heavily damaged. None of the treatments had obvious damage to the microtubule doublets. PM – Plasma membrane; MT – Mitochondria; MD- Microtubule Doublets. Magnification was either (A, G) 56,000 or (B, C, D, E, F, H, I) 71,000. Scale bar is equivalent to 0.5 µm.

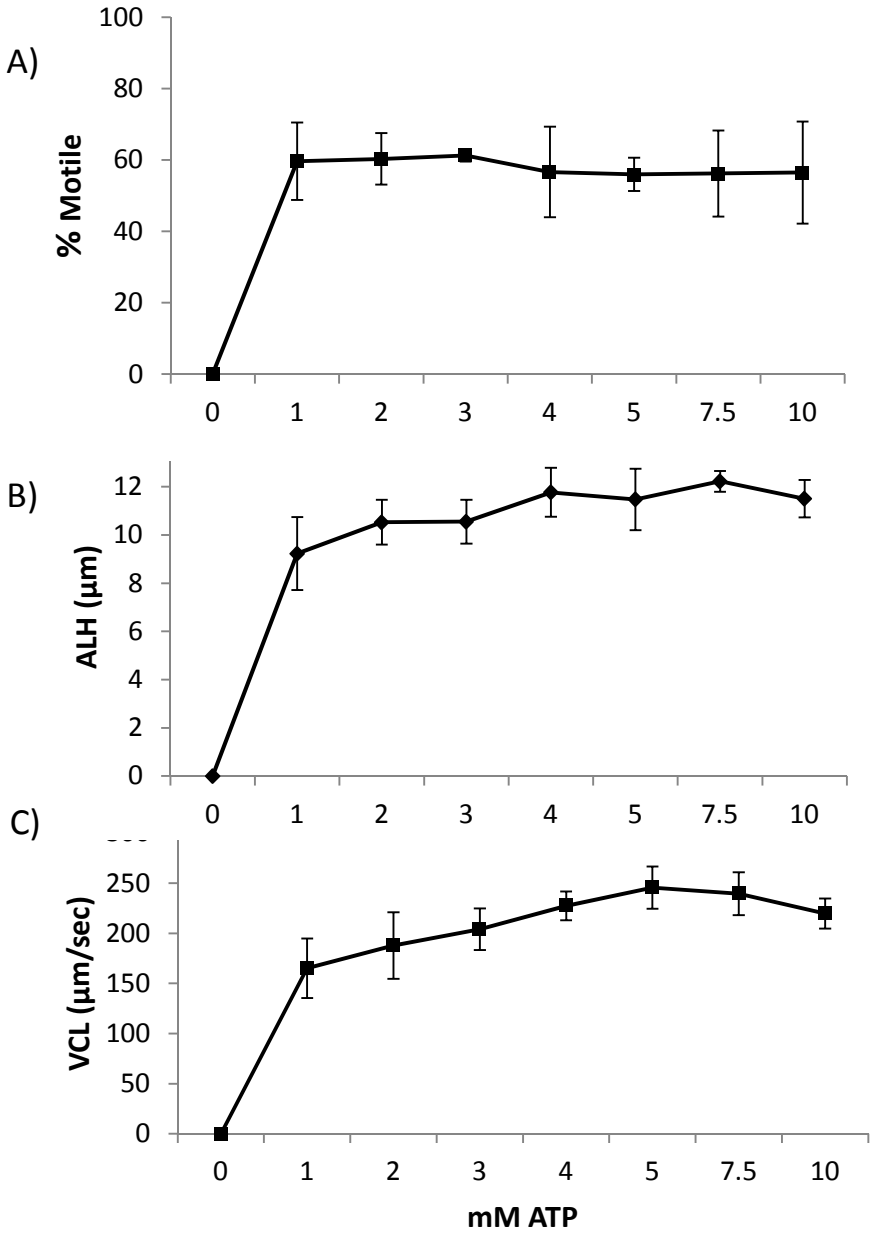

Figure 4.3. Effect of ATP concentration on demembranated sperm motility. Demembranated sperm were held at pH 6.9 with 100 nM free calcium and exposed to ATP between 0 and 10 mM. A) Total % motility, B) ALH and C) VCL were analyzed via CASA. Values represent the mean ± SE for three independent replicates with a different stallion used for each replicate.

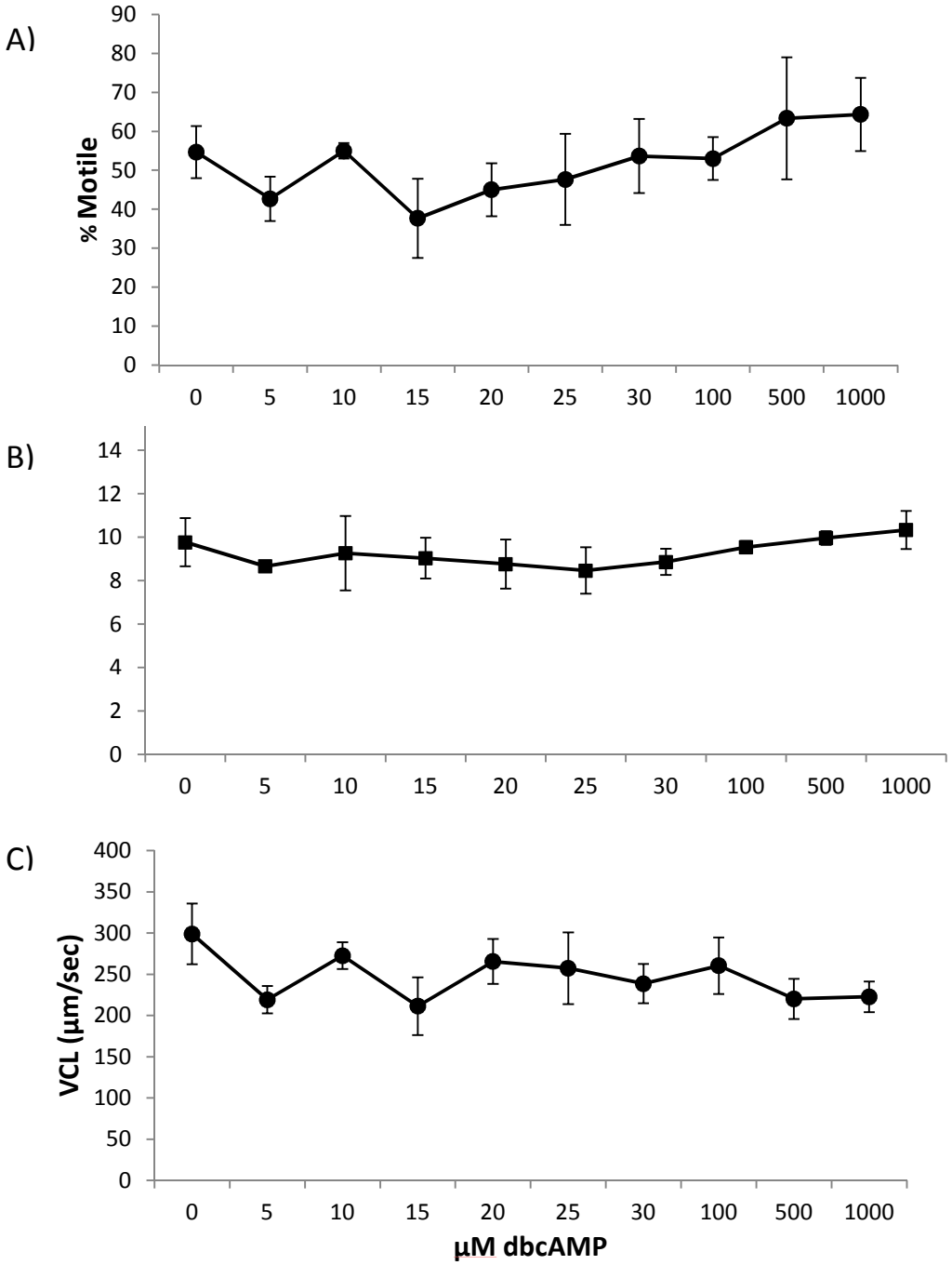

Figure 4.4. Effect of dbcAMP on demembranated sperm motility. Demembranated sperm were held at pH 6.9 with 100 nM free calcium and then exposed to dbcAMP at ranges from 0 and 1 mM. Parameters evaluated include A) total motility, B) amplitude of lateral head movement (ALH) and C) curvilinear velocity (VCL). Values represent the mean ± SE for three independent replicates with two separate stallions.

The effect of pH on motility parameters in demembranated sperm was evaluated from pH 4 to pH 10.5 with calculated free calcium held at 100 nM (Figure 4.5). Motility initiated at pH 5.5, peaked at pH 7, and declined substantially by pH 9. There was no increase in VCL or ALH associated with increasing pH above that required for total motility. At pH 9.5, the medium became viscous, likely due to the denaturation of proteins induced by high pH medium [291]. These results indicate that the hyperactivating effect of high intracellular pH in equine sperm [281] appears to be independent of a direct effect of pH on the axoneme.

To determine the effect of calcium on the equine axoneme, we examined sperm exposed to free calcium levels ranging from 129 pM (8 mM EGTA) to 1 mM (Figure 4.6). Free calcium levels in the media containing 2, 4, 6 or 8 mM EGTA, as calculated by MaxChelator, are presented in Table 4.1. The amount of $CaCl_2$ added in the presence of 2 mM EGTA to achieve the desired free calcium level is presented in Table 4.2. Calculated free calcium concentrations between 129 pM and 400 nM had no significant effect on motility parameters. Sperm began to lose motility at 1 μM ($P < 0.001$) and VCL began to significantly decline at 10 μM free calcium ($P < 0.01$). Notably, equine sperm that were immobilized in the presence of excess calcium had no significant flagellar curvature (Figure 4.7), in marked contrast to the hook-shaped bends and/or curlicue formations described for other species [125, 142].

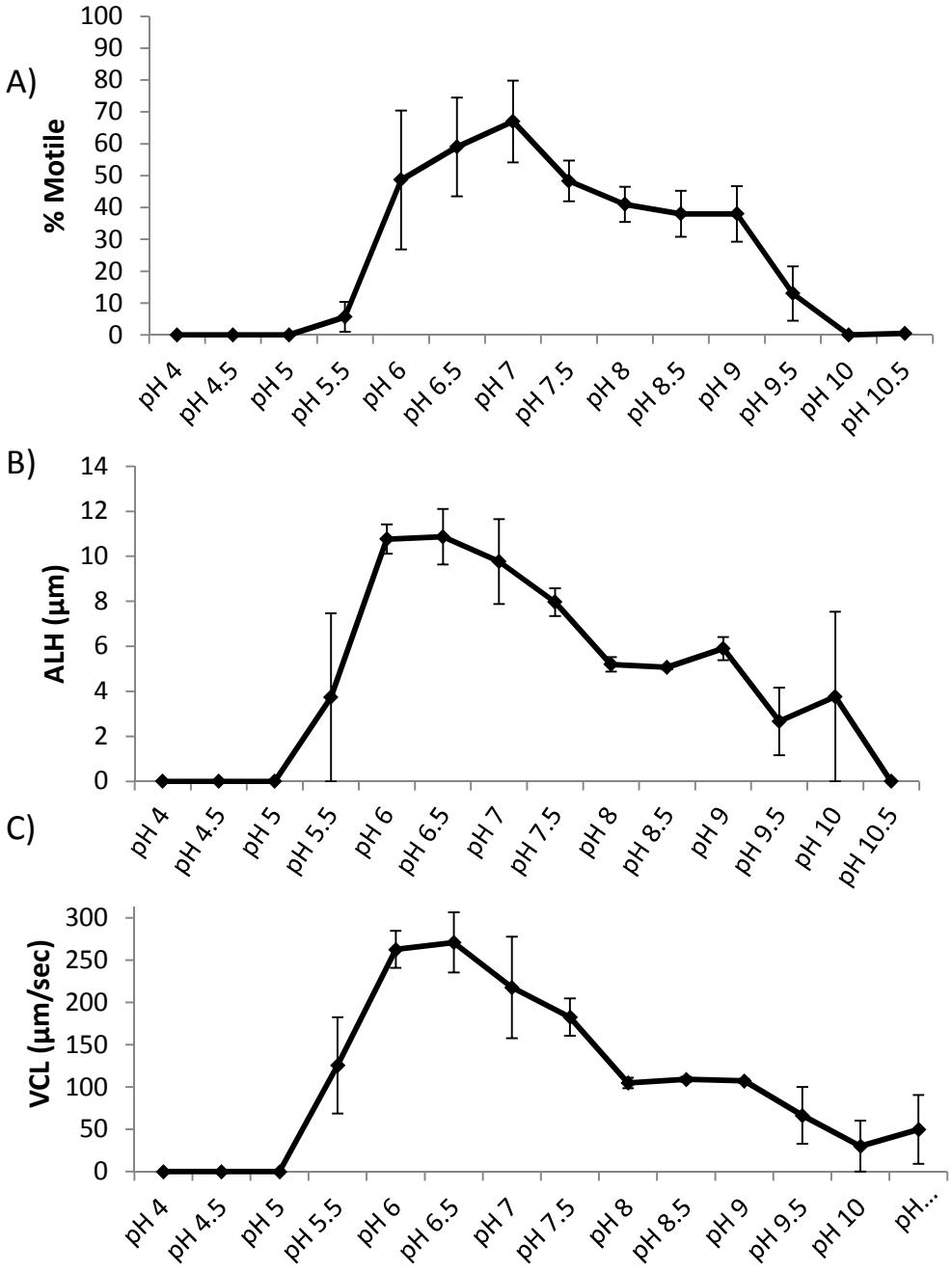

Figure 4.5. Effect of medium pH on demembranated sperm motility. Demembranated sperm were diluted in ReM with the initial medium pH ranging from pH 4 and pH 10.5, with intervals of 0.5 ± 0.02 pH units. Sperm motility was analyzed via CASA including A) percent motile, B) amplitude of lateral head movement (ALH) and C) curvilinear velocity (VCL). Values represent the mean ± SE for three independent replicates with a different stallion used for each replicate.

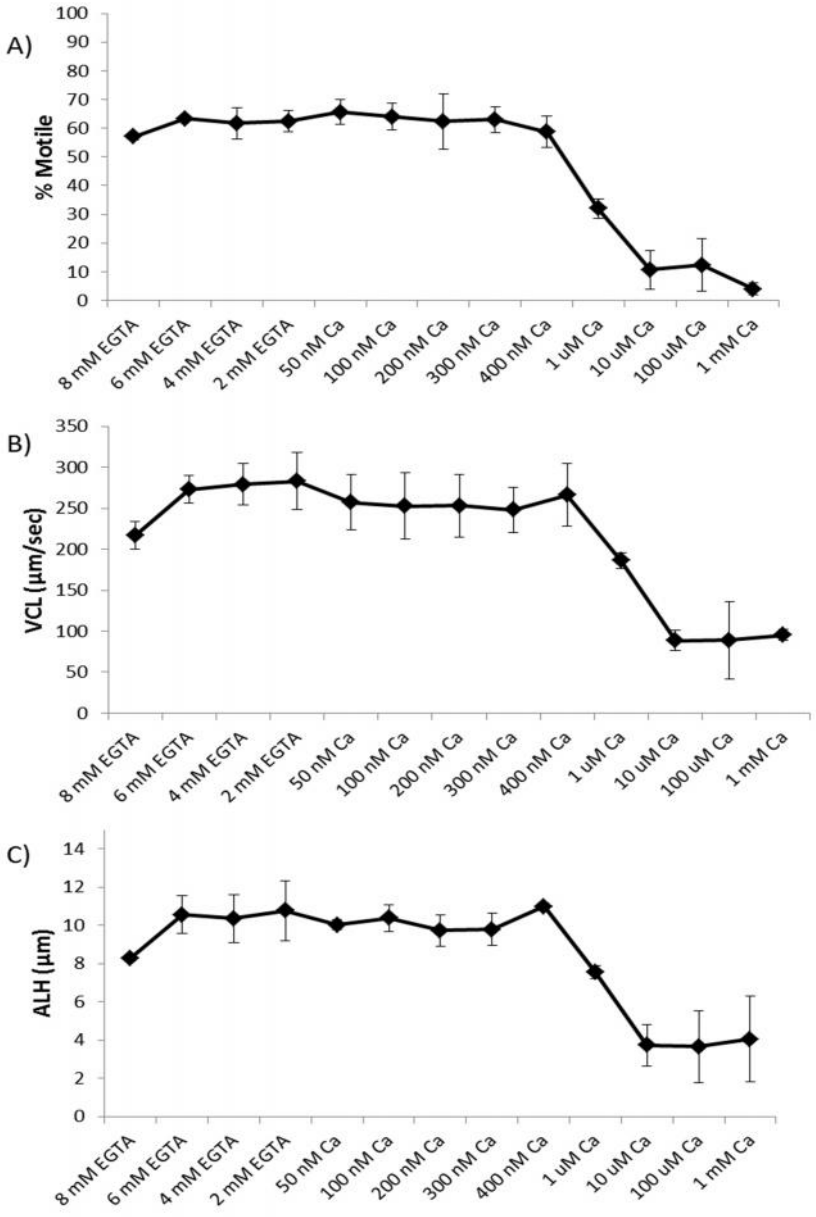

Figure 4.6. Effect of free calcium concentration on demembranated sperm motility. Demembranated sperm were diluted in ReM held constant at pH 6.9 with free calcium chelated to levels from 129 pM to 1 mM. Samples chelated with 8, 6, 4 or 2 mM EGTA contained 129, 172, 258 and 515 pM free calcium, respectively. Sperm motility was analyzed via CASA including A) percent motile, B) curvilinear velocity (VCL) and C) lateral head amplitude (ALH). Values represent the mean ± SE for five independent replicates with four separate stallions.

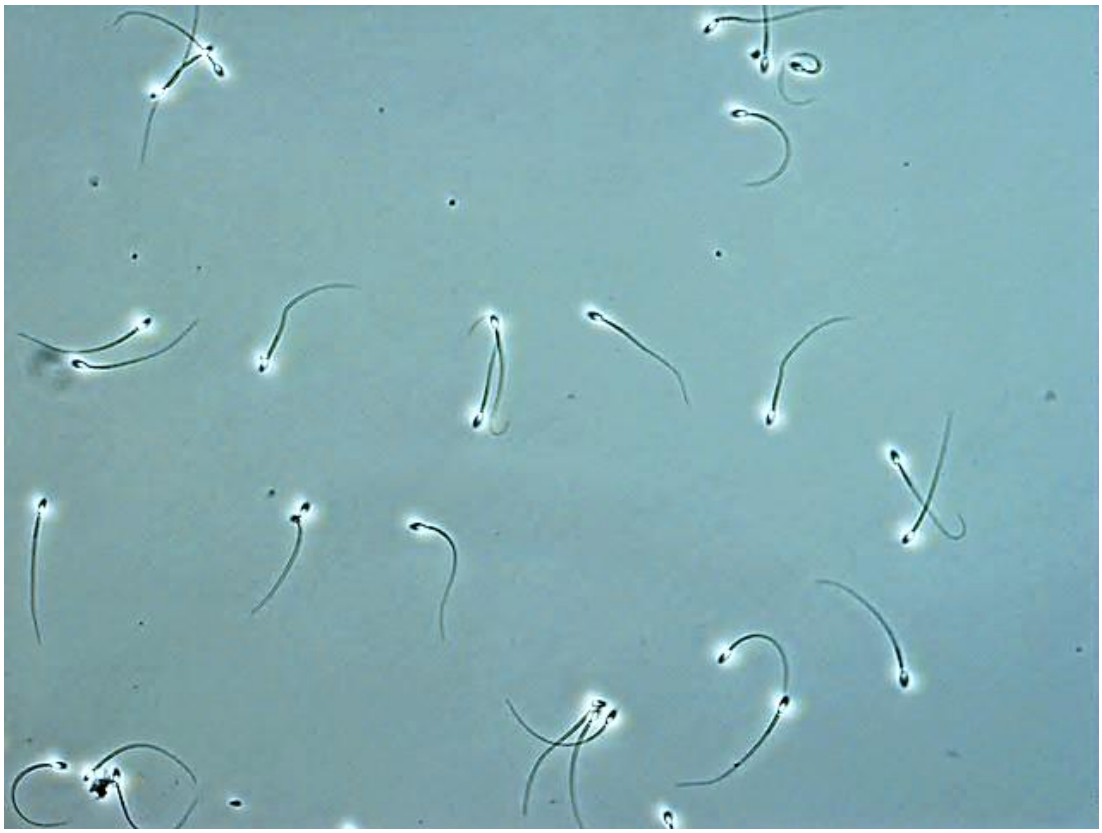

Figure 4.7. Quiescence induced by high calcium. Quiescence was induced by exposing demembranated sperm to 2 mM free calcium. While slight bending was seen in some sperm, there was no consistent curvature on arrest. This image is representative of the sperm immobilized with high calcium levels in 14 different replicates, using six separate stallions.

To determine if there was an interaction between pH and calcium in the initiation of hyperactivated motility, sperm were exposed to pH 5.9, 6.4, 6.9 or 7.4 media with free calcium levels ranging from 50 to 1000 nM, or with no added calcium plus 2, 4, 6 or 8 mM EGTA (Figure 4.8). There was no pH and/or calcium level which significantly increased VCL or ALH independent of a similar increase in total motility. Sperm bathed in pH 5.9 medium experienced a decrease in motility at relatively low calcium levels; at this pH, total motility in 4, 6 or 8 mM EGTA with 0 added calcium was significantly higher than that at all other calcium levels ($P < 0.01$). At pH 7.4, sperm appeared to be sensitive to both high levels of EGTA and high levels of calcium; motility was maximized in the presence of 2 mM EGTA with no added calcium (< 60 pM Ca^{2+}), and was significantly decreased in response to 8 mM EGTA ($P < 0.001$) as well as to 100 nM free calcium ($P < 0.05$).

Sperm experienced a decline in motility in the 8 mM EGTA treatment. To test whether this decline in motility was due to chelation of calcium or magnesium, sperm were reactivated in 8 mM EGTA with either no added calcium or with calcium, magnesium, or both calcium and magnesium added (Figure 4.9). Calcium was added to a calculated free calcium concentration of 100 nM; magnesium was added to a free magnesium concentration equivalent to that in the standard 100 nM calcium treatment. Neither calcium nor magnesium restored either total motility or VCL in the 8 mM EGTA-treated sperm at any pH tested, indicating that the loss of motility in this treatment was not due to absence of free calcium or magnesium (Figure 4.9).

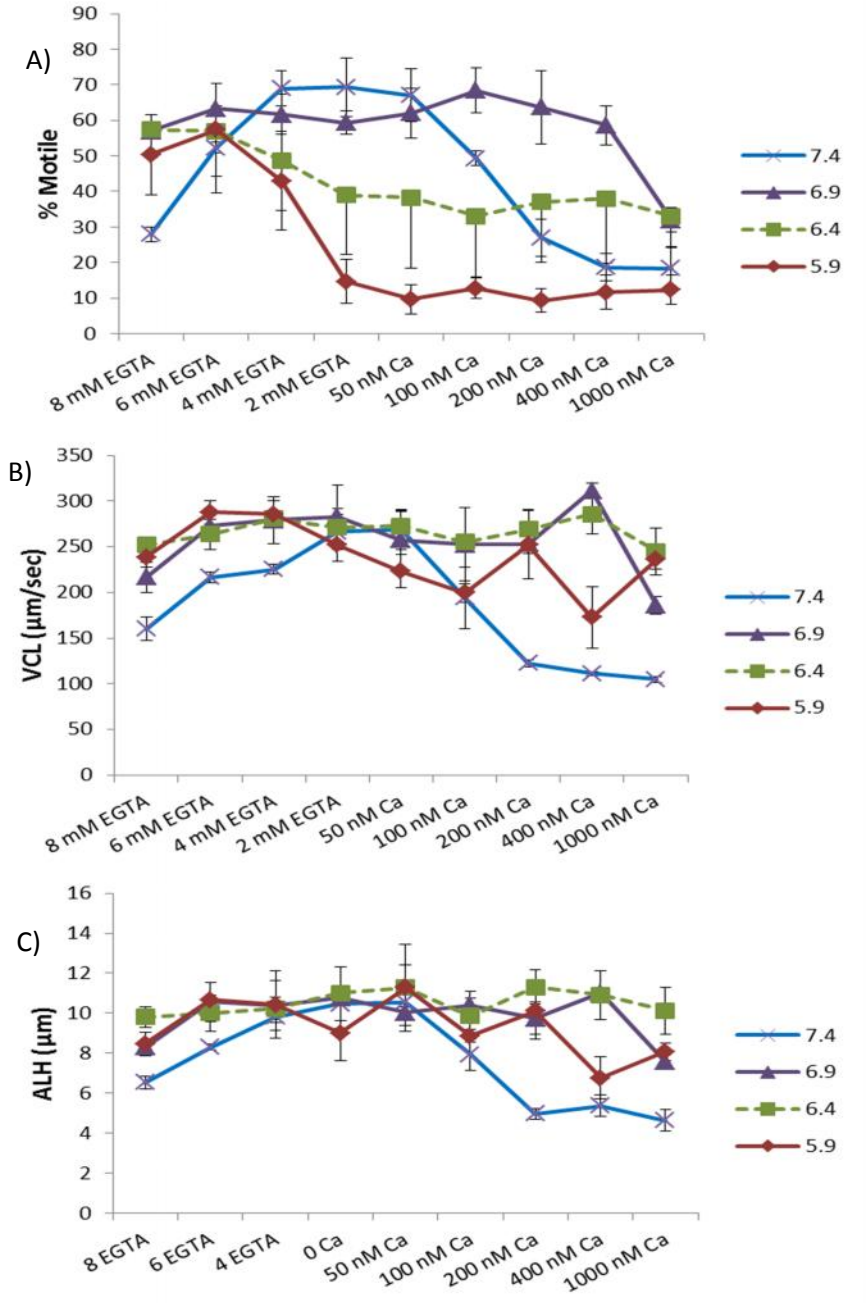

Figure 4.8. Interaction of calcium and pH on sperm motility. Demembranated sperm were diluted in ReM at either pH 5.9, 6.4, 6.9 or 7.4 with calcium levels ranging 13 pM to 1000 nM. The effect of pH and calcium on sperm motility was analyzed via CASA, including A) percent motile, B) curvilinear velocity (VCL) and C) amplitude of lateral head displacement (ALH). Values represent the mean ± SE for three independent replicates with three separate stallions.

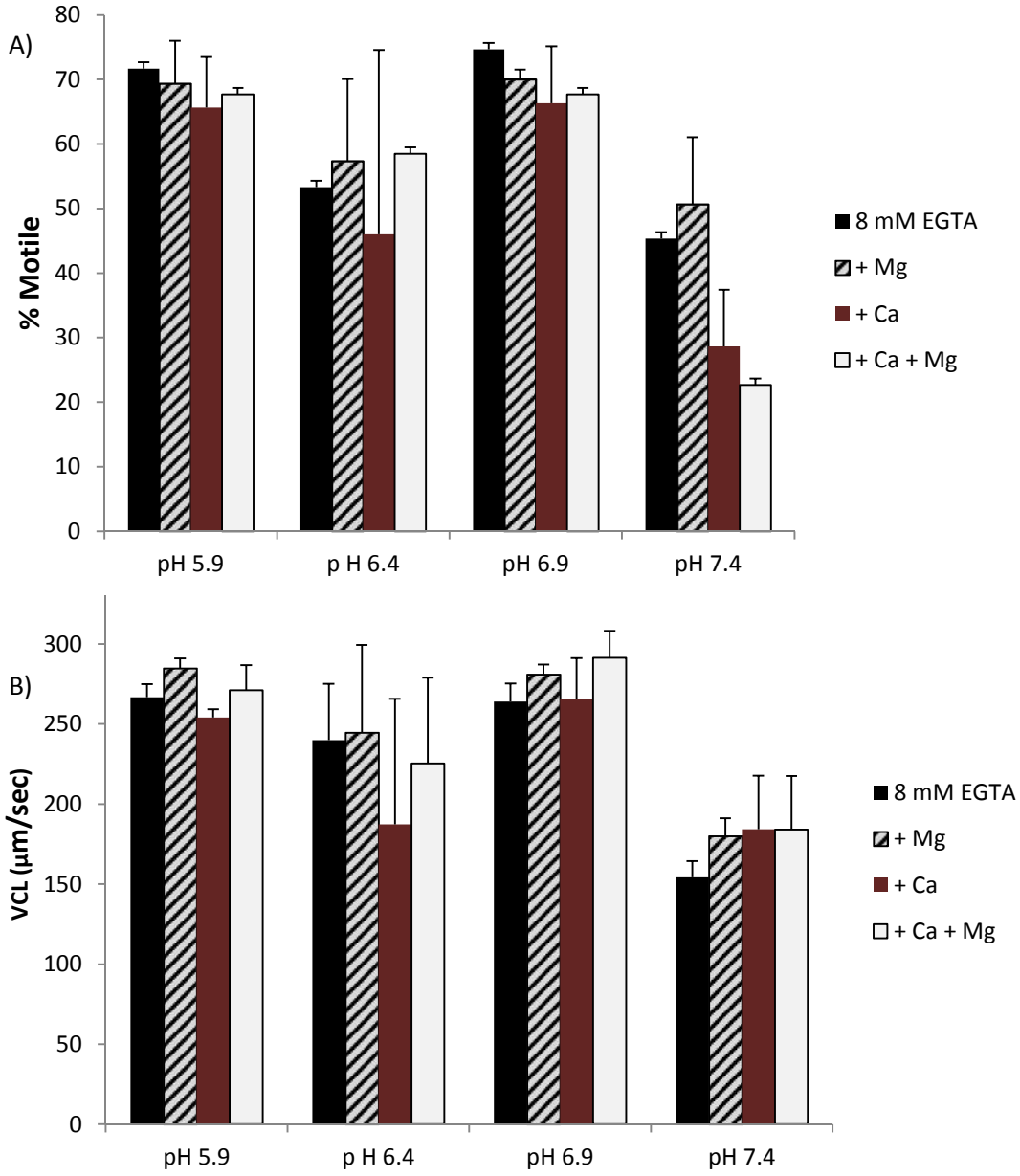

Figure 4.9. Effect of calcium and magnesium on sperm treated with 8 mM EGTA. Demembranated sperm were diluted in ReM with 8 mM EGTA either with no added calcium or magnesium (8 mM EGTA), added magnesium (+ Mg), added calcium (+ Ca) or both calcium and magnesium added (+ Ca + Mg) at either pH 5.9, 6.4, 6.9 or 7.4. Calcium was added so free calcium equaled 100 nM; magnesium was re-added so free magnesium was equivalent to the free magnesium in the 100 nM calcium treatment. A) % motile sperm and B) curvilinear velocity (VCL) were analyzed via CASA. Values represent the mean ± SE for three independent replicates with three separate stallions.

To determine whether the inhibition of motility induced by excess calcium was reversible, demembranated sperm were bathed in medium with or without 2 mM EGTA. The same amount of total $CaCl_2$ was added in each treatment; this was the amount required to generate 400 nM free calcium in the presence of 2 mM EGTA (Figure 4.10). After initial motility evaluation, 2 mM EGTA was added to the treatment without EGTA to evaluate whether chelation of excess calcium restored motility (EGTA replaced treatment). Motility in sperm in the calcium-containing medium without EGTA was significantly reduced compared to that of sperm in the EGTA-containing medium ($P < 0.05$). Replacement of EGTA restored motility, showing that the inhibition of motility by excess calcium was reversible. The restorative effect of EGTA was most pronounced at pH 6.4 to 6.9; in these groups, motility in the EGTA-replaced treatment was not significantly different from that for the 400 nM Ca treatment ($P > 0.1$).

Motility in Sperm Capacitated Before Demembranization

Sperm capacitation in other species is associated with an increase in tyrosine phosphorylation of axonemal proteins [9]. Incubation in calcium-free media has been shown to cause similar phosphorylation in equine sperm [28]. For ease of description, in this study equine sperm incubated in conditions promoting protein tyrosine phosphorylation were designated “capacitated” sperm, whereas sperm demembranated without incubation were designated as “non-capacitated” sperm. In other species,

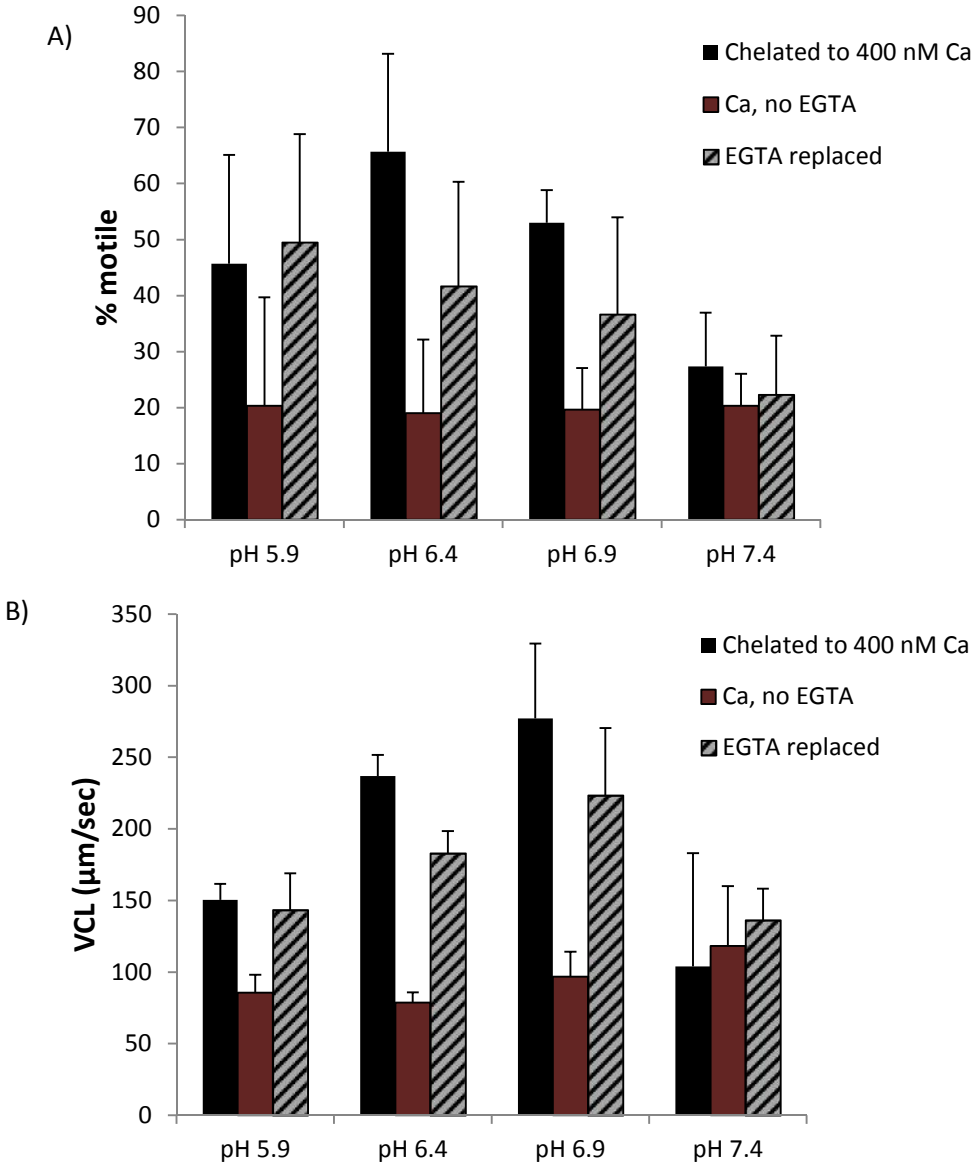

Figure 4.10. Reversal of excess calcium by EGTA. Demembranated sperm were diluted in ReM with calcium (Chelated to 400 nM Ca) with or without added 2 mM EGTA (Ca, no EGTA). Total calcium in all samples was the equivalent of 400 nM free calcium in the presence of 2 mM EGTA. Following initial motility analysis of (Ca, no EGTA) group, 2 mM EGTA was added and motility was re-analyzed (EGTA replaced). A) % motile and B) curvilinear velocity (VCL) were analyzed via CASA. Values represent the mean ± SE for three independent replicates with three separate stallions.

capacitation is also associated with an increase in intracellular calcium [292, 293]; since effective capacitation (ability to fertilize an oocyte) has not been achieved in vitro in the horse, the relationship of intracellular calcium levels to capacitation has not been determined in this species. We found that sperm subjected to incubation in "capacitating" medium before demembranization had significantly higher total motility and higher VCL at 1 µM free calcium than did sperm demembranated without "capacitation" ($P < 0.05$; Figure 4.11). In addition, the sperm of two out of three stallions did not experience a drop in motility in the 10 µM free calcium treatment, suggesting that stallion sperm are less sensitive to the suppressive effects of excess calcium after being subjected to "capacitating" conditions. However, incubation for "capacitation" did not affect the ability of the sperm to undergo hyperactivation after demembranization, as no increase in VCL or ALH was seen at any pH or calcium concentration (Figures 4.11 and 4.12). "Capacitated" sperm demonstrated significantly greater total motility than did "non-capacitated" sperm when exposed to 400 nM free-calcium at pH 7.4 ($P < 0.05$; Figure 4.12).

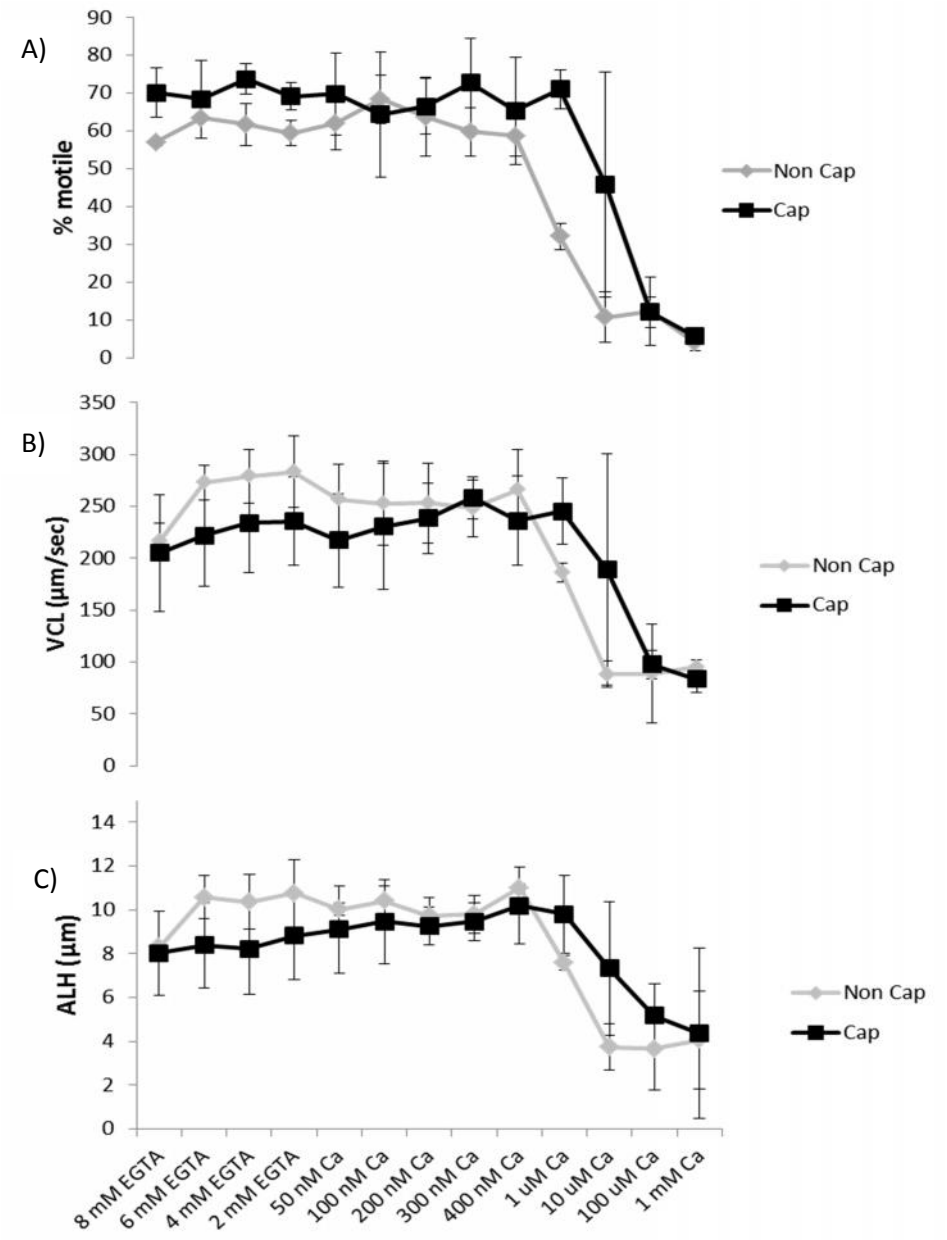

Figure 4.11. Effect of calcium on capacitated and non-capacitated sperm motility. Stallion sperm were analyzed either immediately (Non Cap) or placed into a medium shown to induce protein tyrosine phosphorylation [28] for 4 h prior to analysis (Cap). Both Non Cap and Cap sperm were demembranated then extended in ReM with free calcium levels ranging from 515 pM to 1 mM. A) % of motile sperm, B) curvilinear velocity (VCL) and C) amplitude of lateral head displacement (ALH) were analyzed via CASA. Values represent the mean ± SE for three independent replicates with three separate stallions.

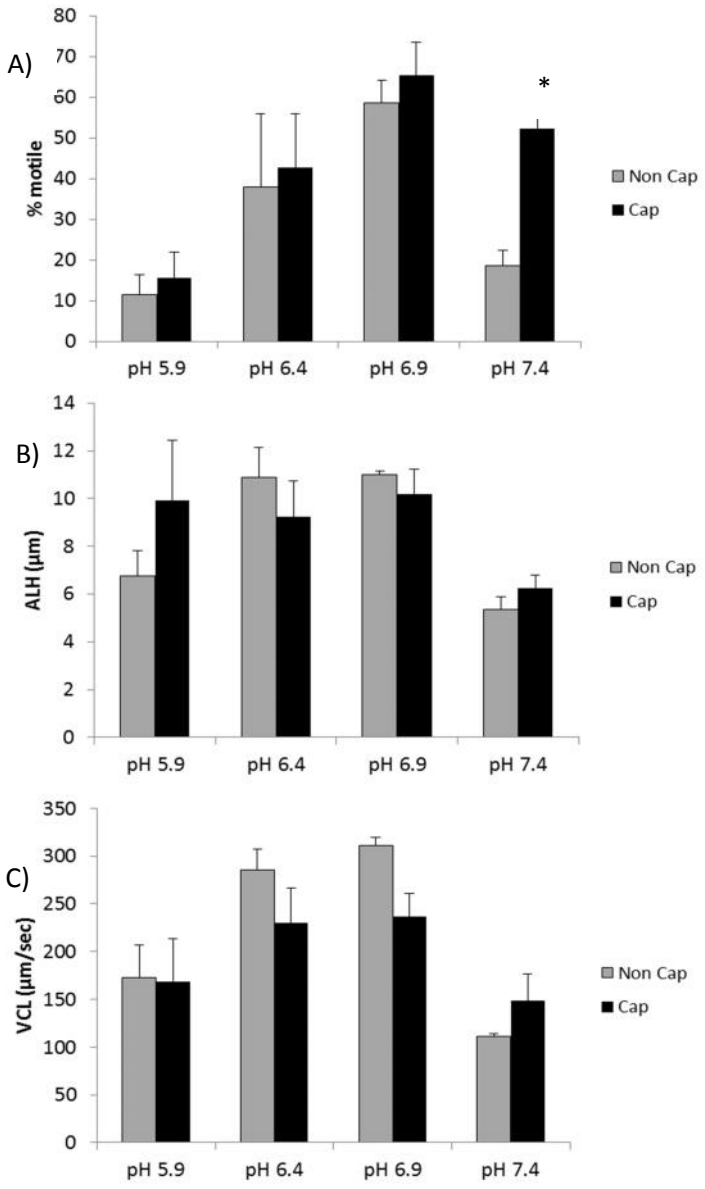

Figure 4.12. Effect of pH on capacitated and non-capacitated sperm motility. Stallion sperm were analyzed either immediately (Non Cap) or placed into conditions shown to increase protein tyrosine phosphorylation [28] for 4 h prior to analysis (Cap). Both Non Cap and Cap sperm were demembranated then extended in ReM with 400 nM free calcium at either pH 5.9, 6.4, 6.9 or 7.4. A) % of motile sperm, B) amplitude of lateral head displacement (ALH) and C) curvilinear velocity (VCL) were analyzed via CASA. In treatments marked with a *, the Cap and Non Cap treatments were significantly different ($P < 0.05$). Values represent the mean ± SE for three independent replicates with three separate stallions.

Effect of Nickel and Cadmium on Demembranated Sperm Motility

The effects of the flagellar motility inhibitors nickel and cadmium on demembranated equine sperm are presented in Figure 4.13. Nickel at 25 to 250 µM induced a dose-dependent decrease in both VCL and total motility, as seen in the rat and the bull (Figure 4.12.A,C) [140, 149, 150, 158, 159]. In contrast, cadmium at 2.5 to 50 µM did not decrease total motility. This is notable, as cadmium at concentrations as low as 1 µM results in a significant decrease in motility in demembranated bull sperm [140]. Interestingly, treatment of equine sperm with cadmium at concentrations up to 20 µM induced a significant, dose-dependent increase in VCL (Figure 4.13.B,D). As cadmium is thought to be a calcium antagonist, the finding that hyperactivated motility parameters increase with cadmium treatment again suggests a suppressive role of calcium on equine sperm hyperactivated motility.

To determine if cadmium was acting as acting as a calcium antagonist, sperm were exposed to either 2 µM free-calcium, 20 µM cadmium or 2 µM calcium with 20 µM cadmium. Sperm exposed to cadmium had significantly higher VCL than those exposed to calcium ($P < 0.05$), however, no protective effect of cadmium was seen on calcium-treated sperm (Figure 4.14).

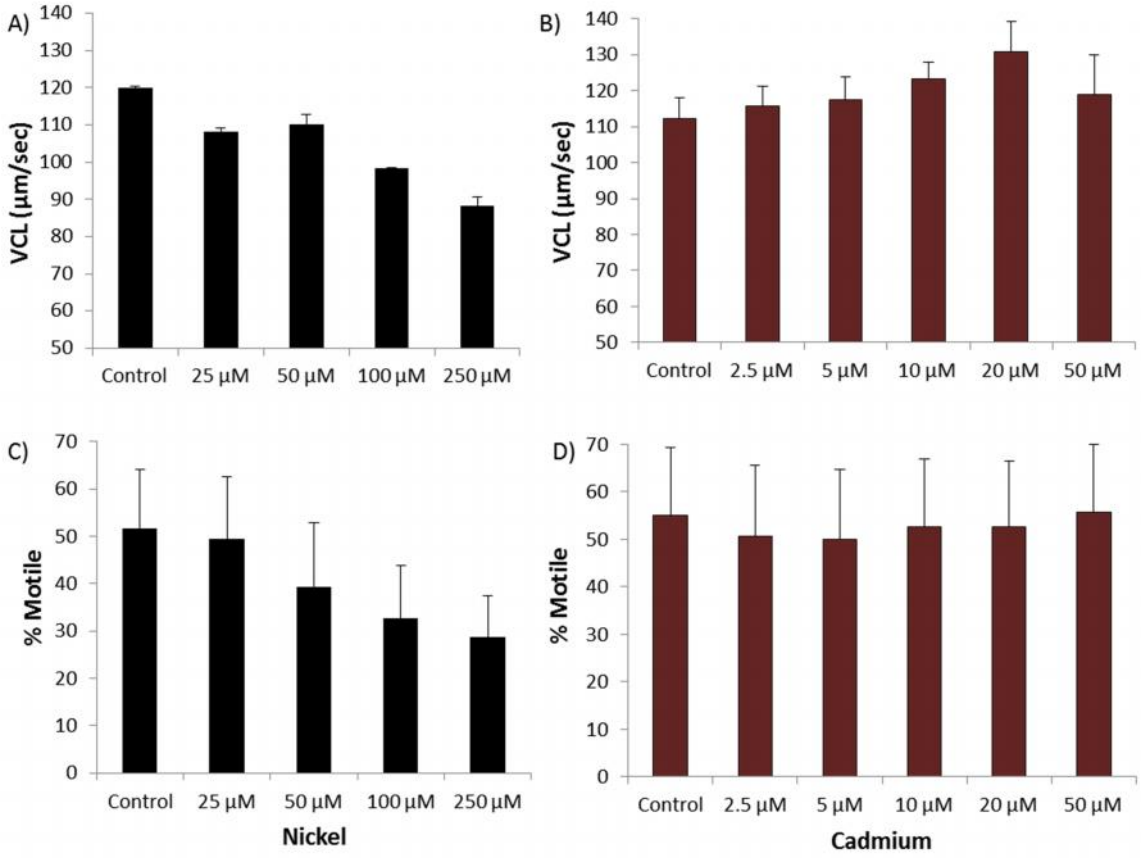

Figure 4.13. Effect of nickel and cadmium on demembranated sperm motility. Motility of sperm held at pH 6.9 with 100 nM free calcium was examined following exposure to either A,C) nickel or B,D) cadmium. Parameters studied include A,B) curvilinear velocity (VCL) and C,D) % motile. Motility parameters were analyzed using CASA. Values represent the mean ± SE for three independent replicates with three separate stallions.

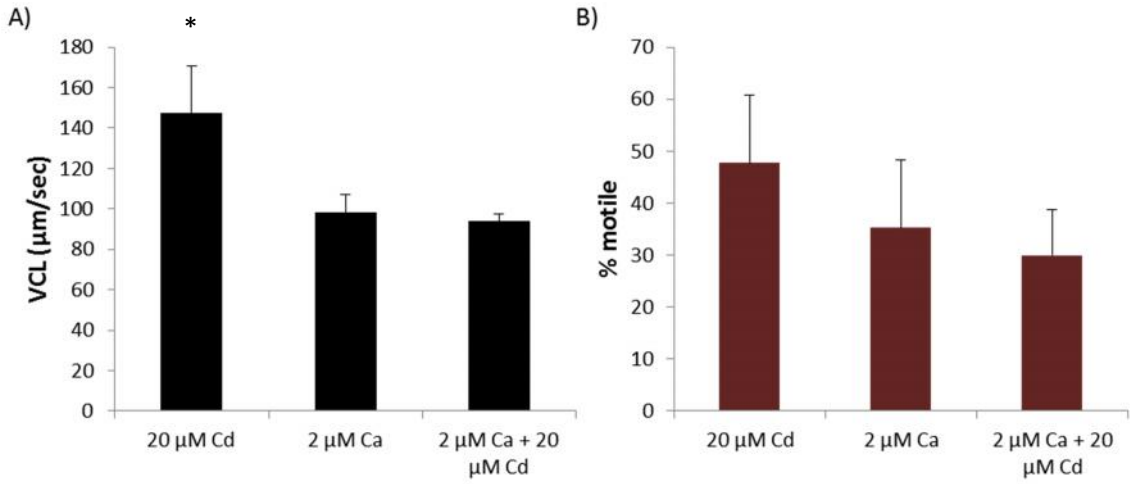

Figure 4.14. Effect of cadmium on sperm exposed to excess calcium. Motility of sperm exposed to either 20 µM cadmium, 2 µM free-calcium or both cadmium and calcium was analyzed via CASA. A) Curvilinear velocity (VCL) and B) % motile were analyzed. Significantly different treatments are denoted by * ($P < 0.05$). Values represent the mean ± SE for three independent replicates with three separate stallions.

Effect of 4-AP and Procaine on Demembranated Sperm Motility

Both procaine and 4-AP induce repeatable, vigorous increases in VCL and ALH in equine sperm [281], however, their modes of action are unknown. Neither 4-AP nor procaine had a significant effect on the percentage of motile sperm or on VCL in demembranated sperm, and neither agent induced a significant change in motility over time, as compared to Time 0 (Figure 4.15). These results suggest that 4-AP and procaine do not act directly on the axoneme to stimulate hyperactivated motility.

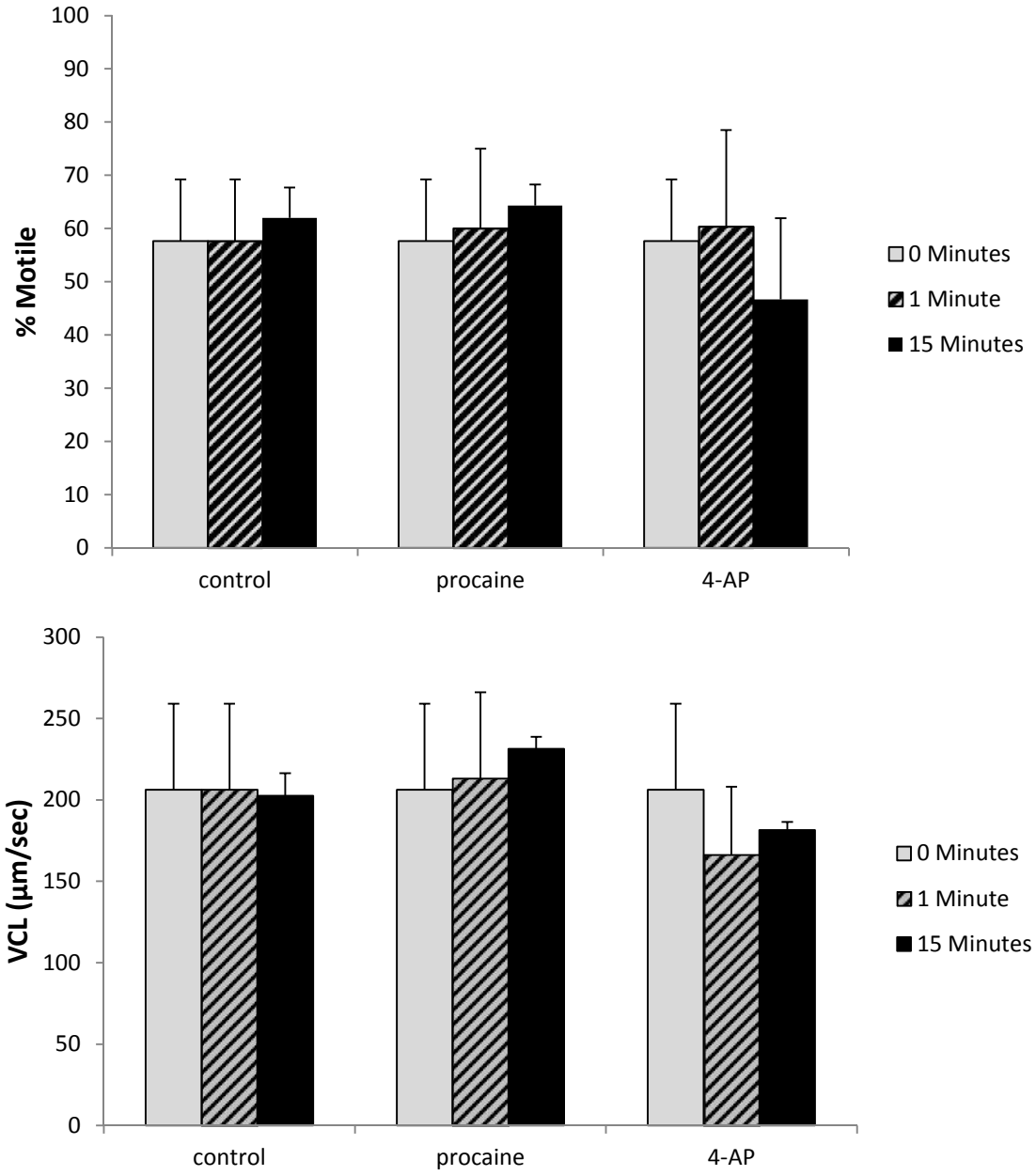

Figure 4.15. Effect of procaine and 4-AP on motility of demembranated sperm. Motility of sperm held at pH 6.9 with 100 nM free calcium was examined following exposure to either media (control), or pharmacological inducers of hyperactivated motility, 5 mM procaine or 4 mM 4-AP at 1 min and 15 min post-exposure. A) % total motility and B) curvilinear velocity (VCL) was analyzed via CASA. Values represent the mean ± SE for three independent replicates with three separate stallions.

DISCUSSION

The results of this study suggest that equine sperm are not regulated by calcium in the same manner as sperm of other species, including the bull, mouse and rat [125, 140, 149, 150, 158, 159]. Demembranated equine sperm maintained motility in the essential absence of calcium (pM quantities, Fig. 4.8); whereas in the bull, sperm showed a marked decrease in motility as free calcium levels decrease below 20 nM [22, 122, 123, 136-138, 294]. Increasing calcium concentrations did not induce the onset of hyperactivated motility, as reported for mouse, rat, bull, monkey and sea urchin sperm [122, 124, 140-142, 208]. Excess calcium suppressed motility in equine sperm at concentrations (> 400 nM) much lower than that seen with motility suppression in other species (1 mM, bull [122], mouse [125] and rat [142]), although at similar levels as seen in demembranated human sperm [153]. When motility was suppressed by calcium, equine sperm did not arrest with a curved axoneme, as seen in calcium-induced arrest in other species [125, 142, 144]. While treatment with nickel suppressed motility as seen in other species, treatment with cadmium up to 50 μM had no effect on total motility of equine sperm and cadmium treatment was, in fact, associated with an increase in VCL, a measure of hyperactivated motility. In contrast, treatment with cadmium at 1 μM causes a significant inhibition of motility in bull sperm [140].

Demembranated equine sperm attained maximum motility in a more acidic environment (pH 7) than that seen in other species. In demembranated bull sperm, motility initiated at pH 7 and maintained a plateau until pH 8 [122, 209]. The pH associated with peak motility in demembranated equine sperm was similar to the

calculated intracellular pH in non-stimulated sperm (7.14). Interestingly, in the bull, demembranated sperm were not motile at pH 6.5 [122], despite a calculated intracellular pH of 6.70 ± 0.03 [295]. Similarly, demembranated human sperm were significantly more motile at pH 7.8 than at 7.1 [154], but the intracellular pH of these sperm was calculated to be 6.94 ± 0.03 [296]. These differences may relate to species-specific effects of pH directly on the axoneme; alternatively, it is possible that, by optimizing the demembranization treatment to conserve axonemal architecture, our model retained a more physiological response to the tested factors. For example, the outer dynein arms play an integral role in pH-related regulation of motility [155]; minimizing permeabilization during demembranization may better maintain the organization of the outer dynein arms and their related proteins, and thus allow these to respond more normally to pH. Increasing medium pH beyond that required for initiation of motility did not further increase either VCL or ALH of demembranated equine sperm, despite the increase in intracellular pH seen after treatment of intact sperm with the effective stimulators of hyperactivated motility, procaine, 4-AP and pH 8.5 medium [281]. The failure of pH to elicit hyperactivation in demembranated equine sperm was unexpected. Since calcium appears to have a suppressive effect on hyperactivation in stallion spermatozoa [281], we hypothesized that, instead, pH may play a direct role in hyperactivated motility in this species. Much further work is needed to determine the factors which stimulate hyperactivated motility at the axonemal level in equine sperm.

Demembranated equine sperm were highly motile even at calculated free calcium levels as low as 13 pM (as found at pH 7.4 and 8 mM EGTA). To the best of our

knowledge, no other study has addressed this low level of calcium in demembranated sperm. The typical intracellular calcium level of sperm is approximately 50 nM [297]. In demembranated human and monkey sperm, a detrimental effect of low calcium levels was not observed, however, free-calcium levels were not taken below 20 nM [124, 138, 153, 298]. In the hamster, [283] decreasing calcium levels was reported to be beneficial to the initiation of hyperactivated motility, however, the concentration of EDTA used to chelate calcium did not exceed 580 µM and the free calcium concentrations would remain well above the nM level.

The lack of a requirement for calcium to initiate motility in demembranated equine sperm may appear surprising, as in intact equine sperm, absence of environmental calcium causes loss of motility [281]. However, in intact sperm, this is likely to be in response to membrane depolarization due to sodium influx through the CatSper channel which occurs when environmental calcium is low [270]. Although a slight decline in motility of demembranated sperm was seen in the 8 mM EGTA treatment in the current study, this did not appear to be due to chelation of either calcium or magnesium (Figure 4.9). This high level of EGTA may be toxic to sperm in itself, or may be chelating another essential medium component.

The failure of increasing calcium to induce hyperactivated motility in demembranated equine sperm is notable in comparison to results in other species. In the mouse, rat, monkey, bull and sea urchin, increasing calcium has been shown to increase asymmetrical bending in sperm [122, 124, 140-142, 157]. However, the failure of increased calcium to induce hyperactivation in demembranated equine sperm support

our previous data from intact equine sperm, in which the degree of hyperactivated motility achieved appeared to be inversely related to the degree of increase in intracellular calcium [281].

Excess calcium has a detrimental effect on total motility of sperm from all species studied, although the concentration at which motility begins to decline varies by species [22, 122, 136-138, 144, 294]. We found that equine sperm began experiencing a decline in motility at 1 μM free calcium, whereas bovine sperm are not affected by excessive calcium levels until they reach a 1000 times higher concentration (1 mM; [122]). The fact that equine sperm immobilized by excess calcium arrest with a relatively straight flagellum appears to be unique, as sperm of other species take on a "fish hook," "candy cane" or "curlicue" appearance under similar conditions [125, 142]. It has been suggested that the excess-calcium induced bend is caused by the suppressive effect of calcium on dyneins on one side of the axoneme, as excess calcium has been shown to preferentially inhibit sliding of specific (1, 2, 3 & 4) doublet pairs, which are the more dominant pairs in the beat cycle when calcium is present [125, 148-150]. The calcium-induced bend has been hypothesized to form the framework upon which the high-amplitude, asymmetric waves of hyperactivated sperm motility propagate [140]. Thus, the lack of curvature in calcium-arrested equine sperm may relate directly to the failure of increased calcium concentrations to induce hyperactivated motility in both intact [281] and demembranated sperm.

Further support for this difference in calcium regulation of axonemal motility in the horse is seen in the response of equine sperm to cadmium. While the mechanism of

action of cadmium is unknown, motility of demembranated rat sperm declines after exposure to cadmium at levels as low as 1 μM [140]. In contrast, demembranated equine sperm maintained motility when treated with cadmium at concentrations up to 50 μM, and in fact, a dose-dependent increase in VCL was seen from 2.5 to 20 μM cadmium ($P < 0.001$; Figure 4.13.B). One possible explanation for the findings that equine sperm are not stimulated by calcium to undergo hyperactivation, and are not inhibited by cadmium, is that there is a calcium-binding protein which is intricately involved in stimulating sperm hyperactivated motility in the bull, mouse and rat which is not present in the horse. This hypothetical protein might be stimulated by calcium and inhibited by cadmium, and directly or indirectly result in an increase in asymmetrical beating. In our study, cadmium did not appear to compete with calcium, as 20 μM cadmium did not restore motility in sperm exposed to excessive levels of calcium (2 μM; Fig. 4.14). The stimulating effect of cadmium on equine sperm motility may be associated with the ability of cadmium to stimulate calmodulin kinase II [163] which has been shown to be involved in increasing hyperactivated motility parameters in bull sperm [139]; this stimulation may be observable in the horse due to the lack of the cadmium-related inhibitory pathway.

Equine sperm experienced a decline in motility in response to nickel, similar to that seen in the rat and the bull [140, 149, 150, 158, 159], suggesting a similar action on motility. However, equine sperm again arrested with a straight flagellum in response to nickel, whereas bull sperm arrest in a C-curve under similar conditions [299]. The action of nickel that causes suppression of motility is unclear, but nickel has been shown

to inhibit 14s dynein in the paramecium [161]. Our findings suggest that the actions of nickel and cadmium on motility suppression, as defined in other species, occur by different pathways; one which is present in horse sperm (nickel) and one which is not (cadmium).

The role of cAMP in sperm motility is controversial; it has been found to be essential for sperm motility in some studies [128, 157, 207, 208, 219], while others have found that the effect of cAMP is calcium dependent [124], or that it has no effect on motility or hyperactivation [122]. In the hamster, sperm are collected from the epididymis, thus not exposed to calcium in ejaculatory fluids during collection. A requirement of demembranated hamster sperm for cAMP is found only in sperm not exposed to calcium before demembranization. Exposure of intact sperm to calcium is thought to generate sufficient cAMP to stimulate axonemal proteins, and thus eliminate the requirement for cAMP in reactivation medium after demembranization [300]. In our studies, there was no significant effect of dbcAMP on equine sperm; however, since these sperm were obtained by ejaculation and were processed in calcium-containing medium, they were exposed to calcium before demembranization.

The inducers of hyperactivated motility, procaine and 4-AP, did not have a significant effect on sperm motility or VCL in demembranated sperm. This establishes that these compounds do not work by direct stimulation of axonemal proteins, and supports our previous hypothesis that 4-AP and procaine act to stimulate hyperactivated motility by modulating ion influx [281]. As these compounds so far appear to be the

most repeatable and robust inducers of hyperactivated motility in equine sperm, further work is needed to determine their mechanisms of action.

In conclusion, in this study we developed a technique for demembranating equine sperm which maximizes not only the percentage of permeabilized sperm but also overall motility. Using the demembranated sperm model, we found species-specific differences in the reaction of demembranated sperm to calcium and pH, specifically a preference for a more physiological pH than in other reported demembranated sperm models, and a response to calcium that reflects both a lack of stimulation and an increased sensitivity to inhibition by this ion. Equine sperm had no apparent loss of motility even at pM calcium levels, suggesting that ongoing calcium stimulation is not a requirement for motility at the axonemal level in equine sperm. Lastly, we found that the inducers of hyperactivated motility, 4-AP and procaine, are unable to hyperactivate demembranated sperm, suggesting that these compounds require intact membranes, and thus ion channels, to exert their function.

CHAPTER V

CONCLUSIONS

The research presented in this dissertation analyzed the role of calcium and pH on hyperactivated motility in both intact and demembranated sperm. In intact sperm, an inverse relationship between calcium levels and the level of hyperactivated motility was found. In fact, procaine, the most potent inducer of hyperactivation used in our study, appeared to be exerting its action without opening the CatSper channel; the intracellular calcium level following procaine treatment was not altered when the CatSper channel was inhibited with mibefradil,. Procaine may even be blocking the CatSper channel, as procaine-treated sperm maintained motility in calcium-free medium for significantly longer than control sperm, potentially due to procaine inhibiting the sodium influx seen in intact sperm exposed to low-calcium media [270].

All hyperactivating stimuli observed, including pH 8.5, procaine and 4-AP, stimulated an increase in intracellular pH. However, a stimulating effect of increased pH on hyperactivated motility of demembranated sperm was not seen, indicating that the relationship of increased intracellular pH to hyperactivation in intact sperm is not direct. While a basal increase in intracellular pH in intact sperm was related to hyperactivated motility, a greater increase (as with treatment with pH 9.5 medium) was detrimental. Treatment with pH 9.5 medium significantly increased calcium levels. This effect was consistent with the inhibition of motility seen at high calcium levels in demembranated sperm [122, 142].

An efficient protocol for demembranating stallion sperm was developed, allowing for the direct analysis of various factors at the axonemal level. Motility was restored only when pH was between 5.5 and 9.5, and pH did not appear to have a direct effect on hyperactivated motility suggesting that the increase in hyperactivation seen with an increase in intracellular pH is due to effects of ion channels such as the CatSper channel, rather than an effect on the axoneme itself.

ATP was required for sperm reactivation following demembranization and was able to stimulate dose-dependent increase in hyperactivated motility parameters; this may be via stimulating the dyneins directly by providing more energy.

Calcium did not stimulate an increase in either VCL or ALH at the axonemal level, in direct contrast with previous reports in the mouse, rat, bull, monkey and sea urchin [122, 124, 140-142]. Increasing quantities of free calcium from 13 pM to 1 mM did not increase hyperactivated motility parameters, regardless of pH. Surprisingly, motility was not affected by reducing free-calcium to levels below 20 pM.

Nickel induced a dose-dependent decrease in motility, consistent with that seen in other species [140, 150, 159], likely due to the inhibitory effect of nickel on the α heavy chain of dynein [160]. However, cadmium did not decrease motility until 100 µM, considerably higher than the level of 1 µM required to decrease motility in the rat [140]. Even more surprising, cadmium was able to increase VCL in a dose-dependent manner from 2.5 µM to 20 µM without affecting total motility, possibly due to the stimulatory action of cadmium on calmodulin kinase II [163].

In conclusion, we found significant differences in the responses of equine sperm to calcium. Not only did excess calcium have an inhibitory effect on motility, calcium itself was unable to stimulate hyperactivated motility in equine sperm, in direct contrast to responses seen in other species. The lack of inhibition of cadmium at low levels is also indicative of differential calcium response. Much more work is needed to uncover the underlying differences in equine sperm which are behind these physiological differences.

REFERENCES

1. Roasa LM, Choi YH, Love CC, Romo S, Varner DD, Hinrichs K. Ejaculate and type of freezing extender affect rates of fertilization of horse oocytes in vitro. Theriogenology 2007; 68:560-566.
2. Hinrichs K, Love CC, Brinsko SP, Choi YH, Varner DD. In vitro fertilization of in vitro-matured equine oocytes: Effect of maturation medium, duration of maturation, and sperm calcium ionophore treatment, and comparison with rates of fertilization in vivo after oviductal transfer. Biol Reprod 2002; 67:256-262.
3. Dell'aquila ME, Fusco S, Lacalandra GM, Maritato F. In vitro maturation and fertilization of equine oocytes recovered during the breeding season. Theriogenology 1996; 45:547-560.
4. Torner A, Mlodawska, Warnke, Gollnitz, Blottner, Okolski. Determination of development in horse zygotes and spermatozoa during fertilization in vitro. Theriogenology 2002; 58:693-696.
5. Alm H, Torner H, Blottner S, Nurnberg G, Kanitz W. Effect of sperm cryopreservation and treatment with calcium ionophore or heparin on in vitro fertilization of horse oocytes. Theriogenology 2001; 56:817-829.
6. Mcpartlin LA, Suarez SS, Czaya CA, Hinrichs K, Bedford-Guaus SJ. Hyperactivation of stallion sperm is required for successful in vitro fertilization of equine oocytes. Biol Reprod 2009; 81:199-206.

7. Chang MC. Fertilizing capacity of spermatozoa deposited into the fallopian tubes. Nature 1951; 168:697-698.

8. Austin CR. Observations on the penetration of the sperm in the mammalian egg. Aust J Sci Res B 1951; 4:581-596.

9. Visconti PE, Bailey JL, Moore GD, Pan D, Olds-Clarke P, Kopf GS. Capacitation of mouse spermatozoa. I. Correlation between the capacitation state and protein tyrosine phosphorylation. Development 1995; 121:1129-1137.

10. Parrish JJ, Susko-Parrish JL, First NL. Capacitation of bovine sperm by heparin: Inhibitory effect of glucose and role of intracellular ph. Biol Reprod 1989; 41:683-699.

11. Zeng Y, Oberdorf JA, Florman HM. Ph regulation in mouse sperm: Identification of na(+)-, cl(-)-, and hco3(-)-dependent and arylaminobenzoate-dependent regulatory mechanisms and characterization of their roles in sperm capacitation. Dev Biol 1996; 173:510-520.

12. Galantino-Homer HL, Florman HM, Storey BT, Dobrinski I, Kopf GS. Bovine sperm capacitation: Assessment of phosphodiesterase activity and intracellular alkalinization on capacitation-associated protein tyrosine phosphorylation. Mol Reprod Dev 2004; 67:487-500.

13. Lishko PV, Botchkina IL, Fedorenko A, Kirichok Y. Acid extrusion from human spermatozoa is mediated by flagellar voltage-gated proton channel. Cell 2010; 140:327-337.

14. Yanagimachi R. Mammalian fertilization. In: Neill K (ed.) Physiology of reproduction. New York: Raven Press; 1994: 189.

15. Baldi E, Casano R, Falsetti C, Krausz C, Maggi M, Forti G. Intracellular calcium accumulation and responsiveness to progesterone in capacitating human spermatozoa. J Androl 1991; 12:323-330.

16. Dasgupta S, Mills CL, Fraser LR. Ca(2+)-related changes in the capacitation state of human spermatozoa assessed by a chlortetracycline fluorescence assay. J Reprod Fertil 1993; 99:135-143.

17. Gadella BM, Harrison RA. The capacitating agent bicarbonate induces protein kinase A-dependent changes in phospholipid transbilayer behavior in the sperm plasma membrane. Development 2000; 127:2407-2420.

18. Harrison RA, Miller NG. Camp-dependent protein kinase control of plasma membrane lipid architecture in boar sperm. Mol Reprod Dev 2000; 55:220-228.

19. Yanagimachi R. The movement of golden hamster spermatozoa before and after capacitation. J Reprod Fertil 1970; 23:193-196.

20. Suarez SS, Varosi SM, Dai X. Intracellular calcium increases with hyperactivation in intact, moving hamster sperm and oscillates with the flagellar beat cycle. Proc Natl Acad Sci U S A 1993; 90:4660-4664.

21. Singh JP, Babcock DF, Lardy HA. Increased calcium-ion influx is a component of capacitation of spermatozoa. Biochem J 1978; 172:549-556.

22. Babcock DF, Stamerjohn DM, Hutchinson T. Calcium redistribution in individual cells correlated with ionophore action on motility. J Exp Zool 1978; 204:391-399.

23. Chen H, Kui C, Chan HC. Ca2+ mobilization in cumulus cells: Role in oocyte maturation and acrosome reaction. Cell Calcium 2013; 53:68-75.

24. Davis BK. Influence of serum albumin on the fertilizing ability in vitro of rat spermatozoa. Proc Soc Exp Biol Med 1976; 151:240-243.

25. Go KJ, Wolf DP. Albumin-mediated changes in sperm sterol content during capacitation. Biol Reprod 1985; 32:145-153.

26. Suzuki F, Yanagimachi R. Changes in the distribution of intramembranous particles and filipin-reactive membrane sterols during in vitro capacitation of golden hamster spermatozoa. Gamete Res 1989; 23:335-347.

27. Wennemuth G, Carlson AE, Harper AJ, Babcock DF. Bicarbonate actions on flagellar and Ca2+ -channel responses: Initial events in sperm activation. Development 2003; 130:1317-1326.

28. Gonzalez-Fernandez L, Macias-Garcia B, Velez IC, Varner DD, Hinrichs K. Calcium-calmodulin and ph regulate protein tyrosine phosphorylation in stallion sperm. Reproduction 2012; 144:411-422.

29. Gonzalez-Fernandez L, Macias-Garcia B, Loux SC, Varner DD, Hinrichs K. Focal adhesion kinases and calcium/calmodulin-dependent protein kinases regulate protein tyrosine phosphorylation in stallion sperm. Biol Reprod 2013; 88.

30. Suarez SS. Regulation of sperm storage and movement in the mammalian oviduct. Int J Dev Biol 2008; 52:455-462.

31. Demott RP, Suarez SS. Hyperactivated sperm progress in the mouse oviduct. Biol Reprod 1992; 46:779-785.

32. Ho K, Wolff CA, Suarez SS. CatSper-null mutant spermatozoa are unable to ascend beyond the oviductal reservoir. Reprod Fertil Dev 2009; 21:345-350.

33. Chang H, Suarez SS. Unexpected flagellar movement patterns and epithelial binding behavior of mouse sperm in the oviduct1. Biol Reprod 2012; 86:Article 140, 141-148.

34. Florman HMDT. Fertilization in mammals. New York: Raven Press; 2006: 55-112..

35. Jin M, Fujiwara E, Kakiuchi Y, Okabe M, Satouh Y, Baba SA, Chiba K, Hirohashi N. Most fertilizing mouse spermatozoa begin their acrosome reaction before contact with the zona pellucida during in vitro fertilization. Proceedings of the National Academy of Sciences 2011; 108:4892-4896.

36. Meyers SA, Rosenberger AE. A plasma membrane-associated hyaluronidase is localized to the posterior acrosomal region of stallion sperm and is associated with spermatozoal function. Biol Reprod 1999; 61:444-451.

37. Suarez SS, Katz DF, Owen DH, Andrew JB, Powell RL. Evidence for the function of hyperactivated motility in sperm. Biol Reprod 1991; 44:375-381.

38. Litscher ES, Wassarman PM. Characterization of a mouse ZP3-derived glycopeptide, GP55, that exhibits sperm receptor and acrosome reaction-inducing activity in vitro. Biochemistry (Mosc) 1996; 35:3980-3985.

39. Shur BD. Reassessing the role of protein-carbohydrate complementarity during sperm-egg interactions in the mouse. Int J Dev Biol 2008; 52:703-715.

40. Buffone MG, Rodriguez-Miranda E, Storey BT, Gerton GL. Acrosomal exocytosis of mouse sperm progresses in a consistent direction in response to zona pellucida. J Cell Physiol 2009; 220:611-620.

41. Dunbar BS, Dudkiewicz AB, Bundman DS. Proteolysis of specific porcine zona pellucida glycoproteins by boar acrosin. Biol Reprod 1985; 32:619-630.

42. Howes E, Pascall JC, Engel W, Jones R. Interactions between mouse ZP2 glycoprotein and proacrosin; a mechanism for secondary binding of sperm to the zona pellucida during fertilization. J Cell Sci 2001; 114:4127-4136.

43. Buffone MG, Foster JA, Gerton GL. The role of the acrosomal matrix in fertilization. Int J Dev Biol 2008; 52:511-522.

44. Bedford JM. Mammalian fertilization misread? Sperm penetration of the eutherian zona pellucida is unlikely to be a lytic event. Biol Reprod 1998; 59:1275-1287.

45. Inoue N, Satouh Y, Ikawa M, Okabe M, Yanagimachi R. Acrosome-reacted mouse spermatozoa recovered from the perivitelline space can fertilize other eggs. Proc Natl Acad Sci U S A 2011; 108:20008-20011.

46. Stauss CR, Votta TJ, Suarez SS. Sperm motility hyperactivation facilitates penetration of the hamster zona pellucida. Biol Reprod 1995; 53:1280-1285.

47. Ren D, Navarro B, Perez G, Jackson AC, Hsu S, Shi Q, Tilly JL, Clapham DE. A sperm ion channel required for sperm motility and male fertility. Nature 2001; 413:603-609.

48. Yanagimachi R. Sperm-egg fusion. In: Current topics in membranes and transport, Vol. 32. San Diego, CA: Academic Press; 1988: 3-43..

49. Yanagimachi R, Noda YD. Physiological changes in the postnuclear cap region of mammalian spermatozoa: A necessary preliminary to the membrane fusion between sperm and egg cells. J Ultrastruct Res 1970; 31:486-493.

50. Bedford JM, Moore HD, Franklin LE. Significance of the equatorial segment of the acrosome of the spermatozoon in eutherian mammals. Exp Cell Res 1979; 119:119-126.

51. Longo FJ, Chen DY. Development of surface polarity in mouse eggs. Scan Electron Microsc 1984; 2:703-716.

52. Kaji K, Oda S, Shikano T, Ohnuki T, Uematsu Y, Sakagami J, Tada N, Miyazaki S, Kudo A. The gamete fusion process is defective in eggs of CD9-deficient mice. Nat Genet 2000; 24:279-282.

53. Miyado K, Yamada G, Yamada S, Hasuwa H, Nakamura Y, Ryu F, Suzuki K, Kosai K, Inoue K, Ogura A, Okabe M, Mekada E. Requirement of CD9 on the egg plasma membrane for fertilization. Science 2000; 287:321-324.

54. Miyado K, Yoshida K, Yamagata K, Sakakibara K, Okabe M, Wang X, Miyamoto K, Akutsu H, Kondo T, Takahashi Y, Ban T, Ito C, et al. The fusing ability of sperm is bestowed by CD9-containing vesicles released from eggs in mice. Proc Natl Acad Sci U S A 2008; 105:12921-12926.

55. Dale B, Wilding M, Coppola G, Tosti E. How do spermatozoa activate oocytes? Reprod Biomed Online 2010; 21:1-3.

56. Hoodbhoy T, Talbot P. Characterization, fate, and function of hamster cortical granule components. Mol Reprod Dev 2001; 58:223-235.

57. Tsai PS, Garcia-Gil N, Van Haeften T, Gadella BM. How pig sperm prepares to fertilize: Stable acrosome docking to the plasma membrane. PLoS ONE 2010; 5:0011204.

58. Bleil JD, Wassarman PM. Sperm-egg interactions in the mouse: Sequence of events and induction of the acrosome reaction by a zona pellucida glycoprotein. Dev Biol 1983; 95:317-324.

59. Schroeder AC, Schultz RM, Kopf GS, Taylor FR, Becker RB, Eppig JJ. Fetuin inhibits zona pellucida hardening and conversion of ZP2 to ZP2f during spontaneous mouse oocyte maturation in vitro in the absence of serum. Biol Reprod 1990; 43:891-897.

60. Kalab P, Kopf GS, Schultz RM. Modifications of the mouse zona pellucida during oocyte maturation and egg activation: Effects of newborn calf serum and fetuin. Biol Reprod 1991; 45:783-787.

61. Iwao Y, Jaffe LA. Evidence that the voltage-dependent component in the fertilization process is contributed by the sperm. Dev Biol 1989; 134:446-451.

62. Jaffe LA. Fast block to polyspermy in sea urchin eggs is electrically mediated. Nature 1976; 261:68-71.

63. Larson SM, Lee HJ, Hung PH, Matthews LM, Robinson DN, Evans JP. Cortical mechanics and meiosis ii completion in mammalian oocytes are mediated by myosin-II and ezrin-radixin-moesin (erm) proteins. Mol Biol Cell 2010; 21:3182-3192.

64. Gardner AJ, Williams CJ, Evans JP. Establishment of the mammalian membrane block to polyspermy: Evidence for calcium-dependent and -independent regulation. Reproduction 2007; 133:383-393.

65. Wolf DP, Nicosia SV, Hamada M. Premature cortical granule loss does not prevent sperm penetration of mouse eggs. Dev Biol 1979; 71:22-32.

66. Horvath PM, Kellom T, Caulfield J, Boldt J. Mechanistic studies of the plasma membrane block to polyspermy in mouse eggs. Mol Reprod Dev 1993; 34:65-72.

67. Maleszewski M, Kimura Y, Yanagimachi R. Sperm membrane incorporation into oolemma contributes to the oolemma block to sperm penetration: Evidence based on intracytoplasmic sperm injection experiments in the mouse. Mol Reprod Dev 1996; 44:256-259.

68. Wortzman-Show GB, Kurokawa M, Fissore RA, Evans JP. Calcium and sperm components in the establishment of the membrane block to polyspermy: Studies of ICSI and activation with sperm factor. Mol Hum Reprod 2007; 13:557-565

69. Odor DL, Blandau RJ. The frequency of occurrence of supernumerary sperm in rat ova. Anat Rec 1949; 104:1-9.

70. Hunter RH. Fertilization of pig eggs in vivo and in vitro. J Reprod Fertil Suppl 1990; 40:211-226.

71. Sengoku K, Tamate K, Horikawa M, Takaoka Y, Ishikawa M, Dukelow WR. Plasma membrane block to polyspermy in human oocytes and preimplantation embryos. J Reprod Fertil 1995; 105:85-90.

72. Perry E. The artificial insemination of farm animals. In. New Brunswick, NJ: Rutgers University Press; 1968..

73. Heape. The artificial insemination of mammals. Proceedings of the Royal Society of London 1897; 61:52-63.

74. Bezard J MM, Duchamp G, Palmer E. Chronology of equine fertilisation and embryonic development in vivo and in vitro. Equine Veterinary Journal Supplement 1989; 8:105-110.

75. Alm H, Torner H, Blottner S, Rnberg G, Kanitz W. Effect of sperm cryopreservation and treatment with calcium ionophore or heparin on in vitro fertilization of horse oocytes. Theriogenology 2001; 56:817-829.

76. Dell'aquila ME, Fusco S, Lacalandra GM, Maritato F. In vitro maturation and fertilization of equine oocytes recovered during the breeding season. Theriogenology 1996; 45:547-560.

77. Palmer E, Bézard J, Magistrini M, Duchamp G. In vitro fertilisation in the horse: A retrospective study. J Reprod Fertil 1991; Supp. 44:375-384.

78. Hinrichs K, Love CC, Brinsko SP, Choi YH, Varner DD. In vitro fertilization of in vitro-matured equine oocytes: Effect of maturation medium, duration of maturation, and sperm calcium ionophore treatment, and comparison with rates of fertilization in vivo after oviductal transfer. Biol Reprod 2002; 67:256-262.

79. Del Campo MR, Donoso MX, Parrish JJ, Ginther OJ. In vitro fertilization of in vitro-matured equine oocytes. Equine Veterinary Science 1990; 10:18-22.

80. Zhang JJ, Muzs LZ, Boyle MS. In vitro fertilization of horse follicular oocytes matured in vitro. Mol Reprod Dev 1990; 26:361-365.

81. Bohlmann MK. Effects and effectiveness of heparin in assisted reproduction. J Reprod Immunol 2011; 90:82-90.

82. Cormier N, Sirard MA, Bailey JL. Premature capacitation of bovine spermatozoa is initiated by cryopreservation. J Androl 1997; 18:461-468.

83. Choi YH, Okada Y, Hochi S, Braun J, Sato K, Oguri N. In vitro fertilization rate of horse oocytes with partially removed zonae. Theriogenology 1994; 42:795-802.

84. Li LY, Meintjes M, Graff KJ, Paul JB, Denniston RS, Godke RA. In vitro fertilization and development of in vitro-matured oocytes aspirated from pregnant mares. Biol Reprod 1995; Monograph 1:309-317.

85. Lange-Consiglio A, Cremonesi F. Hyperactivation of stallion sperm in follicular fluid for in vitro fertilization of equine oocytes. Reproduction, Fertility, and Development 2011; 24:193-194.

86. Ambruosi B, Accogli G, Douet C, Canepa S, Pascal G, Monget P, Moros Nicolas C, Holmskov U, Mollenhauer J, Robbe-Masselot C, Vidal O, Desantis S, et al. Deleted in malignant brain tumour 1 (DMBT1) is secreted in the oviduct and involved in the mechanism of fertilization in equine and porcine species. Reproduction 2013.

87. Marquez B, Suarez SS. Different signaling pathways in bovine sperm regulate capacitation and hyperactivation. Biol Reprod 2004; 70:1626-1633.

88. Fawcett DW. The anatomy of the spermatozoon after 300 years. Kaibogaku Zasshi 1975; 50:326-327.

89. Afzelius BA. On the numbering of peripheral doublets in cilia and flagella. Tissue Cell 1988; 20:473-475.

90. Olson GE, Sammons DW. Structural chemistry of outer dense fibers of rat sperm. Biol Reprod 1980; 22:319-332.

91. Sathananthan AH, Kola I, Osborne J, Trounson A, Ng SC, Bongso A, Ratnam SS. Centrioles in the beginning of human development. Proc Natl Acad Sci U S A 1991; 88:4806-4810.

92. Manandhar G, Sutovsky P, Joshi HC, Stearns T, Schatten G. Centrosome reduction during mouse spermiogenesis. Dev Biol 1998; 203:424-434.

93. Manandhar G, Simerly C, Salisbury JL, Schatten G. Centriole and centrin degeneration during mouse spermiogenesis. Cell Motil Cytoskeleton 1999; 43:137-144.

94. Woolley DM, Fawcett DW. The degeneration and disappearance of the centrioles during the development of the rat spermatozoon. Anat Rec 1973; 177:289-301.

95. Manandhar G, Schatten H, Sutovsky P. Centrosome reduction during gametogenesis and its significance. Biol Reprod 2005; 72:2-13.

96. Manandhar G, Schatten G. Centrosome reduction during rhesus spermiogenesis: Gamma-tubulin, centrin, and centriole degeneration. Mol Reprod Dev 2000; 56:502-511.

97. Manandhar G, Simerly C, Schatten G. Highly degenerated distal centrioles in rhesus and human spermatozoa. Hum Reprod 2000; 15:256-263.

98. Turner RM. Tales from the tail: What do we really know about sperm motility? J Androl 2003; 24:790-803.

99. Eddy EM, Toshimori K, O'brien DA. Fibrous sheath of mammalian spermatozoa. Microscopy Research and Technique 2003; 61:103-115.

100. Fulcher KD, Welch JE, Klapper DG, O'brien DA, Eddy EM. Identification of a unique mu-class glutathione s-transferase in mouse spermatogenic cells. Mol Reprod Dev 1995; 42:415-424.

101. Carter AP. Crystal clear insights into how the dynein motor moves. J Cell Sci 2013; 126:705-713.

102. Gibbons IR. Studies on the protein components of cilia from tetrahymena pyriformis. Proc Natl Acad Sci U S A 1963; 50:1002-1010.

103. Ogawa K, Kamiya R, Wilkerson CG, Witman GB. Interspecies conservation of outer arm dynein intermediate chain sequences defines two intermediate chain subclasses. Mol Biol Cell 1995; 6:685-696.

104. Gibbons IR, Gibbons BH, Mocz G, Asai DJ. Multiple nucleotide-binding sites in the sequence of dynein beta heavy chain. Nature 1991; 352:640-643.

105. Toba S, Gibson TM, Shiroguchi K, Toyoshima YY, Asai DJ. Properties of the full-length heavy chains of tetrahymena ciliary outer arm dynein separated by urea treatment. Cell Motil Cytoskeleton 2004; 58:30-38.

106. Gennerich A, Vale RD. Walking the walk: How kinesin and dynein coordinate their steps. Curr Opin Cell Biol 2009; 21:59-67.

107. Carter AP, Garbarino JE, Wilson-Kubalek EM, Shipley WE, Cho C, Milligan RA, Vale RD, Gibbons IR. Structure and functional role of dynein's microtubule-binding domain. Science 2008; 322:1691-1695.

108. Burgess SA, Knight PJ. Is the dynein motor a winch? Curr Opin Struct Biol 2004; 14:138-146.

109. Inaba K, Kagami O, Ogawa K. Tctex2-related outer arm dynein light chain is phosphorylated at activation of sperm motility. Biochem Biophys Res Commun 1999; 256:177-183.

110. Tash JS, Krinks M, Patel J, Means RL, Klee CB, Means AR. Identification, characterization, and functional correlation of calmodulin-dependent protein phosphatase in sperm. J Cell Biol 1988; 106:1625-1633.

111. Padma P, Hozumi A, Ogawa K, Inaba K. Molecular cloning and characterization of a thioredoxin/nucleoside diphosphate kinase related dynein intermediate chain from the ascidian, ciona intestinalis. Gene 2001; 275:177-183.

112. Wargo MJ, Smith EF. Asymmetry of the central apparatus defines the location of active microtubule sliding in chlamydomonas flagella. Proc Natl Acad Sci U S A 2003; 100:137-142.

113. Porter ME, Sale WS. The 9 + 2 axoneme anchors multiple inner arm dyneins and a network of kinases and phosphatases that control motility. J Cell Biol 2000; 151:F37-42.

114. Gaillard AR, Diener DR, Rosenbaum JL, Sale WS. Flagellar radial spoke protein 3 is an a-kinase anchoring protein (akap). J Cell Biol 2001; 153:443-448.

115. Yang P, Fox L, Colbran RJ, Sale WS. Protein phosphatases pp1 and pp2a are located in distinct positions in the chlamydomonas flagellar axoneme. J Cell Sci 2000; 113:91-102.

116. Kon T, Sutoh K, Kurisu G. X-ray structure of a functional full-length dynein motor domain. Nat Struct Mol Biol 2011; 18:638-642.

117. Kikkawa M. Big steps toward understanding dynein. J Cell Biol 2013; 202:15-23.

118. Szent-Gyorgyi A. Free-energy relations and contraction of actomyosin. Biol Bull 1949; 96:140-161.

119. Hoffmann-Berling H. [flagellum models and adenosinetriphosphate (atp)]. Biochim Biophys Acta 1955; 16:146-154.

120. Brokaw CJ, Benedict B. Mechanochemical coupling in flagella. I. Movement-dependent dephosphorylation of atp by glycerinated spermatozoa. Arch Biochem Biophys 1968; 125:770-778.

121. Gibbons BH, Gibbons IR. Flagellar movement and adenosine triphosphatase activity in sea urchin sperm extracted with triton x-100. J Cell Biol 1972; 54:75-97.

122. Ho HC, Granish KA, Suarez SS. Hyperactivated motility of bull sperm is triggered at the axoneme by Ca2+ and not cAMP. Dev Biol 2002; 250:208-217.

123. He S, Jenkins-Keeran K, Woods LC, 3rd. Activation of sperm motility in striped bass via a cAMP-independent pathway. Theriogenology 2004; 61:1487-1498.

124. Ishijima S, Mohri H, Overstreet JW, Yudin AI. Hyperactivation of monkey spermatozoa is triggered by Ca2+ and completed by cAMP. Mol Reprod Dev 2006; 73:1129-1139.

125. Lesich KA, Kelsch CB, Ponichter KL, Dionne BJ, Dang L, Lindemann CB. The calcium response of mouse sperm flagella: Role of calcium ions in the regulation of dynein activity. Biol Reprod 2012; 86:105.

126. Mildvan AS. Role of magnesium and other divalent cations in atp-utilizing enzymes. Magnesium 1987; 6:28-33.

127. Bhattacharyya A, Pakrashi A. Specificity of ATP for the initiation of flagellar motility of hamster sperm. Arch Androl 1993; 31:159-165.

128. Cosson MP, Cosson J, Andre F, Billard R. CAMP/ATP relationship in the activation of trout sperm motility: Their interaction in membrane-deprived models and in live spermatozoa. Cell Motil Cytoskeleton 1995; 31:159-176.

129. Houdusse A, Carter AP. Dynein swings into action. Cell 2009; 136:395-396.

130. Ishida K, Okuno M, Morisawa S. Initiation of sperm motility induced by cyclic AMP in hamster and boar. Dev Growth Differ 1987; 28:47-56.

131. Kinukawa M, Oda S, Shirakura Y, Okabe M, Ohmuro J, Baba SA, Nagata M, Aoki F. Roles of cAMP in regulating microtubule sliding and flagellar bending in demembranated hamster spermatozoa. FEBS Lett 2006; 580:1515-1520.

132. Calogero AE, Fishel S, Hall J, Ferrara E, Vicari E, Green S, Hunter A, Burrello N, Thornton S, D'agata R. Correlation between intracellular cAMP content, kinematic parameters and hyperactivation of human spermatozoa after incubation with pentoxifylline. Hum Reprod 1998; 13:911-915.

133. Tash JS, Kakar SS, Means AR. Flagellar motility requires the cAMP-dependent phosphorylation of a heat-stable NP-40-soluble 56 kd protein, axokinin. Cell 1984; 38:551-559.

134. San Agustin JT, Witman GB. Role of cAMP in the reactivation of demembranated ram spermatozoa. Cell Motil Cytoskeleton 1994; 27:206-218.

135. Storey BT, Keyhani E. Energy metabolism of spermatozoa: III. Energy-linked uptake of calcium ion by the mitochondria of rabbit epididymal spermatozoa. Fertil Steril 1974; 25:976-984.

136. Morton B, Harrigan-Lum J, Albagli L, Jooss T. The activation of motility in quiescent hamster sperm from the epididymis by calcium and cyclic nucleotides. Biochem Biophys Res Commun 1974; 56:372-379.

137. Babcock DF, Singh JP, Lardy HA. Alteration of membrane permeability to calcium ions during maturation of bovine spermatozoa. Dev Biol 1979; 69:85-93.

138. Morton BE, Sagadraca R, Fraser C. Sperm motility within the mammalian epididymis: Species variation and correlation with free calcium levels in epididymal plasma. Fertil Steril 1978; 29:695-698.

139. Ignotz GG, Suarez SS. Calcium/calmodulin and calmodulin kinase II stimulate hyperactivation in demembranated bovine sperm. Biol Reprod 2005; 73:519-526.

140. Lindemann CB, Goltz JS. Calcium regulation of flagellar curvature and swimming pattern in triton X-100--extracted rat sperm. Cell Motil Cytoskeleton 1988; 10:420-431.

141. Bannai H, Yoshimura M, Takahashi K, Shingyoji C. Calcium regulation of microtubule sliding in reactivated sea urchin sperm flagella. J Cell Sci 2000; 113:831-839.

142. Moritz MJ, Schmitz KA, Lindemann CB. Measurement of the force and torque produced in the calcium response of reactivated rat sperm flagella. Cell Motil Cytoskeleton 2001; 49:33-40.

143. Brokaw CJ. Calcium sensors in sea urchin sperm flagella. Cell Motil Cytoskeleton 1991; 18:123-130.

144. Gibbons BH, Gibbons IR. Calcium-induced quiescence in reactivated sea urchin sperm. J Cell Biol 1980; 84:13-27.

145. Wais-Steider J, Satir P. Effect of vanadate on gill cilia: Switching mechanism in ciliary beat. J Supramol Struct 1979; 11:339-347.

146. Stommel EW. Mechanical stimulation activates beating in calcium-arrested lateral cilia of mytilus edulis gill. J Muscle Res Cell Motil 1986; 7:237-244.

147. Lesich KA, Zhang Z, Kelsch CB, Ponichter KL, Strauss JF, 3rd, Lindemann CB. Functional deficiencies and a reduced response to calcium in the flagellum of mouse sperm lacking spag16l. Biol Reprod 2010; 82:736-744.

148. Lindemann CB, Orlando A, Kanous KS. The flagellar beat of rat sperm is organized by the interaction of two functionally distinct populations of dynein bridges with a stable central axonemal partition. J Cell Sci 1992; 102:249-260.

149. Lindemann CB, Kanous KS. "Geometric clutch" hypothesis of axonemal function: Key issues and testable predictions. Cell Motil Cytoskeleton 1995; 31:1-8.

150. Kanous KS, Casey C, Lindemann CB. Inhibition of microtubule sliding by Ni2+ and Cd2+: Evidence for a differential response of certain microtubule pairs within the bovine sperm axoneme. Cell Motil Cytoskeleton 1993; 26:66-76.

151. Gibbons IR, Cosson MP, Evans JA, Gibbons BH, Houck B, Martinson KH, Sale WS, Tang WJ. Potent inhibition of dynein adenosinetriphosphatase and of the motility of cilia and sperm flagella by vanadate. Proc Natl Acad Sci U S A 1978; 75:2220-2224.

152. Sale WS, Gibbons IR. Study of the mechanism of vanadate inhibition of the dynein cross-bridge cycle in sea urchin sperm flagella. J Cell Biol 1979; 82:291-298.

153. Williams KM, Ford WC. The motility of demembranated human spermatozoa is inhibited by free calcium ion activities of 500 nmol/l or more. Int J Androl 2001; 24:216-224.

154. Giroux-Widemann V, Jouannet P, Pignot-Paintrand I, Feneux D. Effects of pH on the reactivation of human spermatozoa demembranated with triton X-100. Mol Reprod Dev 1991; 29:157-162.

155. Keskes L, Giroux-Widemann V, Serres C, Pignot-Paintrand I, Jouannet P, Feneux D. The reactivation of demembranated human spermatozoa lacking outer dynein arms is independent of pH. Mol Reprod Dev 1998; 49:416-425.

156. Alasmari W, Costello S, Correia J, Oxenham SK, Morris J, Fernandes L, Ramalho Santos J, Kirkman-Brown J, Michelangeli F, Publicover S, Barratt CL. Ca2+ signalling through CatSper and Ca2+ stores regulate different behaviours in human sperm. J Biol Chem 2013.

157. Lindemann CB, Gardner TK, Westbrook E, Kanous KS. The calcium-induced curvature reversal of rat sperm is potentiated by cAMP and inhibited by anti-calmodulin. Cell Motil Cytoskeleton 1991; 20:316-324.

158. Lindemann CB, Fentie I, Rikmenspoel R. A selective effect of Ni2+ on wave initiation in bull sperm flagella. J Cell Biol 1980; 87:420-426.

159. Bird Z, Hard R, Kanous KS, Lindemann CB. Interdoublet sliding in bovine spermatozoa: Its relationship to flagellar motility and the action of inhibitory agents. J Struct Biol 1996; 116:418-428.

160. Bean B, Harris A. Selective inhibition of flagellar activity in chlamydomonas by nickel. J Protozool 1979; 26:235-240.

161. Larsen J, Satir P. Analysis of Ni(2+)-induced arrest of paramecium axonemes. J Cell Sci 1991; 99:33-40.

162. Sutoo D, Akiyama K. Effect of cadmium or magnesium on calcium-dependent central function that reduces blood pressure. Arch Toxicol 2000; 74:1-4.

163. Chen S, Xu Y, Xu B, Guo M, Zhang Z, Liu L, Ma H, Chen Z, Luo Y, Huang S, Chen L. CamKII is involved in cadmium activation of mapk and mtor pathways leading to neuronal cell death. J Neurochem 2011; 119:1108-1118.

164. Carr DW, Acott TS. Inhibition of bovine spermatozoa by caudal epididymal fluid: I. Studies of a sperm motility quiescence factor. Biol Reprod 1984; 30:913-925.

165. Hamamah S, Gatti JL. Role of the ionic environment and internal pH on sperm activity. Hum Reprod 1998; 4:20-30.

166. Sato F, Mogami Y, Baba SA. Flagellar quiescence and transience of inactivation induced by rapid pH drop. Cell Motil Cytoskeleton 1988; 10:374-379.

167. Verma RJ. Sperm quiescence in cauda epididymis: A mini-review. Asian J Androl 2001; 3:181-183.

168. Aranha I, Bhagya M, Yajurvedi HN. Concentration of cations in different parts of male reproductive system and their influence on in vitro sperm motility in lizard, mabuya carinata schneider. Indian J Exp Biol 2008; 46:720-724.

169. Moore EW. Ionized calcium in normal serum, ultrafiltrates, and whole blood determined by ion-exchange electrodes. J Clin Invest 1970; 49:318-334.

170. Lishko PV, Kirichok Y, Ren D, Navarro B, Chung JJ, Clapham DE. The control of male fertility by spermatozoan ion channels. Annu Rev Physiol 2012; 74:453-475.

171. Carlson AE, Hille B, Babcock DF. External Ca2+ acts upstream of adenylyl cyclase sacy in the bicarbonate signaled activation of sperm motility. Dev Biol 2007; 312:183-192.

172. Jimenez T, Mcdermott JP, Sanchez G, Blanco G. Na,K-ATPase alpha4 isoform is essential for sperm fertility. Proc Natl Acad Sci U S A 2011; 108:644-649.

173. Okunade GW, Miller ML, Pyne GJ, Sutliff RL, O'connor KT, Neumann JC, Andringa A, Miller DA, Prasad V, Doetschman T, Paul RJ, Shull GE. Targeted ablation of plasma membrane Ca2+-ATPase (PMCA) 1 and 4 indicates a major housekeeping function for PMCA1 and a critical role in hyperactivated sperm motility and male fertility for PMCA4. J Biol Chem 2004; 279:33742-33750.

174. Schuh K, Cartwright EJ, Jankevics E, Bundschu K, Liebermann J, Williams JC, Armesilla AL, Emerson M, Oceandy D, Knobeloch KP, Neyses L. Plasma membrane Ca2+ ATPase 4 is required for sperm motility and male fertility. J Biol Chem 2004; 279:28220-28226.

175. Ramsey IS, Moran MM, Chong JA, Clapham DE. A voltage-gated proton-selective channel lacking the pore domain. Nature 2006; 440:1213-1216.

176. Sasaki M, Takagi M, Okamura Y. A voltage sensor-domain protein is a voltage-gated proton channel. Science 2006; 312:589-592.

177. Lishko PV, Kirichok Y. The role of HV1 and CatSper channels in sperm activation. J Physiol 2010; 588:4667-4672.

178. Wang D, King SM, Quill TA, Doolittle LK, Garbers DL. A new sperm-specific Na+/H+ exchanger required for sperm motility and fertility. Nat Cell Biol 2003; 5:1117-1122

179. Suarez SS, Dai X. Intracellular calcium reaches different levels of elevation in hyperactivated and acrosome-reacted hamster sperm. Mol Reprod Dev 1995; 42:325-333.

180. Chang H, Suarez SS. Two distinct Ca(2+) signaling pathways modulate sperm flagellar beating patterns in mice. Biol Reprod 2011; 85:296-305.

181. Alasmari W, Barratt CLR, Publicover SJ, Whalley KM, Foster E, Kay V, Martins Da Silva S, Oxenham SK. The clinical significance of calcium-signalling pathways mediating human sperm hyperactivation. Hum Reprod 2013; 28:866-876.

182. Beuckmann CT, Sinton CM, Miyamoto N, Ino M, Yanagisawa M. N-type calcium channel alpha1b subunit (cav2.2) knock-out mice display hyperactivity and vigilance state differences. J Neurosci 2003; 23:6793-6797.

183. Saegusa H, Kurihara T, Zong S, Minowa O, Kazuno A, Han W, Matsuda Y, Yamanaka H, Osanai M, Noda T, Tanabe T. Altered pain responses in mice lacking alpha 1e subunit of the voltage-dependent Ca2+ channel. Proc Natl Acad Sci U S A 2000; 97:6132-6137.

184. Kim D, Song I, Keum S, Lee T, Jeong MJ, Kim SS, Mcenery MW, Shin HS. Lack of the burst firing of thalamocortical relay neurons and resistance to absence seizures in mice lacking alpha(1g) t-type ca(2+) channels. Neuron 2001; 31:35-45.

185. Qi H, Moran MM, Navarro B, Chong JA, Krapivinsky G, Krapivinsky L, Kirichok Y, Ramsey IS, Quill TA, Clapham DE. All four CatSper ion channel proteins are required for male fertility and sperm cell hyperactivated motility. Proc Natl Acad Sci U S A 2007; 104:1219-1223.

186. Kirichok Y, Navarro B, Clapham DE. Whole-cell patch-clamp measurements of spermatozoa reveal an alkaline-activated Ca2+ channel. Nature 2006; 439:737-740

187. Carlson AE, Burnett LA, Del Camino D, Quill TA, Hille B, Chong JA, Moran MM, Babcock DF. Pharmacological targeting of native CatSper channels reveals a required role in maintenance of sperm hyperactivation. PLoS ONE 2009; 4:0006844.

188. Marquez B, Suarez SS. Bovine sperm hyperactivation is promoted by alkaline-stimulated ca2+ influx. Biol Reprod 2007; 76:660-665.

189. Chung JJ, Navarro B, Krapivinsky G, Krapivinsky L, Clapham DE. A novel gene required for male fertility and functional CATSPER channel formation in spermatozoa. Nat Commun 2011; 2:153.

190. Navarro B, Kirichok Y, Chung JJ, Clapham DE. Ion channels that control fertility in mammalian spermatozoa. Int J Dev Biol 2008; 52:607-613.

191. Hildebrand MS, Avenarius MR, Fellous M, Zhang Y, Meyer NC, Auer J, Serres C, Kahrizi K, Najmabadi H, Beckmann JS, Smith RJ. Genetic male infertility and mutation of CATSPER ion channels. Eur J Hum Genet 2010; 18:1178-1184.

192. Avenarius MR, Hildebrand MS, Zhang Y, Meyer NC, Smith LL, Kahrizi K, Najmabadi H, Smith RJ. Human male infertility caused by mutations in the CATSPER1 channel protein. Am J Hum Genet 2009; 84:505-510.

193. Lobley A, Pierron V, Reynolds L, Allen L, Michalovich D. Identification of human and mouse CatSper3 and CatSper4 genes: Characterisation of a common interaction domain and evidence for expression in testis. Reprod Biol Endocrinol 2003; 1:53.

194. Liu J, Xia J, Cho KH, Clapham DE, Ren D. CatSperbeta, a novel transmembrane protein in the CatSper channel complex. J Biol Chem 2007; 282:18945-18952.

195. Wang H, Liu J, Cho KH, Ren D. A novel, single, transmembrane protein CatSperg is associated with CATSPER1 channel protein. Biol Reprod 2009; 81:539-544.

196. Ren D, Xia J. Calcium signaling through CatSper channels in mammalian fertilization. Physiology 2010; 25:165-175.

197. Cai X, Clapham DE. Ancestral Ca2+ signaling machinery in early animal and fungal evolution. Mol Biol Evol 2012; 29:91-100.

198. Cai X, Clapham DE. Evolutionary genomics reveals lineage-specific gene loss and rapid evolution of a sperm-specific ion channel complex: CatSpers and CatSperbeta. PLoS ONE 2008; 3:30.

199. Eisenbach M, Giojalas LC. Sperm guidance in mammals - an unpaved road to the egg. Nat Rev Mol Cell Biol 2006; 7:276-285.

200. Lishko PV, Botchkina IL, Kirichok Y. Progesterone activates the principal Ca2+ channel of human sperm. Nature 2011; 471:387-391.

201. Strunker T, Goodwin N, Brenker C, Kashikar ND, Weyand I, Seifert R, Kaupp UB. The CatSper channel mediates progesterone-induced Ca2+ influx in human sperm. Nature 2011; 471:382-386.

202. Rolke K. Localization of the CatSper1 protein and induction of hyperactivated-like motility in equine spermatozoa. College Station, Tx: Texas A&M; 2008.

203. Olson SD, Suarez SS, Fauci LJ. A model of CatSper channel mediated calcium dynamics in mammalian spermatozoa. Bull Math Biol 2010; 72:1925-1946.

204. Olson SD, Fauci LJ, Suarez SS. Mathematical modeling of calcium signaling during sperm hyperactivation. Mol Hum Reprod 2011; 17:500-510.

205. Summers KE, Gibbons IR. Adenosine triphosphate-induced sliding of tubules in trypsin-treated flagella of sea-urchin sperm. Proc Natl Acad Sci U S A 1971; 68:3092-3096.

206. Storey BT. Energy metabolism of spermatozoa. IV. Effect of calcium on respiration of mature epididymal sperm of the rabbit. Biol Reprod 1975; 13:1-9.

207. Morisawa M, Okuno M. Cyclic AMP induces maturation of trout sperm axoneme to initiate motility. Nature 1982; 295:703-704

208. Brokaw CJ. Regulation of sperm flagellar motility by calcium and cAMP-dependent phosphorylation. J Cell Biochem 1987; 35:175-184.

209. Goltz JS, Gardner TK, Kanous KS, Lindemann CB. The interaction of pH and cyclic adenosine 3',5'-monophosphate on activation of motility in triton X-100 extracted bull sperm. Biol Reprod 1988; 39:1129-1136.

210. Suarez SS, Dai X. Hyperactivation enhances mouse sperm capacity for penetrating viscoelastic media. Biol Reprod 1992; 46:686-691.

211. Kaula N, Andrews A, Durso C, Dixon C, Graham JK. Classification of hyperactivated spermatozoa using a robust minimum bounding square ratio algorithm. Conf Proc IEEE Eng Med Biol Soc 2009; 2009:4941-4944.

212. Chen Y, Cann MJ, Litvin TN, Iourgenko V, Sinclair ML, Levin LR, Buck J. Soluble adenylyl cyclase as an evolutionarily conserved bicarbonate sensor. Science 2000; 289:625-628.

213. Gadella BM. The assembly of a zona pellucida binding protein complex in sperm. Reprod Domest Anim 2008; 5:12-19.

214. Salathe M. Regulation of mammalian ciliary beating. Annu Rev Physiol 2007; 69:401-422.

215. Jaiswal BS, Conti M. Calcium regulation of the soluble adenylyl cyclase expressed in mammalian spermatozoa. Proc Natl Acad Sci U S A 2003; 100:10676-10681.

216. Harrison RA. Rapid PKA-catalysed phosphorylation of boar sperm proteins induced by the capacitating agent bicarbonate. Mol Reprod Dev 2004; 67:337-352.

217. Nolan MA, Babcock DF, Wennemuth G, Brown W, Burton KA, Mcknight GS. Sperm-specific protein kinase a catalytic subunit calpha2 orchestrates cAMP signaling for male fertility. Proc Natl Acad Sci U S A 2004; 101:13483-13488.

218. Xie F, Garcia MA, Carlson AE, Schuh SM, Babcock DF, Jaiswal BS, Gossen JA, Esposito G, Van Duin M, Conti M. Soluble adenylyl cyclase (sac) is indispensable for sperm function and fertilization. Dev Biol 2006; 296:353-362.

219. Si Y, Okuno M. Multiple activation of mouse sperm motility. Mol Reprod Dev 1993; 36:89-95

220. Visconti PE, Krapf D, De La Vega-Beltran JL, Acevedo JJ, Darszon A. Ion channels, phosphorylation and mammalian sperm capacitation. Asian J Androl 2011; 13:395-405.

221. Krapf D, Arcelay E, Wertheimer EV, Sanjay A, Pilder SH, Salicioni AM, Visconti PE. Inhibition of ser/thr phosphatases induces capacitation-associated signaling in the presence of SRC kinase inhibitors. J Biol Chem 2010; 285:7977-7985.

222. Colas C, Cebrian-Perez JA, Muino-Blanco T. Caffeine induces ram sperm hyperactivation independent of cAMP-dependent protein kinase. Int J Androl 2010; 33:1365-2605.

223. Harayama H, Miyake M. A cyclic adenosine 3',5'-monophosphate-dependent protein kinase c activation is involved in the hyperactivation of boar spermatozoa. Mol Reprod Dev 2006; 73:1169-1178.

224. Shahar S, Wiser A, Ickowicz D, Lubart R, Shulman A, Breitbart H. Light-mediated activation reveals a key role for protein kinase A and sarcoma protein kinase in the development of sperm hyper-activated motility. Hum Reprod 2011; 26:2274-2282.

225. Rashidi Im TT. The effects of pentoxifylline on mouse epididymal sperm parameters, fertilization and cleavage rages after short time preservation. Iranian Journal of Reproductive Medicine 2004; 2:51-57.

226. Itach SB, Finklestein M, Etkovitz N, Breitbart H. Hyper-activated motility in sperm capacitation is mediated by phospholipase D-dependent actin polymerization. Dev Biol 2012; 362:154-161.

227. Jayaprakash D, Kumar KS, Shivaji S, Seshagiri PB. Pentoxifylline induces hyperactivation and acrosome reaction in spermatozoa of golden hamsters: Changes in motility kinematics. Hum Reprod 1997; 12:2192-2199.

228. Kumar V, Rangaraj N, Shivaji S. Activity of pyruvate dehydrogenase A (PDHA) in hamster spermatozoa correlates positively with hyperactivation and is associated with sperm capacitation. Biol Reprod 2006; 75:767-777.

229. Suzuki T, Fujinoki M, Shibahara H, Suzuki M. Regulation of hyperactivation by PPP2 in hamster spermatozoa. Reproduction 2010; 139:847-856.

230. Scholer HR, Balling R, Hatzopoulos AK, Suzuki N, Gruss P. Octamer binding proteins confer transcriptional activity in early mouse embryogenesis. EMBO J 1989; 8:2551-2557.

231. Smith EF. Regulation of flagellar dynein by the axonemal central apparatus. Cell Motil Cytoskeleton 2002; 52:33-42.

232. Marin-Briggiler CI, Jha KN, Chertihin O, Buffone MG, Herr JC, Vazquez-Levin MH, Visconti PE. Evidence of the presence of calcium/calmodulin-dependent protein kinase iv in human sperm and its involvement in motility regulation. J Cell Sci 2005; 118:2013-2022.

233. Navarro B, Kirichok Y, Clapham DE. Ksper, a pH-sensitive K+ current that controls sperm membrane potential. Proc Natl Acad Sci U S A 2007; 104:7688-7692.

234. Zeng XH, Yang C, Kim ST, Lingle CJ, Xia XM. Deletion of the SLO3 gene abolishes alkalization-activated K+ current in mouse spermatozoa. Proc Natl Acad Sci U S A 2011; 108:5879-5884.

235. Santi CM, Martinez-Lopez P, De La Vega-Beltran JL, Butler A, Alisio A, Darszon A, Salkoff L. The SLO3 sperm-specific potassium channel plays a vital role in male fertility. FEBS Lett 2010; 584:1041-1046.

236. Decoursey TE. Voltage-gated proton channels: What's next? J Physiol 2008; 586:5305-5324.

237. Musset B, Capasso M, Cherny VV, Morgan D, Bhamrah M, Dyer MJ, Decoursey TE. Identification of thr29 as a critical phosphorylation site that activates the human proton channel hvcn1 in leukocytes. J Biol Chem 2010; 285:5117-5121.

238. Miki K, Qu W, Goulding EH, Willis WD, Bunch DO, Strader LF, Perreault SD, Eddy EM, O'brien DA. Glyceraldehyde 3-phosphate dehydrogenase-s, a sperm-specific glycolytic enzyme, is required for sperm motility and male fertility. Proc Natl Acad Sci U S A 2004; 101:16501-16506.

239. Mukai C, Okuno M. Glycolysis plays a major role for adenosine triphosphate supplementation in mouse sperm flagellar movement. Biol Reprod 2004; 71:540-547.

240. Williams AC, Ford WC. The role of glucose in supporting motility and capacitation in human spermatozoa. J Androl 2001; 22:680-695.

241. Okochi Y, Sasaki M, Iwasaki H, Okamura Y. Voltage-gated proton channel is expressed on phagosomes. Biochem Biophys Res Commun 2009; 382:274-279.

242. Ramsey IS, Ruchti E, Kaczmarek JS, Clapham DE. Hv1 proton channels are required for high-level nadph oxidase-dependent superoxide production during the phagocyte respiratory burst. Proc Natl Acad Sci U S A 2009; 106:7642-7647.

243. Rathi R, Colenbrander B, Bevers MM, Gadella BM. Evaluation of in vitro capacitation of stallion spermatozoa. Biol Reprod 2001; 65:462-470.

244. Filannino A, Stout TA, Gadella BM, Sostaric E, Pizzi F, Colenbrander B, Dell'aquila ME, Minervini F. Dose-response effects of estrogenic mycotoxins

(zearalenone, alpha- and beta-zearalenol) on motility, hyperactivation and the acrosome reaction of stallion sperm. Reprod Biol Endocrinol 2011; 9:1477-7827.

245. Warnke C, Tuchscherer A, Alm H, Kanitz W, Blottner S, Torner H. Characterisation of movement pattern and velocities of stallion spermatozoa depending on donor, season and cryopreservation. Acta Vet Hung 2003; 51:395-408.

246. Ortgies F, Klewitz J, Gorgens A, Martinsson G, Sieme H. Effect of procaine, pentoxifylline and trolox on capacitation and hyperactivation of stallion spermatozoa. Andrologia 2012; 1:130-138.

247. Gavella M, Lipovac V, Marotti T. Effect of pentoxifylline on superoxide anion production by human sperm. Int J Androl 1991; 14:320-327.

248. Silva K, Tap M, Ecb S, Sc G, Mmp G. Efeito da adic¸a˜o de trolox e pentoxifilina na motilidade, integridade do acrossoma e do DNA de espermatozoides equinos apo´ s descongelac¸a˜o. Arq Bras Med Vet Zootec 2009; 61:41-49.

249. Gentry CL, Lukas RJ. Local anesthetics noncompetitively inhibit function of four distinct nicotinic acetylcholine receptor subtypes. J Pharmacol Exp Ther 2001; 299:1038-1048.

250. Endo M. Calcium-induced calcium release in skeletal muscle. Physiol Rev 2009; 89:1153-1176.

251. Grandin N, Charbonneau M. Changes in intracellular free calcium activity in xenopus eggs following imposed intracellular pH changes using weak acids and weak bases. Biochim Biophys Acta 1991; 31:242-250.

252. Kuperman AS, Altura BT, Chezar JA. Action of procaine on calcium efflux from frog nerve and muscle. Nature 1968; 217:673-675.

253. De Boland AR, Jilka RL, Martonosi AN. Passive Ca2+ permeability of phospholipid vesicles and sarcoplasmic reticulum membranes. J Biol Chem 1975; 250:7501-7510.

254. Carlson AE, Quill TA, Westenbroek RE, Schuh SM, Hille B, Babcock DF. Identical phenotypes of CatSper1 and CatSper2 null sperm. J Biol Chem 2005; 280:32238-32244.

255. Marquez B, Ignotz G, Suarez SS. Contributions of extracellular and intracellular Ca2+ to regulation of sperm motility: Release of intracellular stores can hyperactivate CatSper1 and CatSper2 null sperm. Dev Biol 2007; 303:214-221.

256. Alm H, Torner H, Blottner S, Nürnberg G, Kanitz W. Effect of sperm cryopreservation and treatment with calcium ionophore or heparin on in vitro fertilization of horse oocytes. Theriogenology 2001; 56:817-829.

257. Ho HC, Suarez SS. Hyperactivation of mammalian spermatozoa: Function and regulation. Reproduction 2001; 122:519-526.

258. Carlson AE, Westenbroek RE, Quill T, Ren D, Clapham DE, Hille B, Garbers DL, Babcock DF. CatSper1 required for evoked Ca2+ entry and control of flagellar function in sperm. Proc Natl Acad Sci U S A 2003; 100:14864-14868.

259. Avidan N, Tamary H, Dgany O, Cattan D, Pariente A, Thulliez M, Borot N, Moati L, Barthelme A, Shalmon L, Krasnov T, Ben-Asher E, et al. CatSper2, a human autosomal nonsyndromic male infertility gene. Eur J Hum Genet 2003; 11:497-502.

260. Nikpoor P, Mowla SJ, Movahedin M, Ziaee SA, Tiraihi T. CatSper gene expression in postnatal development of mouse testis and in subfertile men with deficient sperm motility. Hum Reprod 2004; 19:124-128.

261. Avenarius MR, Hildebrand MS, Zhang Y, Meyer NC, Smith LL, Kahrizi K, Najmabadi H, Smith RJ. Human male infertility caused by mutations in the CatSper1 channel protein. Am J Hum Genet 2009; 84:505-510.

262. Ho HC, Suarez SS. Characterization of the intracellular calcium store at the base of the sperm flagellum that regulates hyperactivated motility. Biol Reprod 2003; 68:1590-1596.

263. Song C, Gao B, Wu H, Xie Y, Wang X, Li B, Chen G, Mao J. Molecular cloning, spatial and temporal expression analysis of CatSper genes in the chinese meishan pigs. Reprod Biol Endocrinol 2011; 9:132.

264. Villaverde AI, Fioratti EG, Landim-Alvarenga FC, De Carvalho Balieiro JC, Melo CM, Papa FO, Lopes MD. Effect of progesterone and ionomycin on domestic cat sperm motility patterns and acrosome reaction. Reprod Domest Anim 2009; 44 Suppl 2:309-312.

265. Foster ML, Love CC, Varner DD, Brinsko SP, Hinrichs K, Teague S, Lacaze K, Blanchard TL. Comparison of methods for assessing integrity of equine sperm membranes. Theriogenology 2011; 76:334-341.

266. Brenker C, Goodwin N, Weyand I, Kashikar ND, Naruse M, Krahling M, Muller A, Kaupp UB, Strunker T. The CatSper channel: A polymodal chemosensor in human sperm. EMBO J 2012.

267. Schmidt H, Kamp G. Induced hyperactivity in boar spermatozoa and its evaluation by computer-assisted sperm analysis. Reproduction 2004; 128:171-179.

268. Pilikian S, Adeleine P, Czyba JC, Ecochard R, Guerin JF, Mimouni P. Hyperactivated motility of sperm from fertile donors and asthenozoospermic patients before and after treatment with ionophore. Int J Androl 1991; 14:167-173.

269. Suarez SS, Vincenti L, Ceglia MW. Hyperactivated motility induced in mouse sperm by calcium ionophore A23187 is reversible. J Exp Zool 1987; 244:331-336.

270. Torres-Flores V, Picazo-Juarez G, Hernandez-Rueda Y, Darszon A, Gonzalez-Martinez MT. Sodium influx induced by external calcium chelation decreases human sperm motility. Hum Reprod 2011; 26:2626-2635.

271. Cai X, Clapham DE. Evolutionary genomics reveals lineage-specific gene loss and rapid evolution of a sperm-specific ion channel complex: CatSpers and CatSperbeta. PLoS One 2008; 3:e3569.

272. Mishra SK, Hermsmeyer K. Selective inhibition of t-type Ca2+ channels by ro 40-5967. Circ Res 1994; 75:144-148.

273. Santi CM, Santos T, Hernandez-Cruz A, Darszon A. Properties of a novel pH-dependent Ca2+ permeation pathway present in male germ cells with possible roles in spermatogenesis and mature sperm function. J Gen Physiol 1998; 112:33-53.

274. Carlson AE, Burnett LA, Del Camino D, Quill TA, Hille B, Chong JA, Moran MM, Babcock DF. Pharmacological targeting of native CatSper channels reveals a required role in maintenance of sperm hyperactivation. PLoS One 2009; 4:e6844.

275. Mujica A, Neri-Bazan L, Tash JS, Uribe S. Mechanism for procaine-mediated hyperactivated motility in guinea pig spermatozoa. Mol Reprod Dev 1994; 38:285-292.

276. Tang QY, Zhang Z, Xia XM, Lingle CJ. Block of mouse slo1 and slo3 k+ channels by CTX, IBTX, TEA, 4-AP and quinidine. Channels (Austin) 2010; 4:22-41.

277. Gu Y, Kirkman-Brown JC, Korchev Y, Barratt CL, Publicover SJ. Multi-state, 4-aminopyridine-sensitive ion channels in human spermatozoa. Dev Biol 2004; 274:308-317.

278. Bedu-Addo K, Costello S, Harper C, Machado-Oliveira G, Lefievre L, Ford C, Barratt C, Publicover S. Mobilisation of stored calcium in the neck region of

human sperm--a mechanism for regulation of flagellar activity. Int J Dev Biol 2008; 52:615-626.

279. Quill TA, Ren D, Clapham DE, Garbers DL. A voltage-gated ion channel expressed specifically in spermatozoa. Proc Natl Acad Sci U S A 2001; 98:12527-12531.

280. Quill TA, Sugden SA, Rossi KL, Doolittle LK, Hammer RE, Garbers DL. Hyperactivated sperm motility driven by CatSper2 is required for fertilization. Proc Natl Acad Sci U S A 2003; 100:14869-14874.

281. Loux SC, Crawford KR, Ing NH, Gonzalez-Fernandez L, Macias-Garcia B, Love CC, Varner DD, Velez IC, Choi YH, Hinrichs K. CatSper and the relationship of hyperactivated motility to intracellular calcium and pH kinetics in equine sperm. Biol Reprod 2013; In Press.

282. Tamblyn TM, Singh JP, Lorton SP, First NL. Mechanisms controlling motility of stallion spermatozoa. J Reprod Fertil Suppl 1979; 27:31-37.

283. Feng B, Bhattacharyya A, Yanagimachi R. Ca2+ is essential for the motility of plasma membrane-intact, but not of demembranated, hamster spermatozoa. Andrologia 1988; 20:155-162.

284. Mizuno K, Shiba K, Okai M, Takahashi Y, Shitaka Y, Oiwa K, Tanokura M, Inaba K. Calaxin drives sperm chemotaxis by Ca(2+)-mediated direct modulation of a dynein motor. Proc Natl Acad Sci U S A 2012; 109:20497-20502.

285. Ishijima S, Witman GB. Flagellar movement of intact and demembranated, reactivated ram spermatozoa. Cell Motil Cytoskeleton 1987; 8:375-391.

286. Lindemann CB, Gibbons IR. Adenosine triphosphate-induced motility and sliding of filaments in mammalian sperm extracted with triton X-100. J Cell Biol 1975; 65:147-162.

287. Yuan T, Gomes AV, Barnes JA, Hunter HN, Vogel HJ. Spectroscopic characterization of the calmodulin-binding and autoinhibitory domains of calcium/calmodulin-dependent protein kinase I. Arch Biochem Biophys 2004; 421:192-206.

288. Yuan Y, Jiang CY, Xu H, Sun Y, Hu FF, Bian JC, Liu XZ, Gu JH, Liu ZP. Cadmium-induced apoptosis in primary rat cerebral cortical neurons culture is mediated by a calcium signaling pathway. PLoS ONE 2013; 8.

289. Alasmari W, Costello S, Correia J, Oxenham SK, Morris J, Fernandes L, Ramalho-Santos J, Kirkman-Brown J, Michelangeli F, Publicover S, Barratt CL. Ca2+ signals generated by CatSper and Ca2+ stores regulate different behaviors in human sperm. J Biol Chem 2013; 288:6248-6258.

290. Nicoletti I, Migliorati G, Pagliacci MC, Grignani F, Riccardi C. A rapid and simple method for measuring thymocyte apoptosis by propidium iodide staining and flow cytometry. J Immunol Methods 1991; 139:271-279.

291. Ahmad B, Kamal MZ, Khan RH. Alkali-induced conformational transition in different domains of bovine serum albumin. Protein Pept Lett 2004; 11:307-315.

292. White DR, Aitken RJ. Relationship between calcium, cyclic AMP, ATP and intracellular pH and the capacity of hamster spermatozoa to express hyperactivated motility. Gamete Res 1989; 22:163-177.

293. Zhou R, Shi B, Chou KC, Oswalt MD, Haug A. Changes in intracellular calcium of porcine sperm during in vitro incubation with seminal plasma and a capacitating medium. Biochem Biophys Res Commun 1990; 172:47-53.

294. Heffner LJ, Storey BT. The role of calcium in maintaining motility in mouse spermatozoa. J Exp Zool 1981; 218:427-434.

295. Vredenburgh-Wilberg WL, Parrish JJ. Intracellular pH of bovine sperm increases during capacitation. Mol Reprod Dev 1995; 40:490-502.

296. Cross NL, Razy-Faulkner P. Control of human sperm intracellular pH by cholesterol and its relationship to the response of the acrosome to progesterone. Biol Reprod 1997; 56:1169-1174.

297. Brewis IA, Morton IE, Mohammad SN, Browes CE, Moore HD. Measurement of intracellular calcium concentration and plasma membrane potential in human spermatozoa using flow cytometry. J Androl 2000; 21:238-249.

298. Peterson RN, Freund M. Relationship between motility and the transport and binding of divalent cations to the plasma membrane of human spermatozoa. Fertil Steril 1976; 27:1301-1307.

299. Lesich KA. Personal Communication; 2013.

300. Si Y, Okuno M. Regulation of microtubule sliding by a 36-kda phosphoprotein in hamster sperm flagella. Mol Reprod Dev 1999; 52:328-334.

APPENDIX

	Concentration Mibefradil				
Time	**0 µM[a]**	**0.5 µM[a]**	**1 µM[a]**	**2 – 2.5 µM[b]**	**5 µM[c]**
1	0.179343	0.170823	0.161509	0.132133	0.064127
2	0.206119	0.186725	0.1824	0.140975	0.075034
3	0.224931	0.197647	0.201948	0.169019	0.085276
4	0.251447	0.224218	0.211822	0.180964	0.108814
5	0.280146	0.239243	0.229071	0.18719	0.131774
6	0.296248	0.256064	0.247799	0.20939	0.146612
7	0.297771	0.271369	0.267053	0.217884	0.165378
8	0.32983	0.288802	0.281542	0.237262	0.176889
9	0.333594	0.303523	0.298969	0.252663	0.190047
10	0.353609	0.319176	0.312125	0.263795	0.212516
11	0.374923	0.339519	0.318957	0.27412	0.224081
12	0.390671	0.347101	0.338799	0.29506	0.243314
13	0.428739	0.388354	0.369757	0.319111	0.277606
14	0.440317	0.383393	0.372748	0.329008	0.295276
15	0.441353	0.390314	0.386438	0.333125	0.303857
16	0.468275	0.41393	0.403854	0.370312	0.337536
17	0.477225	0.427631	0.419499	0.383169	0.340808
18	0.478677	0.42691	0.425972	0.395575	0.350141
19	0.48889	0.438853	0.439747	0.40566	0.356193
20	0.494115	0.446033	0.453068	0.412151	0.372743
21	0.503837	0.456735	0.450629	0.413115	0.370714
22	0.516082	0.465522	0.464335	0.42616	0.3749
23	0.521039	0.480906	0.471239	0.420978	0.381875
24	0.525706	0.48438	0.476476	0.432054	0.387105

Table A-1. Data for Figure 3.1.A, relative intracellular calcium levels (ΔF/F0). Statistics were performed using one-way repeated measures ANOVA. Significant differences are noted with differing superscripts ($P < 0.05$).

	Concentration Mibefradil		
Time	**0 µM[a]**	**5 µM[b]**	**10 µM[a]**
1	0.875897	0.591044	0.690782
2	0.897607	0.621617	0.740507
3	0.946908	0.664569	0.778403
4	0.982388	0.715936	0.812968
5	1.017876	0.734093	0.858132
6	1.052318	0.771837	0.892286
7	1.089475	0.804941	0.949428
8	1.111285	0.833023	0.983739
9	1.132358	0.848735	1.022003
10	1.155305	0.887091	1.068396
11	1.171732	0.90505	1.096424
12	1.20319	0.926776	1.127871
13	1.215526	0.956423	1.162298
14	1.225998	0.987345	1.185586
15	1.246931	1.014083	1.228651
16	1.266026	1.049487	1.258642
17	1.288665	1.07329	1.281052
18	1.298974	1.092067	1.306524
19	1.312865	1.122947	1.335391
20	1.322078	1.150408	1.376057
21	1.339119	1.169611	1.403727
22	1.351649	1.197264	1.411904
23	1.357398	1.223679	1.440073
24	1.371207	1.247425	1.464337
25	1.366857	1.271664	1.492664
26	1.387567	1.312034	1.515585
27	1.391308	1.343982	1.534624
28	1.398052	1.349723	1.55365
29	1.402999	1.375614	1.570712
30	1.430168	1.399859	1.601309
31	1.429977	1.41621	1.618723

Table A-2. Data for Figure 3.1.B - relative intracellular calcium levels (ΔF/F0).

Average VCL

Time	Initial Medium pH 7.25	7.75	8.25	8.75	9.25
0	222.38	222.38	222.38	222.38	222.38
1	222.38[a]	223.68[a]	237.76[a,b]	283.08[b]	283.38[b]
5	227.88[a]	249.64[a,b]	275.84[a,b]	319.42[b]	299.08[a,b]
10	234.6[a]	261.52[a,b]	286.8[a,b]	332.54[b]	299.24[a,b]
15	243.16	268.06	294.58	330.5	298.04
20	246.02	274.04	297.7	323.74	284.98
30	246.82	281.74	300.42	319	269
40	253.78	285.68	288.28	310.96	252.6
60	243.416	279.1	283.32	288.74	234.86
80	245.38[a,b]	279.84[a]	272.28[a,b]	268.54[a,b]	206.62[b]
100	244.62[a,b]	272.22[a]	267.5[a]	242.3[a,b]	183.56[b]

Standard Error for VCL

Time	Initial Medium pH 7.25	7.75	8.25	8.75	9.25
0	8.754263	8.754263	8.754263	8.754263	8.754263
1	8.754263	9.684396	13.95707	11.14552	10.27959
5	11.22616	17.26105	24.31481	11.38326	8.995661
10	12.21396	21.86461	27.47132	10.31149	14.64302
15	14.22796	20.87576	26.69372	11.14206	19.65304
20	14.51139	23.04202	25.20336	11.4727	16.72482
30	14.21417	24.12356	27.32371	13.14741	21.33311
40	11.85136	20.19036	25.53594	11.46573	16.97108
60	10.20024	20.68224	21.65702	14.47366	15.98538
80	7.990715	15.73286	16.20875	12.51583	14.26844
100	15.34787	13.12166	15.81809	7.022991	15.24185

Table A-3. Data for Figure 3.2.A. Motility data for average VCL (μm/sec) and standard error. Statistics were performed by one-way ANOVA and demonstrate significant differences between the different pH media for each time point ($P < 0.05$). Time points without superscripts had no significant differences

Average ALH

Time	Initial Medium pH				
	7.25	**7.75**	**8.25**	**8.75**	**9.25**
0	7.26	7.26	7.26	7.26	7.26
1	7.26[a]	7.62[a]	8.58[a,b]	10.94[b]	11.54[b]
5	8.54	8.94	10.48	12.68	12.76
10	8.6	9.64	10.98	13.28	12.6
15	9.1	10.04	11.26	13.2	12.48
20	9.1	10.3	11.36	12.86	11.7
30	9.14	10.74	11.32	12.6	11.2
40	9.44	10.72	10.88	12.06	10.32
60	8.7	10.34	10.7	10.96	9.3
80	8.6	10.2	10.12	10.14	7.84
100	8.7[a,b]	9.82[a]	9.86[a]	8.86[a,b]	6.88[b]

Standard Error ALH

Time	Initial Medium pH				
	7.25	**7.75**	**8.25**	**8.75**	**9.25**
0	0.355077	0.355077	0.355077	0.355077	0.355077
1	0.355077	0.581997	0.891919	0.808257	0.73026
5	0.755566	0.900933	1.422505	0.815549	0.397593
10	0.883176	1.099309	1.54723	0.581997	0.383667
15	0.939361	1.08355	1.40331	0.631823	0.481996
20	0.918695	1.074802	1.246307	0.67088	0.525357
30	0.878453	1.103304	1.351266	0.650538	0.639375
40	0.835512	1.038614	1.316176	0.649061	0.499119
60	0.490714	1.055879	1.089587	0.69662	0.589237
80	0.36	0.830903	0.87288	0.671476	0.2751
100	0.475815	0.715206	0.776453	0.466133	0.293121

Table A-4. Data for Figure 3.2.B. Motility data for average VCL (μm/sec) and standard error. Statistics were performed by one-way ANOVA and demonstrate significant differences between the different pH media for each time point ($P < 0.05$). Time points without superscripts had no significant differences

Time of Max VCL	Final pH
80	7.9
30	8.74
10	8.89
15	9.06
80	7.53
100	7.88
100	7.5
15	8.27
15	8.49
80	7.42
100	7.83
20	8.05
10	8.28
15	8.57
30	7.69
30	8.24
30	8.4
5	8.62
1	8.89
100	7.56
60	8.17
30	8.33
10	8.48
1	8.82

Table A-5. Data from Figure 3.2.C. Following motility analysis, the pH of the medium of each sample was measured (final pH), and the time point at which the maximal VCL was noted.

Average VCL (µm)	Time (min)					
	0	1	5	15	30	60
control[a]	208.70	207.93	216.33	237.23	234.75	230.83
procaine[b]	208.70	379.05	406.25	392.45	390.15	328.63
10uM Cal[c]	208.70	78.85	68.93	73.98	58.63	74.78
1uM Cal[a,c]	208.70	154.53	146.23	146.65	160.75	183.53
0.1 uM Cal[c]	208.70	215.95	207.85	233.50	241.53	235.13
pH 8.5[a,c]	207.07	238.03	283.70	305.57	300.43	289.73
pH 9.5[a,c]	206.87	235.80	216.70	175.27	126.93	94.90
4-AP[b]	214.17	311.57	319.53	337.43	338.60	322.20
SE VCL (µm)	**Time (min)**					
	0	1	5	15	30	60
control[a]	13.63	14.92	15.24	14.32	17.28	20.17
procaine[b]	13.63	8.93	11.89	10.43	12.50	18.35
10uM Cal[c]	13.63	16.76	16.85	10.78	25.64	15.73
1uM Cal[a,c]	13.63	40.20	42.68	43.84	55.89	34.12
0.1 uM Cal[c]	13.63	17.78	20.03	18.13	22.60	19.51
pH 8.5[a,c]	13.57	29.66	31.65	29.92	29.13	22.47
pH 9.5[a,c]	13.67	35.59	28.10	31.65	36.25	39.89
4-AP[b]	19.18	28.07	28.78	33.41	23.21	29.56

Table A-6. Data for Figure 3.3.A, D. Motility data for VCL (µm/sec) and standard error. . Statistics were performed by one-way repeated measures ANOVA and demonstrate differences between the different treatments. Differing superscripts following the treatment name indicate significance ($P < 0.05$).

Average pH_i								
Time	control[a]	10uM Cal[b]	1uM Cal[c]	0.1 Cal[d]	pH 8.5[c]	pH 9.5[e]	4-AP[c,f]	Procaine[f]
0	5.09	5.09	5.09	5.12	5.35	5.43	5.14	5.07
2	5.16	7.40	6.45	5.74	6.40	7.93	6.27	6.36
4	5.02	7.58	6.59	5.78	6.47	8.49	6.48	6.46
6	4.96	7.50	6.55	5.74	6.47	8.65	6.45	6.35
8	5.07	7.66	6.71	5.92	6.71	8.88	6.53	6.48
10	5.06	7.69	6.79	5.92	6.75	8.97	6.46	6.43
12	5.04	7.75	6.86	5.98	6.81	9.07	6.43	6.40
14	5.01	7.77	6.81	5.92	6.78	9.12	6.45	6.40
16	5.08	7.82	6.94	6.05	6.87	9.18	6.43	6.43
18	5.09	7.85	7.01	6.11	6.88	9.23	6.45	6.42
20	5.06	7.89	6.99	6.05	6.87	9.25	6.46	6.44
22	5.09	7.92	7.06	6.11	6.92	9.28	6.48	6.42
24	5.15	7.99	7.17	6.22	6.98	9.30	6.50	6.55
26	5.13	8.03	7.15	6.18	6.96	9.30	6.51	6.50
28	5.11	7.96	7.14	6.17	6.93	9.23	6.45	6.45
30	5.12	8.00	7.17	6.19	6.94	9.24	6.49	6.44
SE pH_i								
Time	Control	10uM Cal	1uM Cal	0.1 uM Cal	pH 8.5	pH 9.5	4-AP	Procaine
0	0.14	0.14	0.13	0.13	0.25	0.33	0.13	0.11
2	0.23	0.21	0.53	0.44	0.23	0.28	0.19	0.30
4	0.25	0.14	0.54	0.49	0.22	0.10	0.20	0.26
6	0.29	0.20	0.50	0.55	0.30	0.07	0.29	0.28
8	0.24	0.19	0.50	0.54	0.26	0.09	0.26	0.21
10	0.25	0.20	0.48	0.56	0.27	0.08	0.23	0.16
12	0.25	0.20	0.48	0.57	0.24	0.06	0.22	0.18
14	0.26	0.17	0.45	0.60	0.28	0.09	0.23	0.19
16	0.27	0.20	0.46	0.59	0.26	0.06	0.21	0.18
18	0.26	0.18	0.46	0.60	0.26	0.07	0.22	0.18
20	0.28	0.18	0.46	0.61	0.28	0.07	0.20	0.21
22	0.28	0.18	0.47	0.62	0.27	0.06	0.20	0.19
24	0.28	0.19	0.48	0.65	0.26	0.07	0.20	0.20
26	0.28	0.19	0.47	0.65	0.29	0.08	0.20	0.21
28	0.31	0.21	0.50	0.68	0.32	0.16	0.22	0.26
30	0.32	0.21	0.49	0.70	0.31	0.18	0.24	0.25

Table A-7. Data for Figure 3.3.B,E. Fluorescence data for pH_i (F_{440}/F_{488}) and standard error. . Statistics were performed by one-way repeated measures ANOVA and demonstrate differences between the different treatments. Differing superscripts following the treatment name indicate significance differences ($P < 0.05$).

Average Ca_i								
Time	**Control[a]**	**10uM Cal[b]**	**1uM Cal[b,c]**	**0.1 uM Cal[d]**	**pH 8.5[d,e]**	**pH 9.5[b,d,e]**	**4-AP[f]**	**Procaine[g]**
0	0	0	0	0	0	0	0	0
2	0.03	5.10	3.78	1.89	0.45	2.54	0.07	-0.25
4	0.03	5.40	3.94	2.08	0.46	3.03	0.07	-0.28
6	0.05	5.58	4.05	2.21	0.48	3.36	0.09	-0.31
8	0.05	5.64	4.20	2.34	0.54	3.65	0.10	-0.31
10	0.06	5.72	4.29	2.43	0.58	3.87	0.12	-0.33
12	0.07	5.74	4.40	2.53	0.61	4.03	0.14	-0.34
14	0.09	5.86	4.53	2.61	0.65	4.19	0.15	-0.34
16	0.11	5.83	4.64	2.68	0.71	4.41	0.17	-0.34
18	0.11	5.84	4.72	2.74	0.77	4.60	0.20	-0.33
20	0.13	5.92	4.82	2.76	0.80	4.73	0.20	-0.34
22	0.14	5.95	4.89	2.84	0.84	4.89	0.21	-0.35
24	0.16	5.99	4.93	2.92	0.91	5.09	0.25	-0.34
26	0.17	6.02	5.03	2.94	0.94	5.23	0.25	-0.32
28	0.25	6.14	5.18	3.06	1.05	5.45	0.34	-0.26
30	0.27	6.15	5.24	3.11	1.09	5.58	0.35	-0.24
SE Ca_i								
Time	**Control**	**10uM Cal**	**1uM Cal**	**0.1 uM Cal**	**pH 8.5**	**pH 9.5**	**4-AP**	**Procaine**
0	0	0	0	0	0	0	0	0
2	0.03	0.54	0.35	0.63	0.05	0.31	0.02	0.02
4	0.03	0.64	0.35	0.69	0.05	0.29	0.01	0.02
6	0.03	0.74	0.37	0.70	0.07	0.24	0.01	0.01
8	0.03	0.79	0.38	0.73	0.07	0.24	0.02	0.01
10	0.03	0.81	0.35	0.73	0.09	0.28	0.02	0.01
12	0.03	0.80	0.30	0.73	0.09	0.33	0.02	0.01
14	0.04	0.84	0.28	0.71	0.10	0.35	0.03	0.02
16	0.03	0.82	0.20	0.70	0.10	0.39	0.03	0.02
18	0.03	0.83	0.18	0.70	0.10	0.40	0.03	0.02
20	0.03	0.84	0.16	0.66	0.11	0.44	0.03	0.03
22	0.05	0.87	0.12	0.65	0.11	0.47	0.05	0.03
24	0.04	0.87	0.06	0.64	0.12	0.48	0.03	0.02
26	0.05	0.88	0.06	0.62	0.13	0.52	0.03	0.04
28	0.08	0.91	0.05	0.60	0.06	0.55	0.10	0.05
30	0.08	0.91	0.09	0.59	0.06	0.55	0.09	0.05

Table A-8. Data for Figure 3.3.C,F. Fluorescence data for Cai (ΔF/F0) and standard error. . Statistics were performed by one-way repeated measures ANOVA and demonstrate differences between the different treatments. Superscripts following the treatment name indicate significance differences ($P < 0.05$).

Average Ca_i (pH 7.25)					
Time (min)	Control (Media)	Control (OH)	500 nM P4	2 μM P4	5 μM P4
0	0.0000	0.0000	0.0000	0.0000	0.0000
2	0.0778	0.0423	0.0233	0.0148	0.0402
4	0.0651	0.0442	0.0390	0.0361	0.0632
6	0.0788	0.0573	0.0527	0.0512	0.0843
8	0.0859	0.0611	0.0671	0.0672	0.0924
10	0.0933	0.0678	0.0767	0.0779	0.1095
12	0.0941	0.0779	0.0802	0.0866	0.1159
14	0.1014	0.0869	0.0894	0.0955	0.1247
16	0.1044	0.0889	0.0950	0.1073	0.1345
18	0.1131	0.0962	0.1011	0.1128	0.1396
20	0.1189	0.1020	0.1105	0.1226	0.1492
22	0.1245	0.1050	0.1117	0.1283	0.1517
24	0.1233	0.1103	0.1209	0.1363	0.1541
26	0.1331	0.1132	0.1218	0.1455	0.1584
28	0.1325	0.1123	0.1283	0.1533	0.1667
30	0.1361	0.1198	0.1269	0.1640	0.1702
32	0.1454	0.1210	0.1345	0.1728	0.1735
SE Ca_i (pH 7.25)					
Time (min)	Control (Media)	Control (OH)	500 nM P4	2 μM P4	5 μM P4
0	0.0000	0.0000	0.0000	0.0000	0.0000
2	0.0181	0.0195	0.0395	0.0264	0.0053
4	0.0100	0.0175	0.0477	0.0285	0.0115
6	0.0141	0.0229	0.0502	0.0388	0.0203
8	0.0153	0.0274	0.0537	0.0404	0.0218
10	0.0162	0.0298	0.0554	0.0463	0.0325
12	0.0153	0.0339	0.0568	0.0525	0.0322
14	0.0168	0.0346	0.0632	0.0516	0.0377
16	0.0160	0.0338	0.0647	0.0548	0.0383
18	0.0194	0.0363	0.0609	0.0559	0.0421
20	0.0204	0.0406	0.0658	0.0586	0.0426
22	0.0213	0.0402	0.0662	0.0614	0.0465
24	0.0222	0.0421	0.0677	0.0669	0.0470
26	0.0223	0.0448	0.0710	0.0674	0.0486
28	0.0226	0.0432	0.0722	0.0671	0.0494
30	0.0228	0.0495	0.0731	0.0684	0.0519
32	0.0253	0.0528	0.0749	0.0703	0.0556

Table A-9. Data for Figure 3.5.A. Fluorescence data for Ca_i ($\Delta F/F0$) and standard error for sperm treated with progesterone (P4) at pH 7.25. Statistics were performed by one-way ANOVA and no significant differences were found.

Average Ca_i (pH 8)

Time (min)	Control (Media)	Control (OH)	500 nM P4	2 µM P4	5 µM P4
0	0.0000	0.0000	0.0000	0.0000	0.0000
2	0.0714	0.0461	0.0418	0.0505	0.0155
4	0.0737	0.0618	0.0583	0.0697	0.0469
6	0.0857	0.0784	0.0727	0.0911	0.0638
8	0.0935	0.0859	0.0856	0.1074	0.0823
10	0.1103	0.0978	0.0962	0.1208	0.0929
12	0.1132	0.1074	0.1095	0.1320	0.1102
14	0.1242	0.1149	0.1095	0.1490	0.1235
16	0.1289	0.1226	0.1271	0.1576	0.1298
18	0.1406	0.1305	0.1337	0.1760	0.1403
20	0.1436	0.1396	0.1403	0.1831	0.1564
22	0.1546	0.1474	0.1524	0.1914	0.1600
24	0.1643	0.1591	0.1621	0.2085	0.1701
26	0.1734	0.1648	0.1647	0.2131	0.1779
28	0.1812	0.1764	0.1700	0.2247	0.1878
30	0.1877	0.1804	0.1825	0.2353	0.1961
32	0.1950	0.1855	0.1921	0.2409	0.2020

SE Ca_i (pH 8)

Time (min)	Control (Media)	Control (OH)	500 nM P4	2 µM P4	5 µM P4
0	0.0000	0.0000	0.0000	0.0000	0.0000
2	0.0080	0.0288	0.0209	0.0063	0.0317
4	0.0059	0.0279	0.0248	0.0140	0.0372
6	0.0091	0.0291	0.0271	0.0185	0.0412
8	0.0078	0.0332	0.0339	0.0242	0.0453
10	0.0109	0.0331	0.0332	0.0256	0.0516
12	0.0085	0.0351	0.0392	0.0331	0.0553
14	0.0114	0.0368	0.0403	0.0322	0.0573
16	0.0088	0.0377	0.0411	0.0362	0.0570
18	0.0111	0.0376	0.0406	0.0377	0.0573
20	0.0095	0.0392	0.0410	0.0443	0.0601
22	0.0104	0.0338	0.0401	0.0430	0.0673
24	0.0131	0.0389	0.0435	0.0471	0.0665
26	0.0152	0.0328	0.0468	0.0479	0.0672
28	0.0152	0.0365	0.0485	0.0515	0.0704
30	0.0150	0.0396	0.0484	0.0540	0.0748
32	0.0154	0.0381	0.0516	0.0556	0.0748

Table A-10. Data for Figure 3.5.B. Fluorescence data for Ca_i (ΔF/F0) and standard error for sperm treated with progesterone (P4) at pH 8. Statistics were performed by one-way ANOVA and no significant differences were found.

Average VCL

Treatment	pH	Time (Min) 0	1	15	30	60
Control (media)	pH 7.25	188.7333	188.7333	213.0667	225.2	224.4333
Control (OH)	pH 7.25	188.7333	195.2333	229.6333	223.1667	235.5
500 nM P_4	pH 7.25	188.7333	189.1333	225.4333	236.5333	236.2
2 µM P_4	pH 7.25	188.7333	195.9667	224.9	234.8667	242.1333
5 µM P_4	pH 7.25	188.7333	190.9667	226.7	225.4	229.2333
Control (media)	pH 8	188.7333	220.4	261.7667	243.2	244.6
Control (OH)	pH 8	188.7333	220.0667	252.3	246	245.9667
500 nM P_4	pH 8	188.7333	224.2	244	247.9	248.8
2 µM P_4	pH 8	188.7333	228.4	246.5333	249.3667	256.3667
5 µM P_4	pH 8	188.7333	223.6667	255.0333	243.8667	243.8667

SE VCL

Treatment	pH	Time (Min) 0	1	15	30	60
Control (media)	pH 7.25	25.08335	25.08335	25.11509	26.43943	23.81584
Control (OH)	pH 7.25	25.08335	16.76269	22.83377	30.65096	18.65512
500 nM P_4	pH 7.25	25.08335	19.73333	27.10316	29.82428	23.41993
2 µM P_4	pH 7.25	25.08335	21.24573	27.44376	32.20281	21.81531
5 µM P_4	pH 7.25	25.08335	21.63518	23.92871	23.98256	22.39065
Control (media)	pH 8	25.08335	28.6247	31.73223	18.69037	26.90527
Control (OH)	pH 8	25.08335	28.48241	24.24404	26.15996	31.37304
500 nM P_4	pH 8	25.08335	22.81469	22.13572	27.35276	25.20959
2 µM P_4	pH 8	25.08335	30.46922	23.43959	28.97438	32.75497
5 µM P_4	pH 8	25.08335	22.41981	22.46674	23.01719	29.34714

Table A-11. Data for Figure 3.5.C,D Motility data for VCL (µm/sec) and standard error. . Statistics were performed by one-way repeated measures ANOVA; however, no significant differences were seen.

Average Ca_i (pH 7.25)

Time (min)	Control (Media)	Control (OH)	500 nM PGE1	2 μM PGE1	5 μM PGE1
0	0	0	0	0	0
2	0.0577	0.0523	0.0482	0.0307	0.0322
4	0.0520	0.0569	0.0578	0.0331*	0.0318*
6	0.0569	0.0562	0.0607	0.0471	0.0423
8	0.0621	0.0678	0.0681	0.0529	0.0528
10	0.0692	0.0770	0.0753	0.0590	0.0654
12	0.0749	0.0772	0.0816	0.0642	0.0693
14	0.0797	0.0830	0.0809	0.0706	0.0759
16	0.0828	0.0893	0.0876	0.0751	0.0807
18	0.0880	0.0884	0.0947	0.0767	0.0895
20	0.0920	0.0908	0.0934	0.0834	0.0915
22	0.0961	0.0976	0.0989	0.0827	0.0959
24	0.0951	0.1011	0.1075	0.0914	0.1010
26	0.1007	0.1026	0.1041	0.0944	0.1053
28	0.1037	0.1021	0.1124	0.0993	0.1070
30	0.1077	0.1062	0.1103	0.0999	0.1097
32	0.1098	0.1092	0.1141	0.1034	0.1186

SE Ca_i (pH 7.25)

Time (min)	Control (Media)	Control (OH)	500 nM PGE1	2 μM PGE1	5 μM PGE1
0	0.0000	0.0000	0.0000	0.0000	0.0000
2	0.0149	0.0136	0.0069	0.0069	0.0030
4	0.0031	0.0106	0.0041	0.0082	0.0046
6	0.0040	0.0124	0.0062	0.0065	0.0074
8	0.0034	0.0120	0.0077	0.0089	0.0086
10	0.0046	0.0125	0.0071	0.0102	0.0109
12	0.0059	0.0125	0.0074	0.0118	0.0173
14	0.0059	0.0123	0.0114	0.0093	0.0175
16	0.0044	0.0180	0.0097	0.0116	0.0216
18	0.0062	0.0126	0.0106	0.0118	0.0224
20	0.0066	0.0148	0.0115	0.0146	0.0239
22	0.0068	0.0140	0.0115	0.0113	0.0266
24	0.0072	0.0156	0.0098	0.0124	0.0285
26	0.0062	0.0114	0.0145	0.0114	0.0279
28	0.0078	0.0177	0.0091	0.0129	0.0301
30	0.0081	0.0153	0.0166	0.0134	0.0308
32	0.0083	0.0160	0.0156	0.0158	0.0341

Table A-12. Data for Figure 3.6.A. Fluorescence data for Ca_i (ΔF/F0) and standard error for sperm treated with prostaglandin E1 (PGE1) at pH 7.25. Statistics were performed by one-way ANOVA for each time point. Treatments significantly different than the control at any given time point are denoted by a * ($P < 0.05$).

Average Ca_i (pH 8)

Time (min)	Control (Media)	Control (OH)	500 nM PGE1	2 μM PGE1	5 μM PGE1
0	0	0	0	0	0
2	0.0613	0.0495	0.0512	0.0377	0.0321
4	0.0585	0.0575	0.0557	0.0486	0.0360
6	0.0655	0.0687	0.0654	0.0588	0.0470
8	0.0725	0.0753	0.0727	0.0668	0.0613
10	0.0810	0.0835	0.0816	0.0774	0.0661
12	0.0858	0.0905	0.0890	0.0843	0.0763
14	0.0976	0.0959	0.0995	0.0931	0.0836
16	0.1024	0.1009	0.1026	0.0978	0.0939
18	0.1042	0.1102	0.1113	0.1043	0.0990
20	0.1159	0.1107	0.1125	0.1114	0.1053
22	0.1189	0.1179	0.1200	0.1143	0.1134
24	0.1277	0.1293	0.1240	0.1255	0.1182
26	0.1281	0.1284	0.1315	0.1246	0.1278
28	0.1382	0.1405	0.1373	0.1329	0.1349
30	0.1423	0.1442	0.1457	0.1351	0.1424
32	0.1492	0.1463	0.1453	0.1409	0.1392

SE Ca_i (pH 8)

Time (min)	Control (Media)	Control (OH)	500 nM PGE1	2 μM PGE1	5 μM PGE1
0	0.0000	0.0000	0.0000	0.0000	0.0000
2	0.0092	0.0043	0.0039	0.0037	0.0062
4	0.0062	0.0041	0.0034	0.0032	0.0074
6	0.0077	0.0022	0.0022	0.0044	0.0054
8	0.0071	0.0018	0.0045	0.0038	0.0052
10	0.0091	0.0026	0.0033	0.0054	0.0040
12	0.0127	0.0009	0.0055	0.0061	0.0012
14	0.0069	0.0035	0.0077	0.0065	0.0031
16	0.0111	0.0043	0.0089	0.0084	0.0030
18	0.0162	0.0062	0.0092	0.0098	0.0051
20	0.0163	0.0103	0.0103	0.0086	0.0068
22	0.0196	0.0100	0.0134	0.0111	0.0087
24	0.0196	0.0077	0.0138	0.0139	0.0101
26	0.0214	0.0100	0.0155	0.0165	0.0090
28	0.0213	0.0107	0.0176	0.0127	0.0139
30	0.0240	0.0141	0.0170	0.0165	0.0133
32	0.0235	0.0150	0.0201	0.0202	0.0189

Table A-13. Data for Figure 3.6.B. Fluorescence data for Ca_i (ΔF/F0) and standard error for sperm treated with prostaglandin E1 (PGE1) at pH 8. Statistics were performed by one-way ANOVA and no significant differences were found.

Average VCL

		Time (Min)				
Treatment	**pH**	**0**	**1**	**15**	**30**	**60**
Control (media)	pH 7.25	238.8	238.8	241.7	254.3	264.5
Control (OH)	pH 7.25	238.8	231.1	238.6	252.6	279.8
500 nM PGE1	pH 7.25	238.8	227.4	246.8	253.1	281.3
2 µM PGE1	pH 7.25	238.8	230.2	237.2	261.6	281.0
5 µM PGE1	pH 7.25	238.8	230.7	240.6	251.6	275.9
Control (media)	pH 8	238.8	256.2	251.6	256.0	251.4
Control (OH)	pH 8	238.8	248.9	255.1	242.4	239.9
500 nM PGE1	pH 8	238.8	259.2	250.7	249.2	246.0
2 µM PGE1	pH 8	238.8	250.9	249.1	234.6	244.2
5 µM PGE1	pH 8	238.8	255.2	253.6	231.8	251.6

SE VCL

		Time (Min)				
Treatment	**pH**	**0**	**1**	**15**	**30**	**60**
Control (media)	pH 7.25	0.000	30.455	33.409	28.978	5.380
Control (OH)	pH 7.25	0.000	27.164	27.655	28.654	1.050
500 nM PGE1	pH 7.25	0.000	24.975	31.752	25.850	4.700
2 µM PGE1	pH 7.25	0.000	27.104	26.241	26.135	7.550
5 µM PGE1	pH 7.25	0.000	27.102	31.595	25.834	12.450
Control (media)	pH 8	0.000	13.988	12.582	14.525	23.450
Control (OH)	pH 8	0.000	17.710	9.031	17.822	24.750
500 nM PGE1	pH 8	0.000	19.113	13.837	18.418	26.150
2 µM PGE1	pH 8	0.000	16.923	13.749	8.000	36.800
5 µM PGE1	pH 8	0.000	11.643	14.534	6.700	25.450

Table A-14. Data for Figure 3.6.C,D. Fluorescence data for Ca_i ($\Delta F/F0$) and standard error for sperm treated with progesterone (P4) at pH 7.25. Statistics were performed by one-way ANOVA and no significant differences were found.

Mibefradil Concentration Curve (Average pH_i)

Time (min)	0 μM[a]	0.5 μM[a]	1 μM[b]	2.5 μM[c]	5 μM[c]	10 μM[c]
0	6.0526	6.0254	6.1046	6.1036	6.0981	6.1439
2	6.0293	6.1422	6.2803	6.3724	6.3852	6.5755
4	6.0798	5.8535	6.2046	6.4307	6.3598	6.4523
6	6.0798	5.9774	6.1629	6.3202	6.3764	6.4035
8	6.0169	5.8746	6.1923	6.2592	6.3345	6.3629
10	5.9335	5.9402	6.1669	6.3895	6.3296	6.3800
12	6.0142	5.8989	6.1894	6.2678	6.4227	6.3596
14	5.9413	5.9124	6.1590	6.3754	6.2732	6.3646
16	5.9514	5.9846	6.1701	6.2725	6.2648	6.2847
18	6.0180	5.9524	6.1321	6.3133	6.3643	6.3592
20	5.9902	5.9349	6.1546	6.2643	6.2801	6.4265
22	6.0553	5.7992	6.1257	6.2264	6.2548	6.2649
24	5.8857	5.8995	6.1777	6.3473	6.3298	6.4320
26	5.9980	5.9110	6.1211	6.3625	6.2983	6.4064
28	5.9284	5.8661	6.1811	6.2274	6.3756	6.1927
30	5.9704	5.9407	6.1283	6.2577	6.2579	6.3431
32	5.9173	5.9110	6.1415	6.2859	6.2735	6.2762

Mibefradil Concentration Curve (SE pH_i)

Time (min)	0 μM	0.5 μM	1 μM	2.5 μM	5 μM	10 μM
0	0.0627	0.0853	0.1172	0.1182	0.0686	0.0766
2	0.1238	0.1765	0.1109	0.0948	0.0863	0.1730
4	0.1680	0.1365	0.2254	0.2152	0.1504	0.1850
6	0.1596	0.0882	0.1237	0.2291	0.1302	0.1251
8	0.1920	0.0533	0.1359	0.1808	0.1249	0.1285
10	0.2336	0.0890	0.1545	0.1369	0.1404	0.1624
12	0.2013	0.0875	0.1594	0.1450	0.1368	0.1049
14	0.1810	0.0093	0.1934	0.2163	0.1593	0.1508
16	0.2395	0.2439	0.1438	0.2066	0.1518	0.0733
18	0.2200	0.1418	0.1406	0.1663	0.0618	0.1192
20	0.1883	0.0214	0.1641	0.2017	0.1390	0.1242
22	0.2494	0.0516	0.1582	0.1884	0.1326	0.1348
24	0.2470	0.0605	0.1330	0.1718	0.1248	0.0861
26	0.2240	0.0036	0.1428	0.0930	0.1316	0.0487
28	0.2660	0.0523	0.1491	0.1518	0.0832	0.1232
30	0.2266	0.0174	0.1796	0.1285	0.1416	0.1133
32	0.2408	0.0187	0.1967	0.1446	0.1351	0.1029

Table A-15. Data for Figure 3.7. Fluorescence data for pH_i (F440/F488) and standard error for sperm treated with varying concentrations of mibefradil. Statistics were performed using one-way repeated measures ANOVA. Significantly different treatments are denoted with differing superscripts ($P < 0.05$)

Average VCL

	Time (Min)				
Treatment	**0**	**1**	**10**	**20**	**30**
Control	194.68	194.68	194.68	195.58	194.13
Control + Mib	194.68	192.65	192.65	206.15	209.55
High pH*	211.97	211.97	224.00	248.25	226.53
High pH + Mib*	211.97	228.77	241.80	259.35	238.27

SE VCL

	Time (Min)				
Treatment	**0**	**1**	**10**	**20**	**30**
Control	7.44	7.44	8.17	8.82	6.26
Control + Mib	7.44	5.39	7.01	6.39	4.92
High pH	18.69	18.69	13.23	17.45	13.95
High pH + Mib	18.69	19.34	14.46	13.54	7.24

Average VCL

	Time (Min)			
Treatment	**0**	**1**	**15**	**30**
Control	230.90	230.90	229.67	246.77
Control + Mib	230.90	234.67	241.33	228.03
4-AP*	230.90	266.87	289.67	291.27
4-AP + Mib*	230.90	277.87	268.80	256.30
Procaine*	230.90	320.17	343.80	336.73
Procaine + Mib*	230.90	311.37	320.77	318.23

SE VCL

	Time (Min)			
Treatment	**0**	**1**	**15**	**30**
Control	27.89	27.89	21.47	19.99
Control + Mib	27.89	23.05	28.36	16.10
4-AP	27.89	15.20	6.20	10.66
4-AP + Mib	27.89	6.70	9.83	20.31
Procaine	27.89	11.40	17.68	27.60
Procaine + Mib	27.89	12.32	17.19	30.24

Table A-16. Data for Figure 3.8.A,B,C. Motility data for VCL (µm/sec) and standard error. . Statistics were performed by paired t-test, comparing treatments with and without 5 µM mibefradil. Significant differences are marked with a * ($P < 0.05$).

	Average Ca_i							
Time	High pH*	High pH + Mib*	4-AP*	4-AP + Mib*	Control*	Control + Mib*	Procaine	Procaine + Mib
0	0.0000	0.0000	0.0000	0.0000	0.0000	0.0000	0.0000	0.0000
1	0.2981	0.1860	0.0265	0.0088	0.0124	-0.0742	-0.2143	-0.2467
2	0.4338	0.2078	0.1026	0.0789	0.0121	-0.0700	-0.2414	-0.2599
3	0.4981	0.2362	0.1378	0.1193	0.0176	-0.0614	-0.2488	-0.2625
4	0.4885	0.2681	0.1526	0.1418	0.0159	-0.0632	-0.2513	-0.2722
5	0.4951	0.2839	0.1628	0.1514	0.0190	-0.0529	-0.2722	-0.2782
6	0.4728	0.3053	0.1786	0.1413	0.0236	-0.0500	-0.2828	-0.2882
7	0.4366	0.2950	0.1890	0.1390	0.0183	-0.0456	-0.2865	-0.2912
8	0.4278	0.3128	0.1953	0.1480	0.0215	-0.0480	-0.2921	-0.2948
9	0.4197	0.3245	0.2059	0.1559	0.0204	-0.0446	-0.2993	-0.2997
10	0.4064	0.3237	0.2115	0.1633	0.0196	-0.0393	-0.3034	-0.3075
11	0.3784	0.3168	0.2246	0.1601	0.0288	-0.0354	-0.3103	-0.3075
12	0.3787	0.3136	0.2317	0.1623	0.0233	-0.0279	-0.3159	-0.3123
13	0.3724	0.3159	0.2371	0.1693	0.0246	-0.0278	-0.3205	-0.3138
14	0.3772	0.3215	0.2437	0.1687	0.0291	-0.0257	-0.3214	-0.3139
15	0.3747	0.3222	0.2471	0.1749	0.0287	-0.0246	-0.3263	-0.3204
16	0.3963	0.3429	0.2624	0.1831	0.0274	-0.0187	-0.3273	-0.3211
17	0.3749	0.3397	0.2608	0.1793	0.0256	-0.0216	-0.3338	-0.3220
18	0.3837	0.3405	0.2715	0.1840	0.0328	-0.0161	-0.3354	-0.3239
19	0.3843	0.3399	0.2716	0.1895	0.0274	-0.0176	-0.3390	-0.3258
20	0.3836	0.3468	0.2698	0.1895	0.0252	-0.0157	-0.3399	-0.3270
21	0.3858	0.3474	0.2743	0.1926	0.0280	-0.0165	-0.3441	-0.3292
22	0.3773	0.3451	0.2776	0.1977	0.0347	-0.0103	-0.3451	-0.3322
23	0.3830	0.3520	0.2756	0.1979	0.0297	-0.0041	-0.3479	-0.3376
24	0.3876	0.3520	0.2785	0.1960	0.0357	-0.0098	-0.3497	-0.3320
25	0.3870	0.3557	0.2792	0.2069	0.0336	-0.0007	-0.3516	-0.3369
26	0.3890	0.3498	0.2808	0.2076	0.0363	-0.0028	-0.3547	-0.3354
27	0.3850	0.3574	0.2912	0.2154	0.0382	-0.0033	-0.3539	-0.3386
28	0.3907	0.3537	0.2889	0.2115	0.0382	0.0021	-0.3574	-0.3415
29	0.3926	0.3558	0.2854	0.2191	0.0334	0.0067	-0.3569	-0.3434
30	0.3944	0.3624	0.2965	0.2202	0.0430	0.0034	-0.3570	-0.3460
31	0.3989	0.3631	0.3011	0.2257	0.0378	0.0039	-0.3583	-0.3483

Table A-17. Data for Figure 3.8.D,E,F. Average relative calcium levels (Ca_i; $\Delta F/F0$). Statistics were performed by paired t-test, comparing treatments with and without 5 µM mibefradil. Significant differences are marked with a * ($P < 0.001$).

Standard Error Ca_i								
Time	High pH*	High pH + Mib	4-AP*	4-AP + Mib	Control	Control + Mib	Procaine	Procaine + Mib
0	0.0000	0.0000	0.0000	0.0000	0.0000	0.0000	0.0000	0.0000
1	0.0682	0.0746	0.0328	0.0534	0.0044	0.0261	0.0208	0.0177
2	0.1710	0.0698	0.0495	0.0782	0.0056	0.0252	0.0175	0.0208
3	0.1717	0.0655	0.0533	0.0960	0.0041	0.0261	0.0141	0.0246
4	0.1443	0.0577	0.0467	0.1054	0.0021	0.0271	0.0182	0.0241
5	0.1183	0.0563	0.0410	0.1065	0.0044	0.0272	0.0256	0.0270
6	0.0888	0.0583	0.0433	0.0962	0.0062	0.0268	0.0247	0.0274
7	0.0786	0.0637	0.0429	0.0964	0.0062	0.0261	0.0282	0.0261
8	0.0680	0.0598	0.0401	0.1024	0.0027	0.0280	0.0278	0.0262
9	0.0553	0.0635	0.0469	0.1077	0.0023	0.0297	0.0309	0.0291
10	0.0556	0.0676	0.0499	0.1088	0.0036	0.0296	0.0295	0.0323
11	0.0723	0.0754	0.0505	0.1083	0.0078	0.0361	0.0298	0.0304
12	0.0676	0.0769	0.0558	0.1169	0.0068	0.0334	0.0311	0.0308
13	0.0678	0.0750	0.0600	0.1199	0.0048	0.0353	0.0324	0.0313
14	0.0726	0.0735	0.0613	0.1186	0.0053	0.0350	0.0325	0.0318
15	0.0761	0.0832	0.0676	0.1226	0.0081	0.0373	0.0349	0.0324
16	0.0860	0.0887	0.0794	0.1290	0.0076	0.0358	0.0341	0.0335
17	0.0939	0.0868	0.0843	0.1269	0.0055	0.0368	0.0347	0.0312
18	0.0929	0.0929	0.0921	0.1329	0.0064	0.0378	0.0333	0.0337
19	0.0932	0.0906	0.0976	0.1384	0.0057	0.0378	0.0337	0.0349
20	0.1007	0.0957	0.0968	0.1379	0.0060	0.0373	0.0349	0.0312
21	0.1045	0.0936	0.1033	0.1384	0.0058	0.0377	0.0357	0.0322
22	0.1096	0.0914	0.1076	0.1446	0.0079	0.0358	0.0355	0.0318
23	0.1121	0.0930	0.1105	0.1434	0.0082	0.0377	0.0346	0.0317
24	0.1129	0.0976	0.1172	0.1441	0.0067	0.0383	0.0350	0.0327
25	0.1171	0.0976	0.1213	0.1499	0.0087	0.0389	0.0339	0.0340
26	0.1183	0.0991	0.1211	0.1508	0.0107	0.0409	0.0334	0.0322
27	0.1250	0.1025	0.1264	0.1509	0.0064	0.0418	0.0349	0.0337
28	0.1227	0.1011	0.1251	0.1497	0.0096	0.0403	0.0339	0.0341
29	0.1291	0.0978	0.1305	0.1544	0.0080	0.0427	0.0337	0.0345
30	0.1319	0.1056	0.1385	0.1515	0.0099	0.0393	0.0347	0.0330
31	0.1351	0.1037	0.1396	0.1585	0.0112	0.0419	0.0345	0.0336

Table A-18. Data for Figure 3.8.D,E,F. Standard error for relative calcium levels (Ca_i; $\Delta F/F0$).

	Average VCL (μm/sec)				Standard Error VCL			
	Time (min)				Time (min)			
	0	1	15	30	0	1	15	30
Control	196.3	196.3	186.0	145.2	18.90	18.90	24.14	17.03
pH 8.5	196.3	224.7	74.5*	70.6*	18.90	23.10	10.15	6.78
4-AP	196.3	281.0	212.1	184.9	18.90	34.18	15.36	11.29
Procaine	196.3	344.7*	325.7*	286.2*	18.90	10.80	20.86	25.51
Control + EGTA	183.0	183.0	159.8	123.9	17.62	17.62	9.72	6.32
pH 8.5 + EGTA	183.0	172.7*	83.8	72.1*	17.62	6.28	8.43	4.84
4-AP + EGTA	183.0	224.0	150.9	126.4	17.62	22.02	14.34	3.20
Procaine + EGTA	183.0	282.5	202.5	164.3*	17.62	32.01	15.90	10.39
	Average ALH (μm)				**Standard Error ALH**			
Control	7.4	7.4	8.2	7.7	0.87	0.87	0.81	0.27
pH 8.5	7.4	10.6	5.0	5*	0.87	0.80	0.76	0.47
4-AP	7.4	11.7	9.7	9.4	0.87	0.88	0.79	0.52
Procaine	7.4	12.8*	11.8*	10.7*	0.87	0.46	0.66	0.74
Control + EGTA	7.6	7.6	7.4	6.7	0.95	0.95	0.23	0.55
pH 8.5 + EGTA	7.6	9.0	5.7*	5.3	0.95	0.90	0.03	0.58
4-AP + EGTA	7.6	9.6	6.7	6.6	0.95	0.76	0.32	0.26
Procaine + EGTA	7.6	10.4	7.8	7.3	0.95	0.78	0.22	0.35
	Average Motility (% motile)				**Standard Error Motility**			
Control	75.0	75.0	66.3	43.7	6.43	6.43	3.38	5.36
pH 8.5	75.0	74.0	28.0*	17.7*	6.43	6.56	2.52	6.57
4-AP	75.0	78.0	67.0	54.3	6.43	4.58	1.53	6.49
Procaine	75.0	83.0	81*	77.3*	6.43	4.04	3.79	0.88
Control + EGTA	73.7	73.7	57.0	31.0	4.18	4.18	1.53	5.13
pH 8.5 + EGTA	73.7	60.3	31.7*	21.0	4.18	5.84	8.41	5.77
4-AP + EGTA	73.7	73.3	57.0	40.7	4.18	6.44	2.08	2.19
Procaine + EGTA	73.7	78.0	70.7	53.3*	4.18	5.20	2.03	0.33

Table A-19. Data for Figure 3.9. Motility data, including VCL, ALH and % total motile. Statistics were performed using one-way ANOVA for each time point. Treatments significantly different than control are marked with a * ($P < 0.05$).

		Averages		Standard Error	
Treatment	**Time**	**% PI Stained**	**% Motile**	**SE Stained**	**SE Motile**
Negative Control	N/A	25.17	61.67	7.36	13.30
0.1% Triton-X	Imm	77.57*	56.33	20.28	13.87
0.1% Triton-X	30 sec	85.78*	41.33	6.95	10.37
0.1% Triton-X	60 sec	78.67*	21.00*	6.60	5.03
0.05% Triton-X	Imm	93.99*	36.67	3.98	1.45
0.05% Triton-X	30 sec	83.02*	23.67*	7.26	3.18
0.05% Triton-X	60 sec	78.20*	17.33*	6.47	0.88
0.01% Triton X	Imm	33.27	52.00	2.43	10.79
0.01% Triton X	30 sec	53.09	53.33	9.90	12.20
0.01% Triton X	60 sec	60.99	55.67	9.35	5.78
0.005% Triton X	Imm	25.93	54.00	3.42	9.00
0.005% Triton X	30 sec	32.41	49.67	3.66	7.33
0.005% Triton X	60 sec	34.81	42.33	4.32	6.94
0.001% Triton X	Imm	21.25	46.33	6.50	14.81
0.001% Triton X	30 sec	22.61	54.67	5.31	9.91
0.001% Triton X	60 sec	22.82	55.00	5.59	8.89

Table A-20. Data for Figure 4.1.A. The average and standard error for % of sperm stained with PI and % total motile after exposure to varying concentrations of Triton X-100. Statistics were performed using one-way ANOVA. Treatments significantly different than the negative control are marked with a * ($P < 0.05$).

		Average		Standard Error	
Treatment	**Time**	**% PI Stained**	**% Motile**	**% PI Stained**	**% Motile**
Negative Control	N/A	17.27	67.33	8.23	6.64
0.1% Triton-X	Imm	98.8*	54.00	0.65	5.69
0.1% Triton-X	30 sec	88.58*	20.00*	7.88	4.51
0.1% Triton-X	60 sec	83.81*	5.33*	11.63	3.53
0.05% Triton-X	Imm	97.57*	62.00	0.74	11.93
0.05% Triton-X	30 sec	91.82*	28.00*	4.93	3.00
0.05% Triton-X	60 sec	84.72*	12.67*	10.48	2.33
0.01% Triton X	Imm	72.89*	64.00	13.52	4.62
0.01% Triton X	30 sec	99.29*	44.67	0.22	16.33
0.01% Triton X	60 sec	95.09*	18.67*	3.44	8.09
0.005% Triton X	Imm	57.28	62.00	14.72	8.33
0.005% Triton X	30 sec	99.05*	60.00	0.35	11.02
0.005% Triton X	60 sec	99.33*	43.33	0.25	12.67
0.001% Triton X	Imm	45.12	59.67	8.90	4.18
0.001% Triton X	30 sec	70.37*	58.33	5.10	2.67
0.001% Triton X	60 sec	78.59*	51.33	4.23	4.18

Table A-21. Data for Figure 4.1.B. The average and standard error for % of sperm stained with PI and % total motile after exposure to varying concentrations of Triton X-100. Statistics were performed using one-way ANOVA. Treatments significantly different than the negative control are marked with a * ($P < 0.05$).

VCL (μm/sec)		
mM ATP	**Average**	**Standard Error**
0	0.00	0.00
1	214.03	30.09
2	219.35	20.30
3	231.58	18.07
4	245.67	23.03
5	240.68	26.18
7.5	248.90	11.33
10	234.98	7.08
ALH (μm)		
mM ATP	**Average**	**Standard Error**
0	0.00	0.00
1	9.23	1.51
2	10.53	0.93
3	10.55	0.90
4	11.77	1.02
5	11.48	1.28
7.5	12.23	0.43
10	11.50	0.78
% Motile		
mM ATP	**Average**	**Standard Error**
0	0.00	0.00
1	63.75	13.26
2	70.50	2.10
3	78.00	3.50
4	62.67	9.17
5	69.50	4.80
7.5	68.25	8.67
10	69.00	18.02

Table A-22. Data for Figure 4.4. The raw data for the average VCL, ALH and % motile plus standard error for sperm treated with varying concentrations of ATP. Statistics were performed using a linear regression model. The concentration of ATP had no significant effect on any of the above measurements.

VCL (µm/sec)		
µM cAMP	Average	Standard Error
0	298.90	36.78
5	219.17	16.61
10	272.53	16.17
15	211.37	34.96
20	265.53	27.20
25	257.30	43.65
30	238.60	23.83
100	260.40	34.20
500	220.13	24.38
1000	222.70	18.58
ALH (µm)		
µM cAMP	Average	Standard Error
0	9.77	1.11
5	8.67	0.23
10	9.27	1.71
15	9.03	0.94
20	8.77	1.13
25	8.47	1.07
30	8.87	0.61
100	9.54	0.29
500	9.97	0.32
1000	10.33	0.88
% Motile		
µM cAMP	Average	Standard Error
0	54.67	6.69
5	42.67	5.67
10	55.00	2.00
15	37.67	10.17
20	45.00	6.81
25	47.67	11.72
30	53.67	9.53
100	53.00	5.51
500	63.33	15.65
1000	64.33	9.39

Table A-23. Data for Figure 4.4. The raw data for the average VCL, ALH and % motile plus standard error for sperm treated with varying concentrations of cAMP. Statistics were performed using a linear regression model. The concentration of cAMP has no significant effect on any of the above measurements.

VCL (µm/sec)		
Media pH	**Average**	**Standard Error**
4	0.00*	0.00
4.5	0.00*	0.00
5	0.00*	0.00
5.5	125.73*	56.88
6	262.70	21.85
6.5	271.00	35.45
7	217.77	59.90
7.5	182.73	22.15
8	104.90*	6.08
8.5	109.23	2.88
8	107.30	2.15
9.5	66.53*	33.68
10	30.17*	30.17
10.5	49.80*	40.66
ALH (µm)		
Media pH	**Average**	**Standard Error**
4	0.00*	0.00
4.5	0.00*	0.00
5	0.00*	0.00
5.5	3.73	3.73
6	10.77	0.66
6.5	10.87	1.23
7	9.77	1.89
7.5	7.97	0.62
8	5.20	0.32
8.5	5.07	0.09
8	5.90	0.51
9.5	2.67	1.50
10	3.77	3.77
10.5	0.00*	0.00
% Motile		
Media pH	**Average**	**Standard Error**
4	0.00*	0.00
4.5	0.00*	0.00
5	0.00*	0.00
5.5	5.67*	4.67
6	48.67	21.80
6.5	59.00	15.52
7	67.00	12.86
7.5	48.33	6.39
8	41.00	5.51
8.5	38.00	7.23
8	38.00	8.74
9.5	13.00	8.50
10	0.00*	0.00
10.5	0.50*	0.41

Table A-24. Data for Figure 4.5. The raw data for the average VCL, ALH and % motile plus standard error for sperm extended in medium with varying pH. Statistics were performed using one-way ANOVA. Treatments marked with a * are significantly different than sperm extended at pH 6.5 medium ($P < 0.05$).

VCL (μm/sec)		
Calcium	Average	Standard Error
8 mM EGTA	216.50	16.95
6 mM EGTA	272.90	16.62
4 mM EGTA	279.13	25.64
2 mM EGTA	283.13	34.56
50 nM Ca	257.13	33.71
100 nM Ca	252.73	40.49
200 nM Ca	253.13	38.11
300 nM Ca	248.10	27.30
400 nM Ca	266.27	38.33
1 μM Ca	186.10	9.50
10 μM Ca	88.4*	12.20
100 μM Ca	88.8*	47.39
1 mM Ca	95.43*	6.38
ALH (μm)		
Calcium	Average	Standard Error
8 mM EGTA	8.30	0.15
6 mM EGTA	10.57	0.98
4 mM EGTA	10.37	1.24
2 mM EGTA	10.77	1.55
50 nM Ca	10.03	0.27
100 nM Ca	10.40	0.70
200 nM Ca	9.73	0.81
300 nM Ca	9.80	0.85
400 nM Ca	11.00	0.17
1 μM Ca	7.57	0.33
10 μM Ca	3.73*	1.07
100 μM Ca	3.67*	1.88
1 mM Ca	4.07*	2.23
% Motile		
Calcium	Average	Standard Error
8 mM EGTA	57.00	1.00
6 mM EGTA	63.33	0.67
4 mM EGTA	61.67	5.61
2 mM EGTA	62.33	3.67
50 nM Ca	65.67	4.48
100 nM Ca	64.00	4.62
200 nM Ca	62.33	9.74
300 nM Ca	63.00	4.58
400 nM Ca	58.67	5.49
1 μM Ca	32*	3.46
10 μM Ca	10.67*	6.69
100 μM Ca	12.33*	9.06
1 mM Ca	4.00*	2.08

Table A-25. Data for Figure 4.6. The raw data for the average VCL, ALH and % motile plus standard error for sperm extended in medium with varying free calcium concentrations. Statistics were performed using one-way ANOVA. Treatments marked with a * are significantly different than sperm extended with 2 mM EGTA ($P < 0.05$).

VCL (µm/sec)	Average VCL				Standard Error			
Calcium	pH 5.9	pH 6.4	pH 6.9	pH 7.4	pH 5.9	pH 6.4	pH 6.9	pH 7.4
8 mM EGTA	238.77	252.23	216.50	160.17*	10.72	4.95	16.95	12.99
6 mM EGTA	287.70	263.73	272.90	216.57	12.61	16.57	16.62	5.58
4 mM EGTA	285.73	280.90	279.13	225.53	14.55	8.54	25.64	5.47
2 mM EGTA	252.30	271.27	283.13	266.47	18.57	20.63	34.56	19.44
50 nM Ca	223.40	272.63	257.13	268.60	18.47	16.40	33.71	21.35
100 nM Ca	199.40	255.37	252.73	194.07	10.49	5.90	40.49	33.89
200 nM Ca	252.10	269.37	253.13	122.77*	9.62	19.85	38.11	3.88
400 nM Ca	172.70	285.93	311.30	111.20*	33.86	21.45	7.94	2.60
1 mM Ca	236.03	245.17	186.10	105.10*	10.74	25.70	9.50	3.15
ALH (µm)	**Average ALH**				**Standard Error**			
Calcium	pH 5.9	pH 6.4	pH 6.9	pH 7.4	pH 5.9	pH 6.4	pH 6.9	pH 7.4
8 mM EGTA	8.47	9.80	8.30	6.53*	0.59	0.49	0.15	0.32
6 mM EGTA	10.67	10.00	10.57	8.30	0.87	0.90	0.98	0.15
4 mM EGTA	10.43	10.23	10.37	9.80	1.70	0.58	1.24	0.25
2 mM EGTA	9.00	11.00	10.77	10.47	1.35	0.38	1.55	0.85
50 nM Ca	11.27	11.27	10.03	10.53	2.19	1.13	0.27	1.14
100 nM Ca	8.87	9.87	10.40	7.93	0.32	0.88	0.70	0.79
200 nM Ca	10.10	11.30	9.73	4.97*	1.42	0.86	0.81	0.26
400 nM Ca	6.77	10.90	11.00	5.37*	1.05	1.23	0.17	0.54
1000 nM Ca	8.07	10.13	7.57	4.63*	0.43	1.18	0.33	0.52
% Motile	**Average Motility**				**Standard Error**			
Calcium	pH 5.9	pH 6.4	pH 6.9	pH 7.4	pH 5.9	pH 6.4	pH 6.9	pH 7.4
8 mM EGTA	50.33*	57.33	57.00	28.00*	11.26	7.84	1.00	2.08
6 mM EGTA	57.33*	57.00	63.33	52.33	13.02	17.39	0.67	1.45
4 mM EGTA	43.00*	48.67	61.67	69.00	13.86	13.96	5.61	4.93
2 mM EGTA	14.67	39.00	59.33	69.33	6.17	16.74	3.38	8.21
50 nM Ca	9.67	38.33	62.00	67.00	4.06	20.00	7.09	7.37
100 nM Ca	12.67	33.00	68.33	49.33*	2.91	17.06	6.33	2.19
200 nM Ca	9.33	37.00	63.67	27.00*	3.18	17.01	10.33	5.29
400 nM Ca	11.67	38.00	58.67	18.67*	4.81	18.08	5.49	3.84
1000 nM Ca	12.33	33.00	32.00*	18.33*	4.10	8.50	3.46	5.84

Table A-26. Data for Figure 4.8. The raw data for the average VCL, ALH and % motile plus standard error for sperm extended in medium with varying free calcium concentrations extended in medium between pH 5.9 and 7.4. Statistics were performed using one-way ANOVA. Treatments marked with a * are significantly different than sperm extended with 2 mM EGTA at the same respective pH ($P < 0.05$).

VCL (µm/sec)	Average VCL				Standard Error			
Treatment	pH 5.9	pH 6.4	pH 6.9	pH 7.4	pH 5.9	pH 6.4	pH 6.9	pH 7.4
8 mM EGTA	266.70	240.00	263.97	154.17	8.30	35.08	11.28	10.13
+ Mg	284.87	244.77	281.13	180.13	6.14	54.56	5.97	11.04
+ Ca	254.13	187.35	265.97	184.37	5.12	78.34	25.23	33.38
+ Mg + Ca	271.20	225.35	291.37	184.13	15.65	53.52	16.81	33.45
ALH (µm)	**Average ALH**				**Standard Error**			
Treatment	pH 5.9	pH 6.4	pH 6.9	pH 7.4	pH 5.9	pH 6.4	pH 6.9	pH 7.4
8 mM EGTA	10.73	9.43	10.60	7.33	0.67	1.28	0.10	0.33
+ Mg	12.17	10.03	10.87	7.70	0.58	1.56	0.20	0.61
+ Ca	11.13	8.55	10.40	9.23	0.41	2.25	1.04	1.39
+ Mg + Ca	10.40	9.95	11.20	8.20	0.70	1.84	0.17	0.95
% Motile	**Average Motility**				**Standard Error**			
Treatment	pH 5.9	pH 6.4	pH 6.9	pH 7.4	pH 5.9	pH 6.4	pH 6.9	pH 7.4
8 mM EGTA	71.67	53.33	74.67	45.33	6.49	13.62	6.49	12.20
+ Mg	69.33	57.33	70.00	50.67	6.64	12.73	1.53	10.40
+ Ca	65.67	46.00	66.33	28.67	7.80	28.58	8.82	8.76
+ Mg + Ca	67.67	58.50	67.67	22.67	1.20	20.00	7.26	5.21

Table A-27. Data for Figure 4.9. The raw data for the average VCL, ALH and % motile plus standard error for sperm extended in medium between pH 5.9 and 7.4 with 8 mM EGTA added, with or without added calcium and magnesium. Statistics were performed using one-way ANOVA, comparing sperm at each pH with and without calcium and magnesium. No treatments were significantly different.

VCL (μm/sec)	Average VCL				Standard Error			
Treatment	pH 5.9	pH 6.4	pH 6.9	pH 7.4	pH 5.9	pH 6.4	pH 6.9	pH 7.4
400 nM Ca	150.47	236.83[a]	277.13[a]	104.00	79.08	52.32	14.87	11.06
Ca, no EGTA	85.63	78.63[b]	96.8[b]	118.33	41.64	17.48	7.21	12.56
EGTA replaced	143.33	182.87[a]	223.37[c]	136.03	22.26	46.98	15.64	25.69
ALH (μm)	**Average ALH**				**Standard Error**			
Treatment	**pH 5.9**	**pH 6.4**	**pH 6.9**	**pH 7.4**	**pH 5.9**	**pH 6.4**	**pH 6.9**	**pH 7.4**
400 nM Ca	5.83	10.10	10.87[a]	4.70	0.44	0.98	1.99	2.97
Ca, no EGTA	3.07	3.90	3.47[b]	5.57	0.73	1.73	1.95	3.07
EGTA replaced	5.30	5.60	10.2[a]	6.30	0.96	0.67	2.01	2.73
% Motile	**Average Motility**				**Standard Error**			
Treatment	**pH 5.9**	**pH 6.4**	**pH 6.9**	**pH 7.4**	**pH 5.9**	**pH 6.4**	**pH 6.9**	**pH 7.4**
400 nM Ca	27.33	53.00	65.67[a]	45.67	9.60	5.81	17.50	19.46
Ca, no EGTA	20.33	19.67	19[b]	20.33	5.70	7.37	13.17	19.33
EGTA replaced	22.33	36.67	41.67[a,b]	49.50	10.52	17.32	18.67	19.34

Table A-28. Data for Figure 4.10. The raw data for the average VCL, ALH and % motile plus standard error for sperm extended in medium with added calcium with and without 2 mM EGTA. Sperm were extended in medium between pH 5.9 and 7.4. Statistics were performed using one-way ANOVA by pH. Significant differences are noted by varying superscripts ($P < 0.05$). An absence of a superscript indicates that a significant difference was not present for that variable at that specific pH.

VCL (µm/sec)	Average VCL		Standard Error VCL	
Calcium	Capacitated	Non-Capacitated	Capacitated	Non-Capacitated
8 mM EGTA	205.13	216.50	56.03	16.95
6 mM EGTA	222.13	272.90	49.53	16.62
4 mM EGTA	233.93	279.13	47.90	25.64
2 mM EGTA	235.83	283.13	42.37	34.56
50 nM Ca	217.17	257.13	45.33	33.71
100 nM Ca	230.63	252.73	60.84	40.49
200 nM Ca	238.67	253.13	34.16	38.11
300 nM Ca	258.23	248.10	20.44	27.30
400 nM Ca	236.33	311.30	42.64	38.33
1 µM Ca*	245.30	186.10	31.81	9.50
10 µM Ca	189.23	88.40	111.28	12.20
100 µM Ca	97.60	88.80	13.45	47.39
1 mM Ca	83.80	95.43	13.33	6.38
ALH (µm)	**Average ALH**		**Standard Error ALH**	
Calcium	Capacitated	Non-Capacitated	Capacitated	Non-Capacitated
8 mM EGTA	8.03	8.30	1.92	0.15
6 mM EGTA	8.40	10.57	1.95	0.98
4 mM EGTA	8.23	10.37	2.06	1.24
2 mM EGTA	8.83	10.77	2.03	1.55
50 nM Ca	9.10	10.03	2.00	0.27
100 nM Ca	9.47	10.40	1.93	0.70
200 nM Ca	9.27	9.73	0.85	0.81
300 nM Ca	9.47	9.80	0.85	0.85
400 nM Ca	10.20	11.00	1.77	0.17
1 µM Ca	9.80	7.57	1.76	0.33
10 µM Ca	7.33	3.73	3.04	1.07
100 µM Ca	5.17	3.67	1.46	1.88
1 mM Ca	4.37	4.07	3.90	2.23
% Motile	**Average Motility**		**Standard Error Motility**	
Calcium	Capacitated	Non-Capacitated	Capacitated	Non-Capacitated
8 mM EGTA	70.00	57.00	6.56	1.00
6 mM EGTA	68.33	63.33	10.26	0.67
4 mM EGTA	73.67	61.67	4.04	5.61
2 mM EGTA	69.00	59.33	3.61	3.38
50 nM Ca	69.67	62.00	10.97	7.09
100 nM Ca	64.33	68.33	16.50	6.33
200 nM Ca	66.33	63.67	7.37	10.33
300 nM Ca	72.67	59.67	11.72	6.49
400 nM Ca	65.33	58.67	14.19	5.49
1 µM Ca	71.00	32.00	5.20	3.46
10 µM Ca	45.67	10.67	29.74	6.69
100 µM Ca	12.00	12.33	4.00	9.06
1 mM Ca	5.67	4.00	1.53	2.08

Table A-29. Data for Figure 4.11. The raw data for the average VCL, ALH and % motile plus standard error for sperm extended in medium with varying calcium concentrations, before (Non-Capacitated) and after (Capacitated) incubation in conditions promoting protein tyrosine phosphorylation. Significant differences between cap and non-cap treatments are noted with a * ($P < 0.05$).

VCL (μm/sec)	Average VCL		Standard Error	
Medium pH	**Capacitated**	**Non-Capacitated**	**Capacitated**	**Non-Capacitated**
7.4	148.77	111.20	27.77	2.60
6.9	236.33	311.30	24.62	7.94
6.4	230.13	285.93	35.96	21.45
5.9	168.13	172.70	44.97	33.86
ALH (μm)	**Average ALH**		**Standard Error**	
Medium pH	**Capacitated**	**Non-Capacitated**	**Capacitated**	**Non-Capacitated**
7.4	6.23	5.37	0.58	0.54
6.9	10.20	11.00	1.02	0.17
6.4	9.23	10.90	1.52	1.23
5.9	9.93	6.77	2.52	1.05
% Motile	**Average Motility**		**Standard Error**	
Medium pH	**Capacitated**	**Non-Capacitated**	**Capacitated**	**Non-Capacitated**
7.4	52.33	18.67	14.67	3.84
6.9	65.33	58.67	8.19	5.49
6.4	42.67	38.00	13.28	18.08
5.9	15.67	11.67	6.33	4.81

Table A-30. Data for Figure 4.12. The raw data for the average VCL, ALH and % motile plus standard error for sperm extended in medium with varying pH, before (Non-Capacitated) and after (Capacitated) incubation in conditions promoting protein tyrosine phosphorylation. Statistics were performed by paired t-tests between capacitated and non-capacitated sperm at each pH. Significant differences between cap and non-cap treatments are noted with a * ($P < 0.05$).

VCL (µm/sec)	Nickel			Cadmium	
µM $NiSO_4$	Average*	Standard Error	µM $CdSO_4$	Average	Standard Error
0	119.87	0.59	**0**	112.23	5.65
25	108.23	0.96	**2.5**	115.60	5.74
50	110.13	2.62	**5**	117.57	6.39
100	98.45	0.10	**10**	123.27	4.60
250	88.27	2.43	**20**	130.80	8.47
			50	118.77	11.27
ALH (µm)	**Nickel**			**Cadmium**	
µM $NiSO_4$	Average	Standard Error	µM $CdSO_4$	Average	Standard Error
0	5.97	0.03	**0**	5.77	0.29
25	5.80	0.95	**2.5**	6.23	0.22
50	7.80	1.76	**5**	6.37	0.61
100	6.18	1.11	**10**	6.57	0.29
250	5.43	0.70	**20**	6.83	0.46
			50	6.17	0.42
% Motile	**Nickel**			**Cadmium**	
µM $NiSO_4$	Average	Standard Error	µM $CdSO_4$	Average	Standard Error
0	51.67	12.35	**0**	55.00	14.22
25	49.33	13.17	**2.5**	50.67	14.95
50	39.33	13.45	**5**	50.00	14.57
100	32.67	11.17	**10**	52.67	14.17
250	28.67	8.67	**20**	52.67	13.68
			50	55.67	14.19

Table A-31. Data for Figure 4.13. The raw data for the average VCL, ALH and % motile plus standard error for sperm treated with either nickel or cadmium. Statistics were performed by linear regression. Treatments significantly affected by the concentration of nickel or cadmium are marked with a * ($P < 0.05$).

	VCL (µm/sec)	
Treatment	**Average**	**Standard Error**
20 µM Cd[a]	147.55	23.07
2 µM Ca[b]	98.43	8.80
2 µM Ca + 20 µM Cd[b]	93.78	3.54

Treatment	**Average**	**Standard Error**
20 µM Cd	5.60	0.58
2 µM Ca	4.68	0.54
2 µM Ca + 20 µM Cd	5.50	0.47

Treatment	**Average**	**Standard Error**
20 µM Cd	47.75	13.10
2 µM Ca	35.25	13.01
2 µM Ca + 20 µM Cd	30.00	8.82

Table A-32. Data for Figure 4.14. The raw data for the average VCL, ALH and % motile plus standard error for sperm treated with cadmium, calcium or both cadmium and calcium. Statistics were performed by one-way ANOVA. Significantly different treatments are denoted by differing superscripts ($P < 0.05$). Treatments without a superscript did not significantly differ.

VCL (μm/sec)

	Average			Standard Error		
Treatment	**0 Min**	**1 Min**	**15 Min**	**0 Min**	**1 Min**	**15 Min**
Control	206.30	206.30	202.47	52.83	52.83	13.98
Procaine	206.30	213.10	231.40	52.83	53.04	7.38
4-AP	206.30	166.13	181.50	52.83	41.99	4.97

ALH (μm)

	Average			Standard Error		
Treatment	**0 Min**	**1 Min**	**15 Min**	**0 Min**	**1 Min**	**15 Min**
Control	7.60	7.60	8.43	0.20	0.20	0.70
Procaine	7.60	8.80	9.10	0.20	0.47	0.53
4-AP	7.60	7.57	7.93	0.20	0.27	0.12

% Motile

	Average			Standard Error		
Treatment	**0 Min**	**1 Min**	**15 Min**	**0 Min**	**1 Min**	**15 Min**
Control	57.67	57.67	62.00	11.57	11.57	5.69
Procaine	57.67	60.00	64.33	11.57	15.01	3.93
4-AP	57.67	60.33	46.67	11.57	18.17	15.30

Figure A-33. Data for Figure 4.15. The raw data for the average VCL, ALH and % motile plus standard error for sperm treated with media (control), procaine or 4-AP. Statistics were performed by one-way ANOVA. Treatments did not significantly vary.